DISRUPTION OF ANGIOGENESIS BY METHYL TERT-BUTYL ETHER (MTBE) IS MEDIATED BY A DYSREGULATION OF THE VASCULAR ENDOTHELIAL GROWTH FACTOR (VEGF) PATHWAY

by

JOSEPHINE ANN BONVENTRE

A Dissertation submitted to the

Graduate School–New Brunswick

Rutgers, The State University of New Jersey

in partial fulfillment of the requirements

for the degree of

Doctor of Philosophy

Graduate Program in Environmental Sciences

Written under the direction of

Professor Keith R. Cooper

and approved by

_____

_____

_____

_____

_____

New Brunswick, New Jersey

October, 2012

ABSTRACT OF THE DISSERTATION

DISRUPTION OF ANGIOGENESIS BY METHYL TERT-BUTYL ETHER (MTBE)
IS MEDIATED BY A DYSREGULATION OF THE
VASCULAR ENDOTHELIAL GROWTH FACTOR (VEGF) PATHWAY

BY JOSEPHINE ANN BONVENTRE

Dissertation Director:

Keith R. Cooper, PhD

Vascular endothelial growth factor (VEGF) is an essential mitogenic factor required for normal angiogenesis. In development, the primary inducer of this protein is hypoxia via hypoxia inducible factors (HIFs). Methyl tert-butyl ether (MTBE) was hypothesized to disrupt angiogenesis by altering the HIF-VEGF pathway. Exposure of zebrafish embryos to MTBE caused vascular lesions, specifically pooled blood in the common cardinal vein (CCV), cranial hemorrhages, and abnormal intersegmental vessels (ISV). These lesions occurred throughout development and were preceded by a critical period between 6-somites and Prim-5 stages during which there was a significant decrease in mRNA transcript levels of *vegf-a*, *vegf-c* and *vegf receptor 2 (vegfr2)*. Lesions other than those associated with the vasculature were not observed. Embryonic exposure to the two primary metabolites, tert-butyl alcohol and formaldehyde, did not induce vascular lesions, indicating the parent chemical was responsible for the anti-angiogenesis. When embryos were exposed to two structurally related chemicals, ethyl tert-butyl ether

(ETBE) or tert-amyl methyl ether (TAME), some vascular lesions were observed, but zebrafish also exhibited lesions in the heart, whole body edema, and craniofacial abnormalities. Unlike MTBE, ETBE, and TAME exposure did not significantly alter *vegf* expression. Of the 3 structurally similar ethers, MTBE appears unique in its ability to target developing endothelial cells. An analysis of the global gene expression changes in zebrafish exposed to MTBE during the critical period identified the cardiovascular system was among the most altered pathways affected by MTBE toxicity. Finally, manipulation of the HIF-VEGF pathway to rescue the specific MTBE-induced vascular lesions, via an over-expression of *vegf-a* and inhibition of HIF degradation, convincingly demonstrated that MTBE toxicity is mediated by the down regulation of VEGF at a critical time during cardiovascular development. Understanding the underlying mechanisms of angiogenesis is important to developing new therapies used to quell solid tumor growth, enhance wound repair, and reduce diabetes induced vascular damage, among others. Chemicals with anti-angiogenic properties, such as MTBE, can be used to advance the science of angiogenesis in both a disease state and during development.

DEDICATION

I dedicate this work to my first two teachers – my mother and my father, Maria and Joseph Bonventre. Together they instilled in me, among other valuable life lessons, the importance of education, knowledge, and curiosity. Both of my parents were the first of their families to pursue college degrees, and my father continued on to a Doctorate of Science in chemistry. From a young age my father fostered my interest in science, taking me to work at the New York City Department of Health, playing with my "science kit", and helping me with my science fair projects. My mother, a math teacher, taught me that only by teaching someone else do we truly learn to understand a thing. She has helped me wherever and whenever I needed help at every point me my life, and has always given me the space that I've needed to grow and pursue my education and my career. There are not enough words in all the world's languages to say how much I appreciate and love her and my father for all that they have sacrificed so that I may achieved my dreams. Their love and support brought me to where I am today – on a path to pursuing a career in academic science where I will, everyday, be able to utilize the skills my parents nurtured in me.

ACKNOWLEDGEMENTS

Among the many people to whom I am indebted for assistance, guidance, and encouragement throughout my graduate career at Rutgers, I must single out Dr. Sean Bugel and Dr. Keith Cooper first. Sean and I met on my first day at Rutgers, and it seems almost immediately he became one of my biggest supporters. He was always there to remind me of that which I am capable, and how much I have to offer to the world of science. In the lab and out of the lab, he has been such an important part of my time at Rutgers and my life. I am so grateful to have him in my corner.

About Dr. Cooper, I have no words to truly explain my gratitude. He is, in my humble opinion, the best adviser any graduate student can hope to have the opportunity to work with. Dr. Cooper always has his students' success in mind, and is ever thinking of ways to push the student to his or her goal. He was supportive of me throughout my studies, and understood when things in my personal life needed to be a priority. I have only respect and admiration for him as a teacher, adviser, and scientist.

Dr. Lori White is another person to whom I credit with some of my success at Rutgers. Her door was always open to help me troubleshoot an idea, vent about graduate school (we all do it…), or just to take my mind off my current troubles. I will miss sitting in her office decompressing, but I will also miss her quick scientific mind that knows just the right question to ask - the kind of questions that remind a student that there is something still to be considered. I will also miss the kittens.

Tiffany Kung was, without a doubt, an essential personallity to my graduate studies. I don't think I would have made it through my last year with out her. Beyond her

aptitude as a scientist, her critical thinking skills, and her ability as a teacher, she has been a great friend to me. From the lab to the gym to the meetings to the bar, and everything in between - she's contributed something to every facet of my time at Rutgers, and I'm so grateful to have had the opportunity to work with her.

Dr. Kenneth Reuhl was more than a program director and committee chair to me. From my first moments at Rutgers he established himself as a solid advocate on my behalf. Always ready with a sarcastic remark about the environment or "fish people", he also never neglected to show his support of my research and my growth. He seemed never to have doubted me, even when I doubted myself, and, on a more personal note, I was always touched by his words of kindness regarding my father.

There are so many other people at Rutgers to whom I owe thanks. From the White Lab, I am thankful to have worked with Drs. Kyle Murphy and Caren Villano, from whom I've learned many things of grad school, science, and lab dynamics. From the support staff of the Joint Graduate Program in Toxicology, I would like to acknowledge Elizabeth Rossi, Sandi Selby, and Bernadine Chmielowicz for always finding an answer to my questions. From the Department of Biochemistry and Microbiology, Jessie Maguire, Dr. Bill Belden, and Dr. Tammy Joska, for their assistance on both day to day and particularly problematic moments. I'd like to thanks Kathy Roberts for her assistance and patience in helping me with my histology, and to Dr. Jessica Graham for her aid in learning the Ingenuity Pathway Analysis software, as well as for their friendship. The members of the Rutgers Association of Toxicology Students who were always there for a joke, smile, or a shoulder to cry on, including: Jason Magby, Karma Fussell, Allison

Isola, Kristen Bircsak, Kim Kruz, Craig Harvey, Brian Wall, Cristina Dragomir, Angela Baker, Ashley Green, Dr. Kate Sokolowski, and many others.

I'd like to also thank the Bugel family for their support, and being a family away from my family. To my numerous roommates at 410 Cedar Ave – thanks for picking me up when the lab kicked me to the floor. Many, many thanks to all my family and friends, near and far, for not forgetting me or holding it against me when I missed birthdays and events over the last 6 years.

Finally, I'd like to thank the members of my committee not previously mentioned: Drs. Jason Richardson, Marion Gordon, and Ann McElroy, for helping to make my dissertation what it is, and for all the challenging questions, support, and encouragement along the way.

TABLE OF CONTENTS

TABLE OF CONTENTS (continued)

TABLE OF CONTENTS (continued)

TABLE OF CONTENTS (continued)

TABLE OF CONTENTS (continued)

TABLE OF CONTENTS (continued)

LIST OF TABLES

LIST OF TABLES (continued)

LIST OF TABLES (continued)

LIST OF FIGURES

LIST OF FIGURES

Page

LIST OF FIGURES

ABBREVIATIONS

CoMO	control morpholino
CCV	common cardinal vein
DNA	deoxynucleic acid
dpf	days post fertilization
ECM	extracellular matrix
ETBE	ethyl tert-butyl ether
Fli1-EGFP	friend leukemia integration 1-enhanced green fluorescent protein
HIF	hypoxia inducible factor (human nomenclature, general use)
Hif	hypoxia inducible factor (mouse, zebrafish protein)
hif	hypoxia inducible factor (zebrafish gene nomenclature)
hpf	hours post fertilization
HUVECs	human umbilical vein endothelial cells
ISV	intersegmental vessels
mM	milimolar
μM	micromolar
MMP	matrix metalloproteinases
MO	morpholino
mRNA	messenger ribonucleic acid
MTBE	methyl tert-butyl ether
NOG	N-oxalylglycine
PDGF-B	platelet derived growth factor B
PHD	prolyl-4-hydroxylase domain protein

TAME	tert-amyl methyl ether
TBA	tert-butyl alcohol
TCA	tricarboxylic acid cycle/the citric acid cycle
TCF	the cell factor
VEGF	vascular endothelial growth factor (human nomenclature, general use)
Vegf	vascular endothelial growth factor (mouse, zebrafish protein)
vegf	vascular endothelial growth factor (zebrafish gene nomenclature)
VEGFR	vascular endothelial growth factor receptor (human nomenclature, general)
Vegfr	vascular endothelial growth factor receptor (mouse, zebrafish protein)
vegfr	vascular endothelial growth factor receptor (zebrafish gene nomenclature)
VHL	von Hippel-Lindau protein
VHL-MO	von Hippel-Lindau morpholino
WNT	from *wingless* in drosophila and *integration* in mice

CHAPTER 1

General Introduction

The research presented in this dissertation examined the vascular toxicity of methyl tert-butyl ether (MTBE) in the developing zebrafish and the role of HIF1/VEGF pathway in the observed anti-angiogenesis. In chapter 2, the vascular-specific lesions induced by MTBE were characterized in the developing zebrafish embryos, and the expression of several genes important to angiogenesis was shown to be reduced during the critical period established for MTBE. In chapter 3, the toxicity of two structurally related compounds, ethyl tert-butyl ether (ETBE) and tertiary amyl methyl ether (TAME), were characterized to test the hypothesis that ETBE and TAME would also act as vascular toxicants due to the similarity in structure between MTBE, ETBE and TAME. In chapter 4, Affymetrix gene array analysis was performed to (1) identify vulnerable pathways during early embryonic development and (2) generate hypotheses for MTBE vascular toxicity. Finally, in chapter 5, the relationship between MTBE toxicity and VEGF was demonstrated with over-expression, chemical inhibitor, and morpholino rescue studies that were designed to manipulate different components of the HIF/VEGF pathway. Based on these studies, it can be concluded that MTBE causes vascular lesions in the developing zebrafish by decreasing VEGF expression during a critical time in development, thereby disrupting angiogenesis. Establishing a mode of action by which MTBE is anti-angiogenic, but non-toxic to other tissue types, may provide valuable information in the potential for MTBE to be used as a supplement to anti-angiogenic therapies.

1.1 Vascular system and development

The cardiovascular system is comprised of the heart, blood vessels, and blood cells, and functions in gas exchange, nutrient distribution, metabolic waste removal, and organ development. It is one of the first systems to develop in the fetus, and defects in this system account for a large percentage of embryonic and fetal lethality in both lower and higher vertebrates (Mone *et al.*, 2004; Heideman *et al.*, 2005). According to a recent Center for Disease Control study, the estimated national prevalence for birth defects associated with the cardiovascular system was 14.40 per 10,000 live births (Parker et al., 2010). Proper development of the cardiovascular system is vital to normal growth and development as organogenesis is strongly dependent on the ability of an embryo to provide oxygen to the growing tissues.

The process by which embryos, and tissues in general, overcome oxygen deprivation is angiogenesis, the development of new blood vessels from pre-existing blood vessels. Angiogenesis primarily occurs during embryonic development, but also occurs in the adult in times of tissue repair, wound healing, and at various stages of the female reproductive cycle. Inappropriate and unregulated angiogenesis has been implicated in a variety of human adult diseases, including diabetic retinopathy (reviewed in Mohammed et al. 2007), rheumatoid arthritis (reviewed in Avouac et al. 2008), cancer (reviewed in Folkman 2006), and other vascular dependent diseases.

In development, angiogenesis is preceded by vasculogenesis. The *de novo* blood vessel formation is initiated by angioblasts, endothelial cell precursors derived from progenitor cells (hemangioblasts) in the bone marrow (Choi *et al.*, 1998, Vogeli *et al.*, 2006). Angiogenesis, in turn, regulates the formation endothelial cells, derived from the

mesodermal primary germ layer of the embryo, into the lining of cardiovascular and lymphatic vessels (Fig. 1.1). Externally, an extracellular matrix composed of collagen, elastin, fibronectin, and laminin, all mesodermal in origin, surrounds the endothelial cells. This matrix provides structural support to the vessels and all the body's tissues. Smooth muscle cells also play an important role in the structure of blood vessels, surrounding arteries in multiple layers or tunica, or to a lesser extent, as smaller smooth muscle-like cells in microvasculature.

The developing cardiovascular system is commonly a target for toxicants. There are a number of xenobiotics that target the developing heart with well-characterized effects, including thalidomide (reviewed in DeSanctis *et al.,* 2001), cocaine (Meyer and Zhang, 2009), and 2,3,7,8-TCDD (Cheung et al., 1981; Walker *et al.,* 2000). However, few chemicals are known to specifically target developing blood vessels. Ergot alkaloids, produced by fungi infesting rye and other plants, elicit vascular toxicity at the endothelial cell level and reduce circulation to distal structures in animals that have ingested contaminated grains (Perry, 1977 and McKiernan *et al.,* 1994). More recently, anti-cancer therapies have included drugs, such as Avastin (bevacizumab), specifically targeted to disrupt the molecular signals tumor cells produce to promote angiogenesis (Dranitsaris et al., 2010). The consequence of aberrant vascular growth in knockout mice for key angiogenic proteins is lethality (Fong et al., 1995; Shalaby et al., 1995; Carmielet et al., 1996; Ferrara et al., 1996; Ryan et al., 1998; Ramirez-Bergeron et al., 2004). Therefore, understanding how chemicals target specific components of angiogenesis is important to both developmental biology and designing new drugs to treat vascular-related diseases.

1.1.1. Hypoxia and the regulation of hypoxia inducible factor 1 (HIF1)

The formation of blood vessels in a proliferating and growing tissue (e.g. an embryo) is a dynamic process that begins as lowered oxygen levels trigger the cellular hypoxic response system, a highly conserved process in all eukaryote organisms with closed circulatory systems. The response to hypoxia, the primary inducer of angiogenesis in developing embryos, is mediated by hypoxia inducible factors (HIFs) (Ryan et al. 1998; Lee et al., 2001; Ramirez-Bergeron et al., 2004). HIFs are basic helix loop helix-Per-ARNT-SIM transcription factors with cytoplasmic alpha subunits and nuclear beta subunits that heterodimerically bind to hypoxia response elements (HRE). Three HIF-α homologs are known: HIF1-α, HIF2-α, and HIF3-α, but HIF1 and HIF2 play central roles in the regulation of the cardiovascular system, energy metabolism, and cell survival (reviewed in Keith et al., 2012). HIF1-α was the first to be described, and in terms of embryonic development, seems to play the predominant role (Semenza et al., 1995).

HIF1 is composed of cytoplasmic HIF1-α and nuclear HIF1-β (also known as ARNT, the aryl hydrocarbon receptor nuclear translocator). Together, HIF1 is responsible for the regulation of hypoxia compensatory mechanisms in all cells (Semenza et al., 1995; Forsythe *et al.*, 1996; Adelman *et al.*, 1999). Developing embryos (embryonic day 8.5) in a HIF1-α knock-out mouse have a reduced vascular network in the yolk sac, lack of cephalic vascular development, and reduced numbers of somites (Ryan et al., 1998). The lesions were associated with regions of increased hypoxia in the embryo and lethality occurs by embryonic day 10.5. Moreover, hemangioblast differentiation in HIF1-β/ARNT deficient embryonic stem cells (Ramirez-Bergeron et al., 2004) and in knockout mice (Adelman et al., 1999) was inhibited, indicating that hypoxia

is required for early stage vascular development. Distribution of HIF1-α within the embryo varies based on gestational stage and from organ to organ, with the highest found in brain, heart, kidney, lung, and liver (Madan et al. 2002).

Under normoxic conditions HIF1-α is postranslationally modified and degraded (Fig. 1.2). Prolyl-4-hydroxylase domain proteins (PHDs) and von Hippel-Lindau (VHL) protein primarily regulate the HIF1-α levels in the cytoplasm (Ivan et al., 2001; Jaakkola et al., 2001). In the presence of oxygen, 2-oxoglutarate, and Fe^{2+}, PHDs hydroxylate conserved proline residues 402 and 564 in the oxygen dependent domain of HIF1-α (Jaakkola et al., 2001). Three categories of PHDs have been characterized in vertebrates, and they differ in location within the cell and substrate. PHDs responsible for the hydroxylation of Hif1-α are cytoplasmically located, while prolyl-4-hydroxylases (P4H) known to hydroxylate collagen and transmembrane P4Hs are located in or are associated with the endoplasmic reticulum (Hyvärinen, et al. 2010). HIF and collagen PHDs also differ in that collagen P4Hs associate with protein disulfide isomerases in order to hydroxylate the extracellular matrix protein, while HIF-PHDs do not (Winter et al., 2007). Multiple isozymes of HIF-PHDs exist, PHD1, PHD2, and PHD3, and their distribution throughout the body varies (Berra et al., 2003; Hirsila et al., 2003; reviewed in Fraisl et al., 2009). Counter intuitively, gene expression of both PHD2 and PHD3 are induced by hypoxia, which is suggestive of autoregulation, as an upregulation of PHDs would accelerate degradation of HIF1-α upon reoxygenation of the tissue (Marxsen et al., 2004). The reaction that results in the hydroxylation of prolines 402 and 564 on HIF1-α involves the oxidative decarboxylation of 2-oxoglutarate to succinate and carbon dioxide. Binding of HIF1 to DNA, the expression of both erythropoietin and VEGF, and HIF1-α

protein levels are decreased by an excess 2-oxoglutarate *in vitro* (Masumoto et al., 2006). Similarly, 2-oxoglutarate mimetics, i.e. dimethyloxaloylglycine or N-oxaloylglycine, can be used as PHD inhibitors (Mole et al., 2003; Wirthner et al., 2007; van Rooijen et al., 2009).

The conversion of 2-oxoglutarate to succinate by PHD during HIF1-α hydroxylation suggests that the system is sensitive to dysfunction of the citric acid (TCA) cycle. In fact, Pollard et al. (2005) showed *in vivo* that the accumulation of succinate or fumarate stabilizes HIF1-α, and proposed PHD inhibition as the mechanism by which this occurs. Mackenzie et al. (2007) then demonstrated that elevating 2-oxoglutarate could reverse the succinate- or fumarate-mediated inhibition of PHD, indicating that the inhibition is competitive. Similarly, increased levels of pyruvate and lactate have also been shown to stabilize HIF1-α and increase the expression of HIF1 responsive genes (Lu et al., 2002). The relationship between the TCA cycle or pyruvate/lactate and HIF1-α stabilization is important because it demonstrates a potential hypoxia-independent mechanism of HIF1 transcriptional activity.

Hypoxia-dependent PHD-driven hydroxylation of cytoplasmic HIF1-α allows for VHL binding and the initiation of ubiqutination (Maxwell et al., 1999; Ohh et al., 2000; Ivan et al., 2001). VHL serves as the recognition element in an E3 ubiquitin ligase complex that includes elongin b, elongin c, and cullin-2 (Kibel et al., 1995; Lonergan et al., 1998; Iwai et al., 1999). Degradation of polyubiquitinated proteins by the proteasome occurs to maintain the appropriate balance of proteins within a cell. Ubiquitination begins with the activation of ubiquitin by E1, followed by its conjugation by E2 and addition to

the target protein by E3. The process is repeated until a chain of ubiquitin marks the protein for proteolysis in the proteasome (reviewed in Wilkinson et al, 2000).

VHL, a tumor suppressor, derives its name from the genetic disease von Hippel-Lindau syndrome, in which VHL null hemangioblastomas of the retina and central nervous system develop in 60-80% of all patients with the disease (reviewed in Chew, 2005). Loss of function mutations in the VHL protein is common in sporadic clear cell renal carcinomas (Gnarra et al., 1994). Generally these mutations occur in exon 2 of the protein, and a complete deletion of the exon 2 leads to tumor formation despite the fact that neither the HIF1-α (exon 1) nor elongin c (exon 3) binding domains are within exon 2. Rather, exon 2 is important to chaperonin controlled protein folding, and the without appropriate fold configuration, VHL is unable to bind elongin c (Feldman et al., 1999). A hallmark of VHL inactivation in tumors is the over expression of VEGF-A which results from the increased stabilization of HIF1-α. Not surprisingly, VHL knockout mice models die between embryonic day 10.5 and 12.5 due to vascular aberrations of the placenta (Gnarra et al., 1997). Zebrafish transheterozygote ($vhl^{hu2117}/vhl^{hu2081}$) mutant embryos, with two mutations in the Hif1-α binding domain, developed polycythemia, dilated blood vessels, aberrant intersegmental vessel sprouts, and increased Vegf-a/Vegfr2 signaling (van Rooijen et al., 2009; van Rooijen et al., 2010). The zebrafish mutants are, however, not viable beyond 11 days post fertilization. VHL is important to not only vascular patterning and integrity, but has also been shown to play a role in fibronectin deposition within the extracellular matrix (Ohh et al., 1998; Tang et al., 2006).

VHL-driven ubiquitination of the HIF1-α does not occur under hypoxic conditions, as decreased localized oxygen stabilizes HIF1-α protein by preventing PHD

induced hydroxylation and VHL binding. Kim et al. (2006) demonstrated that VHL does not bind to HIF1-α in the absence of hydroxylated prolines by using HIF variants that could not be hydroxylated. Without oxygen, PHDs cannot hydroxylate HIF1-α, and without hydroxylation, VHL cannot bind HIF1α and promote protein degradation. Therefore, under hypoxic conditions within the cell, HIF1-α accumulates in the cytoplasm, and subsequently translocates into the nucleus. In the nucleus, HIF1-α dimerizes with HIF1-β and binds to DNA at response elements in HIF1 responsive genes (Wang and Semenza, 1993). Two primary hypoxia-related genes are erythropoietin, produced in response to systemic hypoxia (reviewed in Krantz, 1991), and vascular endothelial growth factor (VEGF), responsible for angiogenesis in localized tissues (reviewed in Neufeld *et al*., 1999 and Coultas *et al*. 2005). HIF1 increases VEGF mRNA transcription and stabilization in hypoxic conditions. Minchenko et al. (1994) identified 5' and 3' regulatory elements for HIF1 binding to the human *VEGF* gene, of which the 3' enhancer sequence was highly homologous to that of the erythropoietin gene. However, Shima et al. (1995) showed that *VEGF* mRNA stability contributed more to the up-regulation of the gene than increased transcription alone, as had been previously postulated (Levy et al., 1995; Stein et al., 1995). Under normoxia, the half-life of *VEGF* mRNA is 30-45 minutes, while under hypoxia it is 6-8 hours, suggesting that the prolonged presence of mRNA transcript results in the accumulation of VEGF protein.

During vertebrate development, the relationship between HIF1 and VEGF is crucial to angiogenesis and, therefore, to organogenesis. The proteins discussed in this thesis that play a fundamental role in the HIF1-VEGF relationship are described in Table 1.1. These include various isoforms of VEGF and its receptors, components involved in

vessel stability and cell structural, as well as proteins that regulate the extracellular matrix.

1.1.2. Vascular endothelial growth factor driven angiogenesis

The VEGF protein family is a group of secreted glycoproteins essential to vasculogenesis, angiogenesis, and hematopoiesis (reviewed in: Coultas et al., 2005; Patel-Hett and D'Amore 2011). Homologous VEGF A-F ligands bind to extracellular portions of tyrosine kinase receptors, vascular endothelial growth factor receptors (VEGFR1/Flt1, VEGFR2/Flk1/KDR, and VEGFR3/Flt4, hereafter referred to as VEGFR1, 2, or 3) to regulate the proliferation, migration, and survival of endothelial cells. All VEGF ligands and receptors are required in assorted combinations for endothelial cell differentiation and migration, but have varying capacities as factors in angiogenesis (Habeck *et al*., 2002; Bahary, *et al.*, 2007; Covassin, *et al.*, 2006). VEGF-A is the most studied, and is understood to be the key VEGF ligand involved in angiogenesis. The deletion of one *Vegf-a* allele inhibits blood island formation, angiogenesis, lumen formation, and survival of the embryo (Carmielet et al., 1996; Ferrara et al., 1996). Pre-translational modifications of *VEGF-A* mRNA splice variants contribute to the protein's ability to bind to heparin in the extracellular matrix, and consequently to its ability to bind specific recepters (Cohen et al., 1995).

VEGF-A binds primarily VEGFR1 and VEGFR2, which play different roles in angiogenesis. Both Vegfr1 and Vegfr2 knockout mice are embryonic lethal at E8.5. However, Vegfr1 null mice die of uncontrolled vascular growth, indicating a role for VEGFR1 in inhibiting angiogenesis (Fong *et al.*, 1995). Conversely, Vegfr2 null mice

lack differentiated angioblasts and consequently, any vascular growth, demonstrating its role in promoting angiogenesis (Shalaby et al., 1995). The primary VEGF and VEGFR isoforms stimulating angiogenesis are understood to be VEGF-A via VEGFR2. VEGF-C and D are primarily responsible for lymphangiogenesis via VEGFR3 (Enholm et al., 2001), but VEGF-C/VEGFR3 are thought to also play a role in arterial-venous differentiation (Herbert et al. 2009).

Binding of a VEGF ligand to VEGFR stimulates homo- or hetero-dimerization and autophosphorylation. Phosphorylation of conserved tyrosine sites on the receptor activates various signal transduction pathways that regulate proliferation, migration, cell survival, and vascular permeability in the endothelial cell. For example, VEGF-A signals to MAP kinase through phosphorylation of Tyr1175 on VEGFR2, which in turn phosphorylates PLCγ, and activates the Ras-Raf-MEK1 pathway (Takahashi et al, 1999; Takahashi et al., 2001). Figure 1.3 summarizes some of the signaling pathways activated by VEGF-A/VEGFR2 binding that coordinate the organization of endothelial cells into blood vessels.

1.1.3. Supplemental angiogenesis related proteins

Blood vessels are a contiguous network of endothelial cells linked together by the junction protein vascular endothelial (VE)-Cadherin (reviewed in Vestweber, 2007), supported by pericytes, smooth muscle-like cells (reviewed in Hirschi and D'Amore, 1996; Gerhardt and Betsholtz, 2003) and the extracellular matrix. VE-Cadherin is anchored via α- and β-catenin to actin, linking the junction protein to cytoskeleton within the cell (Lampugnani et al., 1995). β-catenin is also an intracellular signaling protein

involved in the WNT (from *wingless* in drosophila and *integration* in mice) canonical pathway, which plays a critical role in governing embryogenesis in the form of axis orientations, embryonic stem cell pluripotency, germ layer formation, cell fate specifications, and organogenesis (reviewed in Sokol et al., 2011). WNT signaling, through cell surface receptor FRIZZLED, inhibits β-catenin degradation, which allows the protein to bind to TCF (T cell factor) and translocate into the nucleus. β-catenin/TCF bind to DNA and promote transcription of genes involved in the regulation of cell growth, including VEGF (Eswaran et al., 2003). In addition, without WNT, β-catenin is degraded, VE-cadherin junctions in endothelial cells cannot form properly, and cell growth is disrupted. In this way, there is a directed relationship between WNT signaling and angiogenesis.

When the capillary tube is initially formed, endothelial cells secrete platelet derived growth factor B (PDGF-B) to recruit pericytes via the PDGF-B receptor. PDGF-B deficient mice exhibit aberrant kidney glomeruli and cardiac vasculature, decreased blood cells and increased hemorrhages that result in embryo death (Leveen et al., 1994). The microvasculature of PDGF-B null mice lack pericytes and, therefore, support for the vascular walls (Lindahl et al., 1997). Pericytes can regulate vascoconstriction and vasodilation, much the way large smooth muscles regulate flow in larger vessels. The distribution of pericytes varies throughout the body, but these cells are most abundantly found in the brain, where they contribute to the blood-brain barrier (reviewed in Bergers and Song, 2005).

Pericytes can also play a role in the coordinated restructuring of extracellular matrix (ECM) components required for vascular formation and remodeling (Stratman et

al., 2009). Matrix metalloproteinases (MMPs), are a family of zinc-dependent proteins that cleave ECM components, including collagen, laminin, gelatin, and elastin, to allow for tissue restructuring (reviewed in Zitka et al., 2010). MMP-2 and -9, are primarily responsible for the degradation of the ECM associated with blood vessels (reviewed in Rundhaug, 2003; van Hinsbergh and Koolwijk, 2008; Zitka et al., 2010). MMP-2 and MMP-9, gelatinase A and B respectively, hydrolyze collagen type IV, V, and XI, and elastin. VEGF is closely associated with MMP-2 and MMP-9 regulation and activity (Belotti et al., 2003; Poyer et al., 2009). MMP-9 transcription and secretion is upregulated by the VEGF-A/VEGFR2 signaling cascade (Wang and Keiser, 1998; Pufe et al., 2002; Hollborn et al., 2007). MMP-2 or MMP-9 deficient mice are viable, but MMP-2 knockouts exhibit reduced vascular growth (Itoh et al., 1998), while MMP-9 knockouts exhibit increased vascular permeability (Kolaczkowska et al., 2006). The ECM proteins maintained by the MMPs are important for cell adhesion mediated by cell surface receptors. While VE-cadherins are necessary for cell-cell junctions, integrins play a primary role in the cell-ECM connections. Integrins, heterodimeric proteins with an alpha and beta subunit, bind extracellularly to fibronectin, vitronectin, laminin, and collagen, while cytoplasmically they bind cytoskeletal components and signaling proteins (reviewed in Malinin et al., 2012). However, these proteins do more than anchor cells to the ECM. For instance, αvβ3 plays a major role in modulating VEGFR signaling by stimulating autophosphorylation of the receptor (Mahabeleshwar et al., 2006). Integrin α3β1 has been shown to increase *MMP-9* transcripts by stabilizing the mRNA thereby facilitating another VEGF/VEGFR function (Iyer et al., 2005). MMP-9 has also been shown to bind integrin-α4β1 under specific conditions (Redondo-Munoz et al., 2008).

The connections between the cells and ECM, maintained by MMPs and utilized by integrins and other cell surface receptors, enables the cells to migrate to hypoxic regions and establish new blood vessels.

1.1.4. Summary of vascular development

A summary schematic, Figure 1.4, describes HIF1/VEGF regulated angiogenesis. Low oxygen levels resulting from by organogenesis promotes HIF1 activation, which in turn up-regulates VEGF-A both at the mRNA level and the secretion of stored protein. Specific endothelial cells, known as “tip cells” are stimulated by the newly created VEGF-A gradient and begin to migrate toward the hypoxic area (Gerhardt *et al.*, 2003). Other endothelial cells in the area begin to proliferate and migrate in response to VEGFa-VEGFR2 signaling. MMPs are secreted to break down the ECM, which allow for movement of the endothelial cells. Eventually, tip cells fuse with either another tip cell or a pre-existing mature vessel, which stimulates the lumen formation and blood flow in the new vessel. Blood flow increases oxygen in the region and begins the capillary maturation process: VEGF-A decreases and endothelial cells secrete PDGF, which attract pericytes. Pericytes adhere to endothelial cells, forming a mural support for the capillary wall, while VE-Cadherins indirectly anchor adjacent endothelial cell cytoskeletons to one another, forming an inter-endothelial cell support network. The ECM is reformed, and the new vessel is stabilized.

1.2 Zebrafish (Danio rerio) as a model for cardiovascular toxicology

The morphological and biochemical pathways involved in angiogenesis are highly conserved across vertebrate species. This allows for the use of lower vertebrates as models systems in which to study the impact of toxicant chemical exposure on vascular development. The zebrafish has emerged as a powerful model for understanding vertebrate development, in part due to the high degree of conservation in critical processes, including angiogenesis, with higher vertebrates (Spitzbergen and Kent, 2003; Heideman *et al.*, 2005). Zebrafish are an attractive vertebrate model due to the availability of molecular techniques, rapid embryonic development (less than 5 days), inexpensive maintenance, and large clutch sizes of transparent embryos that allow for the visualization of embryogenesis.

Zebrafish embryogenesis and vascular development have been well characterized (Kimmel et al., 1995; Isogai et al., 2001). The stages and relative respective time points discussed in this thesis are based on development at 25 ºC (Fig. 1.6). At 21-somites or 24 hours post fertilization (hpf) major blood vessels are intact, but have no circulation. By the Protruding Mouth stage or 96 hpf, all vessels are fully patent and embryos hatch shortly thereafter. Isogai et al. (2001) used Berlin Blue dye to characterize the zebrafish vasculature during the first 7 days of development. Cell fates and migratory patterns of vascular endothelial precursors have also been studied. Angioblasts comprising intersegmental vessels arise in the posterior lateral mesoderm of the zebrafish embryo migrate from the aorta in a very specific manner to their final place in the dorsal vasculature of the embryo (Childs et al., 2002). The key stages of vascular development with the associated embryonic stage are presented in Table 1.2.

Extensive work has also been carried out to characterize zebrafish orthologs to the human angiogenic proteins described in Table 1.1. Morpholino technology has enhanced the understanding of functions of these and other proteins during development. Morpholinos are antisense oligoneucleotides that knock down expression of a protein by blocking translation or modifying the pre-mRNA splice product (Nasevicius and Ekker, 2000). The Vegf morphant – an embryo which has been micro-injected with a morpholino for Vegf-a at the 1-2 cell stage – phenotypically exhibits pericardial edema, no or reduced circulating red blood cells, and aberrant or absent vasculature (Nasevicius et al., 2000). As previously discussed, Carmielet et al. (1996) reported that a murine Vegf-a knockout was lethal, however, in the case of Nasevicious et al. (2000), the zebrafish morphants survive. Several possible reasons exist for the differences between the mice and zebrafish embryos lacking the growth factor. First, zebrafish embryos are smaller and therefore able to diffuse oxygen into tissues from their rearing solutions. Secondly, zebrafish, like many teleosts, underwent a genome duplication event, which resulted in multiple Vegf-a copies (Taylor et al., 2003; Bahary et al., 2007). Therefore, knocking down one Vegf leaves another copy to perform its normal function. Finally, morpholinos are not permanent, and their ability to knockdown the protein diminishes as the molecules are diluted out in the embryonic cells, generally 72-96 hrs post injection. Bahary et al. (2007) evaluated the differences between the duplicated zebrafish *vegf-a* genes (*vegf-aa*, *vegf-ab*) using morpholinos. Knockdown of either protein results in a similar disruption of ISVs and increased cranial hemorrhages. However, knockdown of both variants simultaneously was still not lethal, which suggests that other Vegf isoforms

or alternative pro-angiogenesis pathways play a greater role in compensating for the loss of Vegf-a in the zebrafish than they do in the mouse model.

A transgenic zebrafish line was utilized in the studies presented in this dissertation to investigate developmental cardiovascular toxicity *in vivo* (Fig. 1.5). *Fli1*-EGFP (Fli1s) express enhanced green fluorescent protein driven by the *fli1* promoter in all vascular endothelial cells (Lawson and Weinstein, 2002). Fli1 is an endothelial cell specific transcription factor, and its presence is limited to blood cells, pharyngeal arch cells and endothelial cells (Melet et al., 1996; Lawson and Weinstein, 2002; Covassin et al., 2006). Expression of EGFP in all endothelial cells of Fli1s provides an excellent tool in which to examine morphology of vasculature in live embryos throughout all stages of development (Fig. 1.5).

The differences notwithstanding, zebrafish provide an excellent vertebrate model of *in vivo* embryonic vascular development, and allows for extrapolation between the aquatic and human health scientific communities.

1.3 Gasoline Oxygenates MTBE, ETBE, and TAME

Early studies in our laboratory demonstrated targeted vascular toxicity by gasoline oxygenate, methyl tert-butyl ether (Longo, 1995). As a result, the studies carried out in this dissertation examined the anti-angiogenesis by methyl tert-butyl ether, and the potential anti-angiogenesis of structurally related chemicals ethyl tert-butyl ether and tert-amyl methyl ether, in the zebrafish embryo model system.

1.3.1 Methyl tert-Butyl Ether (MTBE)

MTBE [$CH_3OC(CH_3)_3$] is a water-soluble (50 g/L) volatile organic compound best known for its use as an oxygenating agent in gasoline, which resulted in widespread groundwater contamination throughout the United States (Brown, 1997; Gullick and Lechevalier 2000; Post, 2001; Squillace and Moran, 2007; Van Wezel et al., 2009). At the peak of its use, workers in the petroleum industry exposed to MTBE reported a high incidence of neurologic symptoms, including headaches, dizziness, and nausea (Beller and Middaugh, 1992; Moolenaar, *et al.*, 1994; Prah, et al., 1994). In combination with dizziness and nausea, the headaches reported to follow MTBE exposure suggested an effect on the cerebrovasculature (Appenzeller, 1978) and/or an alteration of cranial hemodynamics (Hannerz et al., 1998). Headaches associated with chemical exposures are not uncommon and may involve similar physiological and biochemical changes observed following MTBE exposure (Fiedler et al., 2000; Martin and Becker, 1993).

Rodent studies have demonstrated species, strain, and sex specific lesions at high concentrations of MTBE (reviewed in McGregor 2006). A 14 and 90 day oral gavage study with Sprague-Dawley rats yielded no adverse effect at concentrations less than 1200 mg/kg, but males rats exposed to greater than 1200 mg/kg exhibited a rat-specific α2μ-globulin nephropathy (Robinson et al., 1990). In a chronic oral administration (gavage) study, male and female Sprague-Dawley rats were treated with 0, 250, or 1000 mg MTBE/kg 4 days per week for 104 weeks. A statistically significant increase in the incidence of Leydig cell tumors in males of the 1000 mg/kg group was observed, while in females, lymphomas/leukemias were statistically increased in the 250 and 1000 mg/kg group (Belpoggi et al., 1995; Belpoggi et al., 1997). Bird et al. (1997) also reported a

statistical increase in Leydig cell tumors as well as renal tube tumors in Fischer 344 rats exposed via inhalation to 3000 and 8000 ppm. However, the incidence of Leydig cell tumors in male rats is known to increase with age (Cook, 1999). Williams et al. (2000) demonstrated that adult Sprague-Dawley rats treated orally with 800 mg MTBE/kg/day for 15 or 28 days exhibited only mild alterations in endocrine-sensitive parameters. Mice studies, on the other hand, did not show Leydig cell or lymphomas, but rather liver neoplasms (Burleigh-Flayer et al., 1992; Bird et al., 1997). Female CD-1 mice exposed to 8000 ppm MTBE by inhalation exhibited an increase in hepatocellular adenomas, but the same increase was not observed in males (Bird et al., 1997). Recently, two studies examined the effect of repeated long term MTBE administration via drinking water (0, 0.5, 3, 7.5, and 15 mg/ml [6 – 170 mM]) in Wistar rats. After 13 weeks, there was a decrease in water consumption in both males and females that may be a consequence of taste. Only minimal effects in male kidneys were observed at 13 weeks and 1-year, and these were attributed to α2μ-globulin (Bermudez et al. 2011). A 2-year study by the same lab reported chronic progressive nephropathy in both males and females, and statistically increased brain astrocytomas in males, but since the incidence of astrocytomas was within the historical control range for Wistar rats, the authors concluded that the increase was not due to MTBE exposure (Dodd et al., 2011).

In all the rodent studies, the concentrations that induced lesions exceed those encountered in human exposures. Drinking water guidelines created by the EPA are based on taste threshold, and the recommendation is to maintain MTBE levels below 40 ug/L (0.45 μM). When MTBE was used in the formulation of Oxyfuel, gasoline contained upto 15% MTBE by volume, which created an atmospheric exposure of about

1.7 ppm MTBE (Fiedler et al., 2000). According to a human exposure study, MTBE levels in the blood of pre-exposed individuals were less than 0.5 ng/ml (6 nM), while post-exposure, 20 minutes to either 11 % or 15 % MTBE/gasoline, blood concentrations were up to 1.2 or 1.75 ng/ml (13 or 19 nM), respectively. Therefore, while both occupational and nonoccupational exposure to MTBE occurs, the MTBE concentrations observed in humans are significantly lower than those used in rodent toxicity studies. With regards to carcinogenicity, IARC classified MTBE as a Group 3 category – "*Not classifiable as to its carcinogenicity to humans"* (IARC, 2012). In other words, based on available studies, there is little evidence to expect MTBE exposure would cause tumors in humans. Moreover, MTBE is FDA approved for use in humans in cases of inoperable cholelithiasis. MTBE is administered via perfusion into the liver biliary tract to dissolve gallstones, and the therapy involves minimal side effects (Leuschner, 1986; Hellstern et al., 1998).

Our laboratory was the first to report that MTBE disrupts normal vascular development in multiple models of angiogenesis. In Japanese medaka (*Oryzias latipes*), vasculature fails to develop in embryos exposed to with 0.11 – 3.4 mM MTBE, while other non-vascular tissues develop normally, and demonstrated no toxicity until the point where vascularization became essential for further growth (Longo, 1995). Recently, we reported three mammalian angiogenic systems exhibiting decreased vascular growth and development in the presence of MTBE: rat brain endothelial cells, human umbilical vein endothelial cells (HUVECs), and the mice matrigel plug assay Kozlosky et al. (2012). Isolated rat brain endothelial cells exposed to 0.34, 3.4, and 34.0 mM MTBE resulted in a dose-dependent reduction of tube formation, with a significant effect ($p < 0.05$) at all

three concentrations. HUVECs, a primary cell line representing macrovascular cells, were able to form tubes on Matrigel in the presence of MTBE (1.25 – 80 mM), however beginning at 10 mM there was a marked delay in the initiation stage of tube formation, where endothelial cells form projections into different directions (Lamalice et al., 2006) (Fig. 1.7). The tubes that formed in the presence of MTBE were narrower than those formed in the absence of MTBE (Fig. 1.8). The results observed with HUVECs were different from the inhibited tube formation observed with the rate brain endothelial cells, which suggested that micro- and macrovasculature cells have different levels of sensitivity to MTBE. In a mouse Matrigel plug implantation assay, 34.0 mM MTBE completely inhibited vessel invasion into plugs containing Endothelial Cell Growth Supplement (ECGS) compared to control plugs with ECGS alone.

MTBE has anti-angiogenic properties at mM concentrations in multiple model systems: piscine, mouse, rat and human endothelial cells. In addition, in the whole animal studies, no toxicity to other tissues types was observed. Furthremore, it is already approved for use in humans. A potential for the use of MTBE as an anti-angiogenic treatment for solid tumors or other vascular based diseases exists, but further work into the characterization of the vascular disrupting effects at the molecular level, along with animal testing, is required.

1.3.2 Ethyl tert-Butyl Ether (ETBE) and tert-Amyl Methyl Ether (TAME)

While MTBE was the more popular gasoline additive in the United States, other oxygenates, such as ETBE [$CH_3CH_2OC(CH_3)_3$] and TAME [$CH_3OC(CH_3)_2CH_2CH_3$] were also in high demand through the 1990s. Limitations on the use of MTBE in the

United States did not extend to the structurally related chemicals, ETBE and TAME (Coons, 2009; van Wezel et al., 2009), despite the similarities in chemical characteristics (Table 1.2). ETBE and TAME have not been as extensively studied as MTBE. The effect of ETBE and TAME on aquatic organisms is limited to acute toxicity data (MSDS, Chevron Philips, 2010; Huttunen et al., 1997), and their potential as developmental toxicants is unknown. Due to their structural similarity to MTBE, ETBE and TAME may also elicit vascular-specific toxicity. Determining the potential for ETBE and TAME, which differ from MTBE by only one methyl (CH_3) group, to also disrupt vascular growth may shed light on the structural characteristics required for a chemical to specifically target the vasculature.

1.3.3 Metabolism of MTBE, ETBE, and TAME

Primary metabolism of MTBE, ETBE, and TAME in mammals occurs in the liver through oxidative demethylation by cytochrome P450s. Cyp 2A6 is the principle isoform involved in human alkoxyether metabolism, but Cyp3A4 also plays a minor role (Hong et al., 1997, Hong et al., 1999, Le Gal et al., 2001). All three chemicals are readily eliminated via expired air or they can be metabolized and excreted in the urine (Amberg et al., 2001). MTBE and ETBE oxidation results in tertiary butyl ether (TBA) and formaldehyde or acetaldehyde, respectively. TAME is oxidized to formaldehylde and tert-amyl alcohol. TBA can be further metabolized to 2-methyl-1,2-propanediol and 2-hydroxyisobutyric acid but the enzymes required for those steps are unknown (Amberg et al. 2001, Phillips et al. 2008). Formaldehyde is biotransformed to either methanol or formic acid in the presence of alcohol dehydrogenase or aldehyde dehydrogenase,

respectively (Du et al., 2005). Aldehyde dehydrogenase will also convert acetaldehyde to acetate. Tert-amyl alcohol can be glucuronidated and excreted (Collins et al., 1999). In humans, circulating levels of the primary metabolite, *tert*-butyl alcohol (TBA), are directly correlated to amount of MTBE exposure because the tertiary alcohol is metabolized at a much slower rate than MTBE (Ahmed, 2001; Chen, 2007).

1.3.4 Mammalian developmental toxicity studies with MTBE, ETBE and TAME

Studies exploring the developmental toxicity of MTBE inhalation in lab animals report effects at very high concentrations. Gestational exposure to MTBE lead to increased fetal resorption in rats and mice at 2500 ppm, with no effect on the dam (Conaway et al., 1985). However, at 4000 and 8000 ppm, mice exhibited a significant increase in fetal toxicity, post implantation loss, altered sex ratio, craniofacial abnormalities, and skeletal variations, with mild maternal toxicity, while no treatment related toxicity or teratogenicity was observed in rabbits exposed to the same high concentrations (Bevan et al., 1997). Pregnant female rats exposed to at one time gavaged dose of 500 -1500 mg/kg of MTBE did not demonstrate treatment related effects in the pups (Kozlosky et al., 2012).

Similar high concentrations are reported for developmental toxicity studies with ETBE, and TAME. Pregnant rats and rabbits gavaged daily with ETBE (100 – 1000 mg/kg/day) from gestational days 6-27 reveal no adverse effects for ETBE on the fetuses exposed prenatally up to 1,000 mg/kg/day, and only a transient decrease in weight was reported for the rabbit dams (Asano et al., 2011, reviewed in de Peyster, 2010). TAME gestational inhalation studies reported NOAELs of 1500 ppm for rat fetuses and 250 ppm

for mice fetuses (Welsh et al, 2003). The mice in this study exhibited significantly reduced fetal body weights, increased cleft palate and enlarged lateral cerebral ventricles when exposed to 1500 and 3500 ppm TAME. No developmental inhalation studies have been published for ETBE and no gavage studies have been published for TAME. Cardiovascular related lesions were not reported for any of the studies discussed above.

1.4 Research Objectives and Hypothesis

The overall objective of this dissertation was to determine the underlying mode of action by which MTBE exerts a toxic effect on the developing vascular system using zebrafish as a model vertebrate. The hypothesis was that vascular lesions observed with MTBE exposure are mediated by the targeted down regulation of VEGF.

The specific aims of the thesis were to:

(1) Characterize the toxicological effects of MTBE, ETBE and TAME on the developing zebrafish

(2) Identify molecular markers associated with the developmental toxicity of each chemical

(3) Use the toxicants to determine sensitive pathways in early embryonic development

(4) Propose a mechanism/mode of action by which MTBE induces vascular lesions

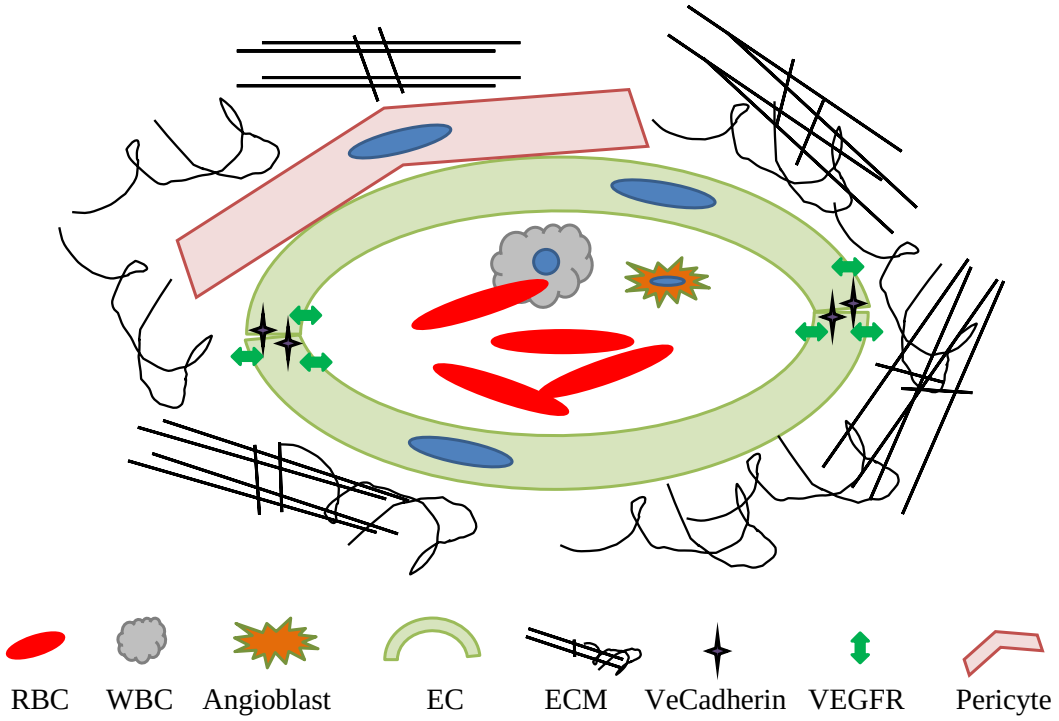

Figure 1.1. Cross-sectional diagram of a capillary. A mature blood vessel is composed of multiple cell types and proteins. The diagram above is a representative figure demonstrating how the different components of a vessel work together. *RBC – red blood cell, WBC – white blood cell, EC – endothelial cell, VEGFR – vascular endothelial growth factor receptor.*

Table 1.1 Proteins involved in HIF1-VEGF regulation of angiogenesis discussed in this thesis.

PROTEIN	FUNCTION	REFERENCE
Hif1-α	transcription factor for hypoxic regulation increases Vegf mRNA transcription and stabilization required for embryonic vascularization	Forsythe *et al*., 1996 Levy *et al.*, 1995 Ryan *et al.*, 1998
PHD	hydroxylation of cytoplasmic HIF1-α	Jaakola *et al.*, 2001
VHL	binds the hydroxylated HIF1-α, promotes ubiquitination and protein degradation	Ohh *et al.*, 2000 Ivan *et al*., 2001
VEGFa	required for blood island formation, angiogenesis, lumen formation, and survival of embryo primary isoform regulating angiogenesis via VEGFR2	Carmielet *et al*., 1996 Ferrara *et al.*, 1996
VEGFc	regulates lymphangiogenesis via VEGFR3 and some angiogenesis via VEGFR2	Lee *et al.*, 1996 Enholm *et al*. 2001
VEGFR1	involved in negative regulation of angiogenesis; lack of VEGFR1 results in death by excessive vascular growth	Kendall & Thomas, 1993 Fong *et al.* 1995
VEGFR2	required in hemangioblast differentiation and angiogenesis primary receptor for VEGFa, upregulated by VEGF	Shalaby et al., 1995
MMP2	gelatinase, activates MMP9 knockouts exhibit reduced vascular growth	Itoh et al., 1998
MMP9	gelatinase, breaks down ECM, is upregulated by VEGF knockouts exhibit increased vascular permeability	Poyer et al., 2009 Kolaczkowska et al., 2006
VE-Cadherin	intercellular junction proteins required for vessel stabilization prohibits vessel disassembly	Carmielet et al., 1999 Crosby et al., 2005
PDGF	attracts pericytes to newly formed capillary	Leveen et al., 1994
WNT	inhibits β-catenin degradation, promotes β-catenin/TCF binding to DNA to upregulate VEGF	Eswaran et al., 2003

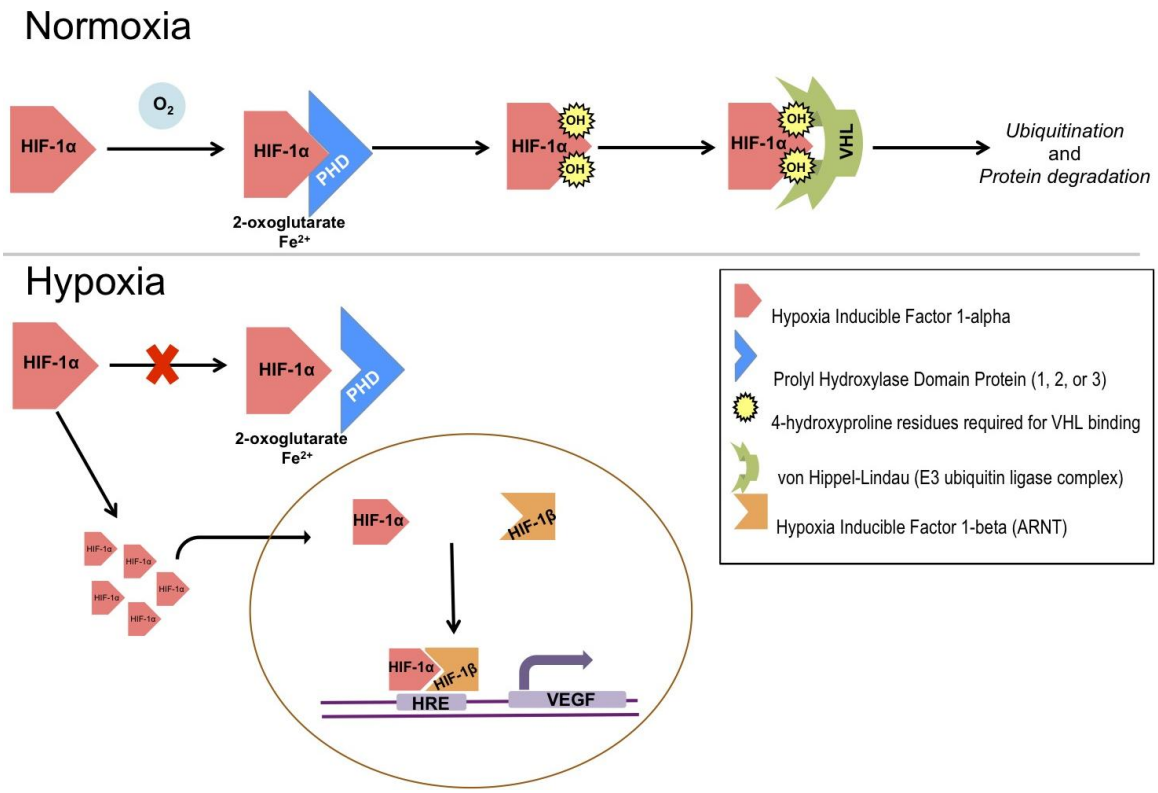

Figure 1.2 HIF-1 post-translational modifications under normoxic or activation under hypoxic conditions. Under normoxic conditions, HIF1-α is hydroxylated, ubiquitinated, and degraded by prolyl-4-hydroxylase domain proteins (PHDs) and von Hippel-Lindau (VHL) protein. Under hypoxic conditions, HIF1-α accumulates and translocates into the nucleus where it heterodimerizes with HIF1-β. Together, HIF1 binds to hypoxic response elements to drive the expression of various genes involved in hypoxia compensatory mechanisms in the cell, including vascular endothelial growth factor (VEGF).

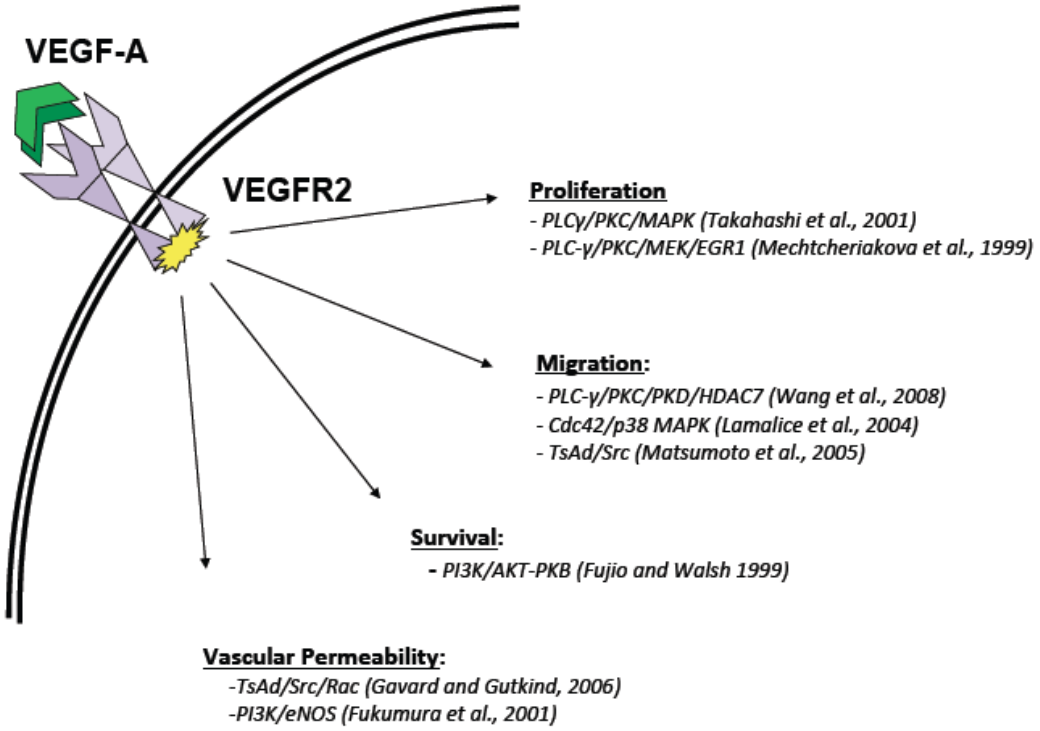

Figure 1.3 Summary of the pathways activated by VEGF-A/VEGFR2 signal transduction. Binding of a VEGF ligand to VEGFR stimulates homo- or hetero-dimerization and autophosphorylation, which in turn induce the signal transduction pathways regulating proliferation, migration, cell survival, and vascular permeability. Abbreviations: *VEGF-A (vascular endothelial growth factor-a); VEGFR2 (vascular endothelial growth factor receptor-2); PLCγ (phospholipase C gamma); PKC (protein kinase C); MAPK (mitogen-activated protein kinase); MEK (mitogen-activated protein kinase/extracellular signal-regulated kinase kinase); EGR1 (early growth response 1); PKD (protein kinase D); HDAC7 (histone deacetylase 7); Cdc42 (cell division cycle 42); TsAd (T-cell specific adaptor); PI3K (phophatidylinositol 3'-kinase); PKB (protein kinase B); eNOS (endothelial nitric oxide synthase).*

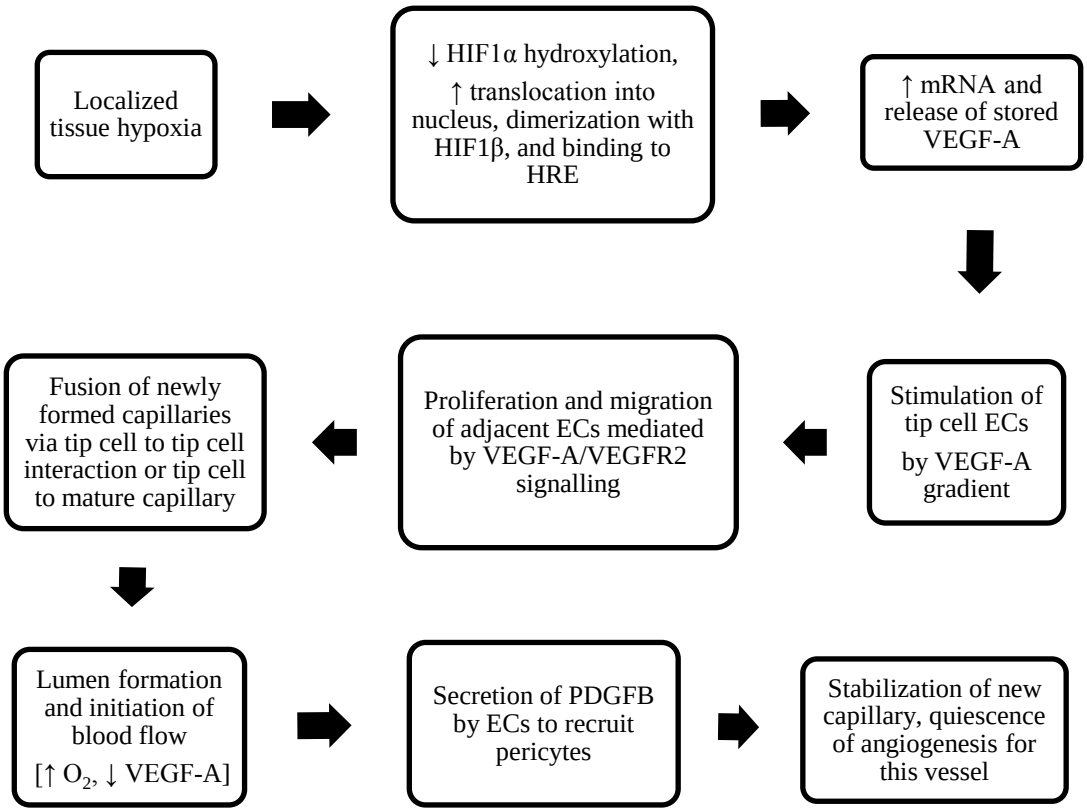

Figure 1.4: Schematic of new capillary formation. Hypoxia in a tissue stimulates the release of pro-angiogenic factors that cause endothelial cells of pre-existing vessels to migrate and proliferate in the direction of the hypoxic tissue. Angiogenesis stops when blood flows through the lumen of the new capillary and transports oxygen to the region in need. Abbreviations: *HIF (hypoxia inducible factor); HRE (hypoxia response element); VEGF-A (vascular endothelial growth factor-a); EC (endothelial cell); VEGFR2 (vascular endothelial growth factor receptor-2; PDGFB (platelet derived growth factor B).*

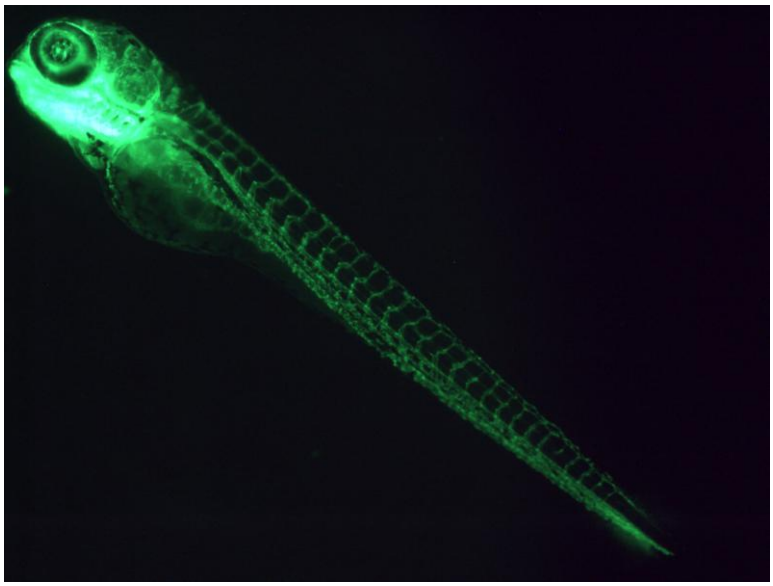

Figure 1.5. Transgenic zebrafish *fli1*-EGFP embryo at 5 days. Fli1s express enhanced green fluorescent protein in all endothelial cells of Fli1s and provides an excellent tool in which to examine morphology of vasculature in live embryos.

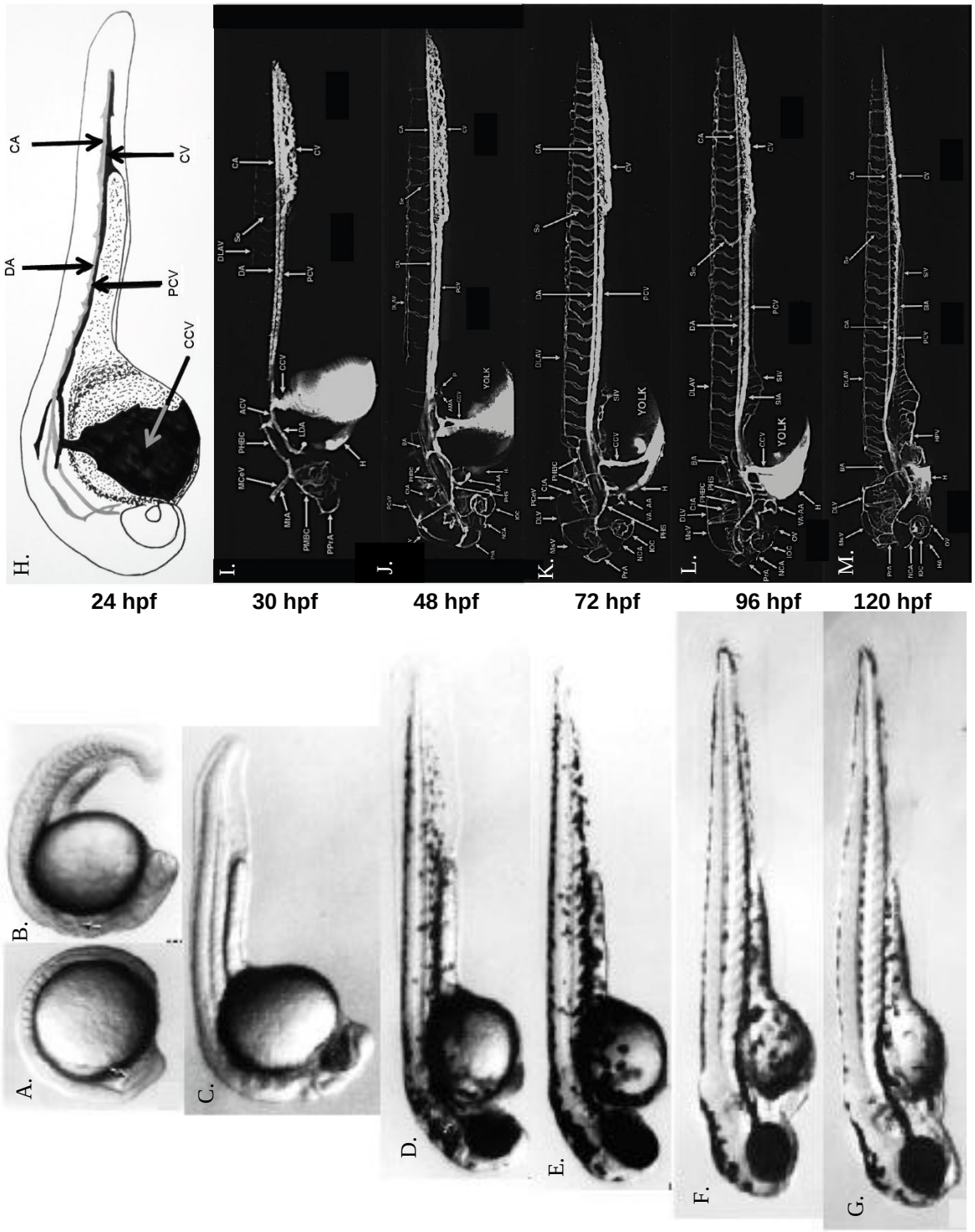

Figure 1.6 Zebrafish stages and timeline of vascular development. All stages are based on development at 25ºC. Embryo stages represented in the figure are A) 6-somites, B) 21-somites, C) Prim-5, D) Prim-25, E) Long Peck, F) Pec Fin, G) Protruding Mouth. A diagram of vasculature in 21-somite embryo (H). Berlin blue dye identifies the vessels with circulation in embryos at the approximate stages of I) Prim-5 J) Prim-25 K) Pec Fin L) Long Pec M) Protruding Mouth. Embryo images B-K are lined up with their approximate hours post fertilization (hpf). The images are adapted from Kimmel et al. 1995 and Isogai et al., 2001. They have been modified from their original format to fit the purposes of this figure.

Table 1.2 Development of the major vascular networks during development in the zebrafish.

6-SOMITES	15 hpf	▪ Intermediate mass precursors commit to hematopoietic stem cell or vascular fate (Liao et al 1997) ▪ Expression of vascular endothelial growth receptor becomes visible in angioblasts (Lawson and Weinstein 2002)
21-SOMITES	24 hpf	▪ Endothelial cells migrate to form the Dorsal Aorta (DA) (Liao et al 1997) ▪ Major vessels of the trunk form
PRIM-5	30 hpf	▪ Heart begins to beat ▪ Most blood cells located in blood island, some move to the rudimental common cardinal veins (CCV) forming across the yolk (Kimmel et al 1995, Isogai et al 2001) ▪ Intersegmental vessel formation begins from DA (Childs et al 2002, Isogai et al 2003)
PRIM-15		▪ DA, Axial vein (AV), Posterior cardinal vein (PCV), and CCV are well-defined (Isogai et al 2001) ▪ Blood slowly circulates ▪ Major vessels of cranium form
PRIM-25	48 hpf	▪ Cartery/vein connection moves distal along tail (Kimmel et al 1995) ▪ CCV is broad and prominent
HIGH PEC		▪ Microvasculature of the head form, continues through 7dpf (Isogai et al 2001) ▪ Blood circulation is strong
LONG PEC		▪ CCV on the yolk is fan-shaped ▪ Circulation through patent cranial vessels ▪ Some circulation in ISVs
PEC FIN	72 hpf	▪ Blood flows in all of the aortic arches and through the subclavian loop (Kimmel et al 1995, Isogai et al 2001) ▪ CCV becomes narrow as it directs blood from PCV rostrally towards the heart ▪ Subintestinal vein forms from cardinal vein (Isogai et al 2001, Childs et al 2002)
PROTRUDING MOUTH	96 hpf	▪ ISVs completely formed (Childs et al 2002, Isogai et al 2003) ▪ Circulation within gills becomes more complex (Kimmel et al 1995) ▪ Early stages of vessel growth in liver and kidney (Isogai et al 2001)

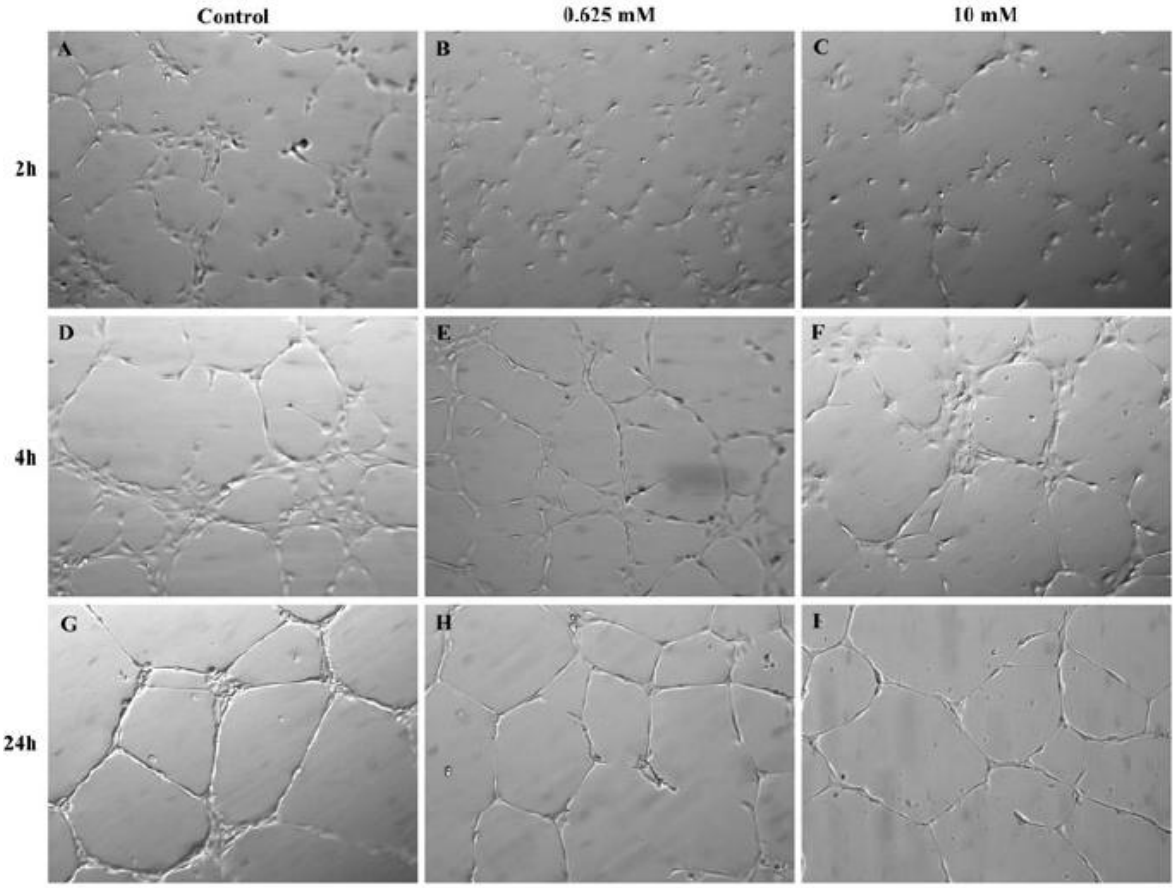

Figure 1.7. MTBE delays initiation of HUVEC tube formation, but not overall network complexity. Representative pictures of HUVEC tube formation time course assay. Untreated control cells A, D, and G, show a clear progression of tube formation form preliminary organization on the Matrigel at 2 h to an elaborate network of capillary rubes at 24 h. MTBE treatments are representative of lowest (0.625 mM: B, E, H) and highest (10 mM: C, F, I) concentrations used for the study. This figure appeared in: J. Appl. Toxicol., 2012, DOI 10.1002/jat.273. Reprinted with permission from the publisher, John Wiley and Sons (License #2902851441655).

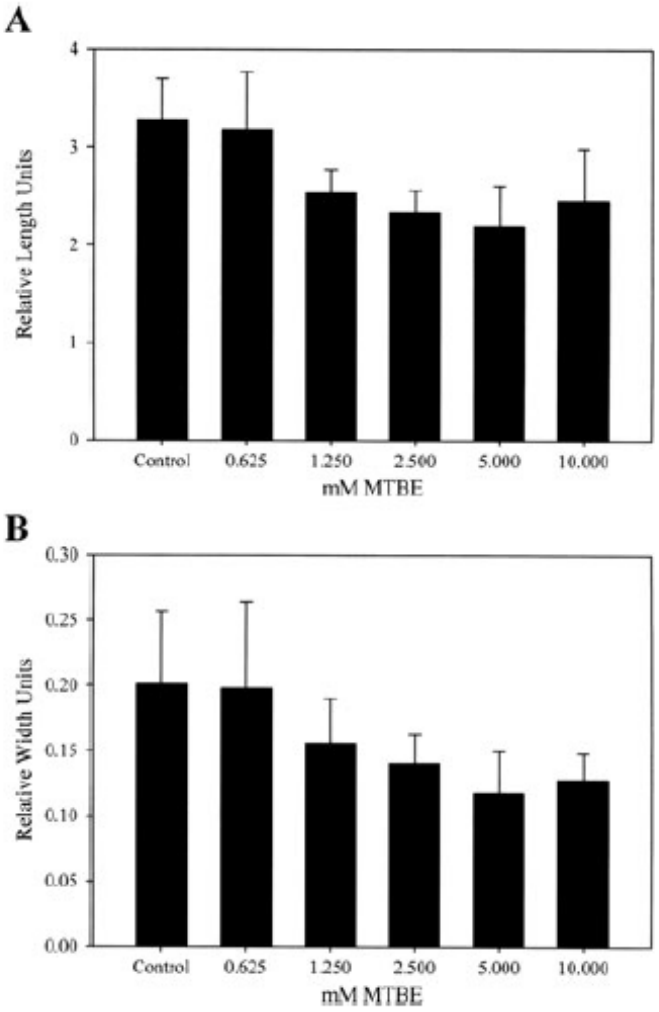

Figure 1.8. The effect of MTBE on HUVEC tube morphometrics. At 24 h, there was not significant difference in the number of tubes per well for any treatment group. There was a significant decreasing trend in the length of tubes formed (A) and tube widths (B). Tubes were measured using Adobe Photoshop measurement tool, and the units are relative. Tube length was measured from the base of one cell projection to another, and the width was the halfway point on the tube. Only tubes for which both ends of the tube were present and measured. The significant trend was determined by one-way analysis of variance ($p < 0.05$), but the Holm-Sidak pairwise comparison ($p < 0.05$) was not significant for any treatment for either length or width. This figure appeared in: J. Appl. Toxicol., 2012, DOI 10.1002/jat.273. Reprinted with permission from the publisher, John Wiley and Sons (License #2902851441655).

Table 1.3: Chemical Properties of Gasoline Oxygenates MTBE, ETBE and TAME.

Chemical	Structure	Molecular Formula	Molecular Weight (g/mol)	Boiling/Melting Point (C°)	Vapor Pressure (mm Hg)	Solubility (per 100g of H20)
Methyl *tert*-butyl ether (MTBE)	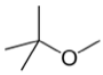	$C_5H_{12}O$	88.15	55/-108	245	4.8g
Ethyl *tert*-butyl ether (ETBE)	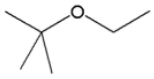	$C_6H_{14}O$	102.18	73/-94	130	1.2g
Tertiary amyl methyl ether (TAME)	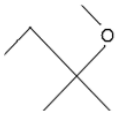	$C_6H_{14}O$	102.18	85/-80	75	1.2g

CHAPTER 2

Methyl tert butyl ether targets developing vasculature in zebrafish (*Danio rerio*) embryos

Josephine A. Bonventre[a,b], Lori A. White[a,b], Keith R. Cooper[a,b]

[a]Rutgers, The State University of New Jersey, Joint Program in Toxicology, United States
[b]Rutgers, The State University of New Jersey, Department of Biochemistry and Microbiology, United States

This manuscript appeared in: Aquatic Toxicology, 2011. 105, 29–40.
Reprinted with permission from the publisher, Elsevier B.V. (License #2823211137788)

Abstract

Disruption of vascular endothelial growth factor (VEGF) signaling during early development results in abnormal angiogenesis and increased vascular lesions. Embryonic exposure to 0.625–10 mM methyl tert butyl ether (MTBE), a highly water soluble gasoline additive, resulted in a dose dependent increase in pooled blood in the common cardinal vein (CCV), cranial hemorrhages and abnormal intersegmental vessels (ISVs). The EC50s for the lesions ranked in terms of likelihood to occur with MTBE exposure were: pooled blood in the CCV, 3.2 mM [95% CI: 2.2–4.7] > cranial hemorrhage, 11 mM [5.9–20.5] > abnormal ISV, 14.5 mM [6.5–32.4]. Organ systems other than the vascular system appear to develop normally, which suggests MTBE toxicity targets developing blood vessels. Equal molar concentrations (0.625–10 mM) of the primary metabolites, tertiary butyl alcohol (TBA) and formaldehyde, did not result in vascular lesions, which suggested that the parent compound is responsible for the toxicity. Stage specific exposures were carried out to determine the developmental period most sensitive to MTBE vascular disruption. Embryos treated until 6–somites or treated after Prim–5

stages did not exhibit a significant increase in lesions, while embryos treated between 6–somites and Prim–5 had a significant increase in vascular lesions ($p \leq 0.05$). During the critical window for MTBE–induced vascular toxicity, expression of vegfa, vegfc, and flk1/kdr were significantly decreased 50, 70 and 40%, respectively. This is the first study to characterize disruption in vascular development following embryonic exposure to MTBE. The unique specificity of MTBE to disrupt angiogenesis may be mediated by the down regulation of critical genes in the VEGF pathway.

2.1. Introduction

The developing cardiovascular system is often a target of chemical toxicants, and cardiovascular defects account for a large percentage of embryo and fetal lethality in lower and higher vertebrates (Mone et al., 2004; Heidman et al., 2005). Organogenesis is closely linked to vascular development because tissue growth is restricted by hypoxia. Formation of the vertebrate closed circulatory system involves both vasculogenesis and angiogenesis. Vasculogenesis is *de novo* blood vessel formation by endothelial cell precursors (angioblasts) derived from progenitor cells (hemangioblasts) in the bone marrow (Choi et al., 1998; Vogeli et al., 2006). Angiogenesis is the development of blood vessels from pre–existing vessels, and is integral to organ growth and repair. Hypoxia–initiated angiogenesis in embryos is mediated by hypoxia inducible factor 1 (HIF1), a heterodimeric transcription factor complex composed of cytoplasmic HIF1–α and nuclear HIF1–β (ARNT) (Ryan et al., 1998; Ramirez–Bergeron et al., 2004). Together, they are responsible for the regulation of hypoxia compensatory mechanisms including the upregulation of a key signaling protein, vascular endothelial growth factor (VEGF) (Levy

et al., 1995; Forsythe et al., 1996; Adelman et al., 1999). VEGF is essential to vasculogenesis, angiogenesis, and hematopoiesis. In mammals, deletion of one vegf allele inhibits blood island formation, angiogenesis, lumen formation, and survival of the embryo (Carmeliet et al., 1996; Ferrara et al., 1996). Multiple VEGF isoforms (VEGF a–d) and vascular endothelial growth factor receptors (VEGFR1/Flt1, VEGFR2/Flk1/KDR, and VEGFR3/Flt4) are required in various combinations for endothelial cell differentiation and migration (Habeck et al., 2002; Covassin et al., 2006; Bahary et al., 2007). Regulation of HIF1, VEGF, and VEGFR in the embryo is crucial to angiogenesis and, therefore, to organogenesis and survival.

Methyl tert butyl ether (MTBE) [$C_5H_{12}O$] is a low molecular weight volatile organic compound (MW 88.15 g/mol) used as a gasoline additive to increase the burning efficiency of fuel in combustion engines. Due to a high water solubility [476 mM, 48 g/L at 25 °C], MTBE can readily contaminate both surface and groundwater at any point in its lifecycle (Brown, 1997; Ahmed, 2001; Squillace and Moran, 2007). As of August 2007, 25 states enacted either complete or partial bans on the use of MTBE in gasoline (US EPA, 2007). Litigation continues over the reparations oil companies were required to pay to municipalities where groundwater supplies were contaminated with MTBE from leaky underground gasoline storage containers. While MTBE use in the US has declined since its peak in the mid-1990s, its use as a gasoline additive continues worldwide (Rosell et al., 2006; Van Wezel et al., 2009). Production of MTBE remains high, averaging just over 1 million barrels per month in 2009 and 2010 (DOE–EIA, 2010).

In humans, MTBE is readily eliminated by expiration or metabolized and excreted in urine (Amberg et al., 2001). Primary metabolism of MTBE in mammals occurs in the

liver through oxidative demethylation by cytochrome P–450 2A6 or 3A4 (Hong et al., 1997, 1999; Le Gal et al., 2001). MTBE oxidation results in the formation of tert–butyl alcohol (TBA) and formaldehyde (Fig. 2.1). Circulating levels of TBA are directly correlated to the MTBE exposure because the tertiary alcohol is metabolized at a much slower rate than MTBE (Amberg et al., 2001).

Other than acute lethality, MTBE's effects on aquatic vertebrates are largely uninvestigated. In a review of early invertebrate and vertebrate LC50 studies, Werner et al. (2001) reported that environmental levels of MTBE were unlikely to cause acute toxic effects in freshwater organisms. LC50s for adult fish were in the 6.8–11.3 mM (600–1000 mg/L) range (Werner et al., 2001; Moreels et al., 2006a; Naddafi et al., 2008). Embryonic exposures to sublethal concentrations of MTBE have thus far been limited to the African catfish (*Clarias gariepinus*) and the Japanese medaka (*Oryzias latipes*). Moreels et al. (2006b) reported that exposure to 0.7–1.3 mM (65–111 mg/L) MTBE reduced the number of viable African catfish embryos at 24 h, decreased survival for 3 day post hatch larvae and led to an increase in craniofacial and spinal abnormalities. In the Japanese medaka embryos, exposure to 10.2 mM (900 mg/L) MTBE resulted in increased prevalence of hypopigmented blood, tail curvature and developmental stage delay, and exposure to 29.5 mM (2600 mg/L) MTBE completely inhibited vascular growth (Longo, 1995).

MTBE is acutely toxic at moderately high concentrations, but the vascular inhibition (Longo, 1995) and developmental lesions (Moreels et al., 2006b) observed in fish embryos occur at lower, sub–lethal concentrations. Here we examined the effect of MTBE on zebrafish embryos (*Danio rerio*) and the developing vascular system.

Embryonic exposure to sub–lethal concentrations of MTBE disrupted angiogenesis and altered VEGF – VEGFR regulation by decreasing transcript levels of vegf–a, vegf–c and flk1/kdr during a critical period of vascular development. This is the first study which explores the vascular disrupting effects of MTBE in an *in vivo* model.

2.2. Materials and methods

2.2.1. Animal handling

Transgenic zebrafish fli1–EGFPs (Fli1s) used for all experiments were obtained from the Zebrafish International Resource Center. Fli1s express enhanced green fluorescent protein driven by the fli1 promoter in all vascular endothelial cells (Lawson and Weinstein, 2002). Expression of EGFP in all endothelial cells of Fli1s allows for *in vivo* examination of vasculature morphology in live embryos. Adults were maintained and bred in an Aquatic Habitat recirculating system on a 14:10 light:dark cycle. Fish system water was maintained between 26 and 28 °C, <0.05 ppm nitrite, <0.2 ppm ammonia, and pH between 7.2 and 7.7. The husbandry (#03– 014) and embryonic exposure protocols (#08–025) were approved by the Rutgers University Animal Care and Facilities Committee. Embryos were raised in 60 µg/mL Instant Ocean in ddH2O (egg water). During exposures, embryos were incubated at 25 °C in an attempt to slow down development. The standard timeline of zebrafish development is based on development at 28.5 °C, but normal development will occur between 25 and 33 °C (Kimmel et al., 1995). The zebrafish stages of development corresponding to hours post fertilization (hpf) for both 25 and 28.5 °C are presented in Table 2.1. The hpf at 25 °C were determined using the conversion equation established by Kimmel et al. (1995): HT = h/(0.055T – 0.57). A

concerted effort was made to ensure that all embryos were at the same stage at the beginning of each experiment.

2.2.2. Chemicals

All chemicals were obtained from Sigma–Aldrich: methyl tert–butyl ether (MTBE) [purity 99.9%], tert–butanol (TBA) [≥99.5%], or Fisher Scientific: Formaldehyde. All chemical solutions were made the day of treatment with aerated egg water.

2.2.3. LC50 studies

Exposures were performed in triplicate at nominal concentrations of 6.25, 12.5, 25, 50, 100 and 200 mM MTBE in sealed glass scintillation vials to avoid volatilization of the chemical (N = 3 vials per concentration, 15 embryos each vial). Exposure began at 3 hpf (512 cell stage) and embryos were observed daily for mortality until 120 hpf. The study was repeated with 6.25, 12.5, 18.75, 25 and 50 mM in triplicate. LC50 and confidence intervals were calculated at 120 hpf using the Litchfield–Wilcoxon method (Litchfield and Wilcoxon, 1949).

2.2.4. Dose-response vial studies

Embryos were exposed individually (N = 20 per treatment) in sealed 4 mL glass vials to static, non–renewal concentrations of 0.625, 1.25, 2.5, 5, and 10 mM nominal concentrations of MTBE, TBA or formaldehyde, and observed under light and fluorescence microscopy. Embryos were observed daily for the 5 day developmental

period characteristic of zebrafish maintained at 25 °C. After hatch, eleutheroembryos (sac–fry) were maintained under the same experimental conditions until 3 day post hatch (dph) observations were made. Three-dph survival was used as a marker of sac fry viability, and is based on normal survival rates of control embryos (Wisk and Cooper, 1990a). Embryos not hatched by 3 dph were considered dead (non–viable). EC50 and confidence intervals for lesion occurrence were determined using the Litchfield–Wilcoxon method (Litchfield and Wilcoxon, 1949). The MTBE, TBA and formaldehyde dose-response studies were each repeated 3 times. A follow up metabolite study used the vial study paradigm to expose embryos to 10 mM TBA, 10 mM formaldehyde, or a mixture of 10 mM TBA and 10 mM formaldehyde (N = 20 per treatment).

2.2.5. Histology

To characterize the lesions histologically, embryos were exposed at the 512 cell stage to 5 mM MTBE. Embryos were selected for fixation at 48, 72 or 96 hpf for histology based on the appearance of a severe lesion. Embryos were fixed over night at room temperature in a solution of 1% formaldehyde, 2% gluteraldehyde, and 1% calcium acetate. Fixed embryos were rinsed with 0.1 M phosphate buffer 4 times and stored in 50% ethanol at 4 °C. Before tissue processing, fixed embryos were stained with 1% osmium tetraoxide. Embryos were further dehydrated with ethanol, then infiltrated with acetone:EPON, and embedded in EPON in BEEM capsules. The EPON resin blocks were trimmed, and thick sections were cut with glass knives. Sections were stained with toluidine blue–O (Gonzalez Santander et al., 1997).

2.2.6. Stage specific exposures

A staggered exposure regime was used to determine the beginning (Study A) and end (Study B) of the critical window for MTBE–induced specific lesions (Fig. 2.2). In Study A, embryos (N = 25) were exposed in individual glass vials to static nonrenewal treatments of 10 mM MTBE at an initial time point: 15, 24, 30, or 48 hpf. In Study B, embryos (N = 25) were treated in individual vials to static nonrenewal treatments of 10 mM MTBE at 3 hpf (time zero) and treatment was discontinued at 15, 24, 30, or 48 hpf. The target time points correspond approximately to the following stages at 25 ◦C: 6–somites (15 hpf), 21–somites (24 hpf), prim–5 (30 hpf), and prim–25 (48 hpf) (Table 2.1). In the third study (Study C, N = 25) embryos were exposed to 10 mM MTBE during the critical period (15 hpf to 30 hpf; 6–somites to prim–5), determined by Study A and B (N = 20 per treatment). Embryos were observed daily under light and fluorescence microscopy for 5 days. Studies A, B and C were each repeated twice. The stage specific exposures were based on previous work with Japanese medaka embryos demonstrating stage specificity following 2,3,7,8–tetrachlorodibenzo–*p*–dioxin exposures (2,3,7,8–TCDD) (Wisk and Cooper, 1990a).

2.2.7. Real–time polymerase chain reaction

Embryos were exposed to a static non–renewal treatment of 0 (control) or 5 mM MTBE until 24 hpf (21–somites) in glass scintillation vials to determine the effect of MTBE on the mRNA expression of key genes associated with angiogenesis. Treatment with 5 mM MTBE was used for these studies because it corresponded to the calculated EC90 for total lesions based on the 3 dose-response studies (2.4). The 21–somite stage

was chosen because it is associated with the formation of the major descending and ascending vessels (Kimmel et al., 1995; Isogai et al., 2001) and an increase in zebrafish vegfa mRNA expression (Liang et al., 1998). Approximately 50 embryos were used per treatment, each treatment was performed in triplicate, and the experiment was repeated three times. Real–time PCR sample preparation was carried out as described in Hillegass et al. (2007). Briefly, embryos were snap frozen in liquid nitrogen at 24 hpf. RNA was isolated (Invitrogen: TRIzol) and DNase treated (Ambion: DNase I [RNase–free]), and cDNA (Biorad: iScript cDNA Synthesis Kit) was made for real–time PCR (Biorad: iQ SYBR Green Supermix). A 2–step qPCR protocol was used: 95–60 °C for 35 cycles, and primer sets were selected to work with the same qPCR protocol. Data were normalized to 28S and quantified using standard curves generated for each primer set. The primer sets were as follows: zf *vegf-a* (NM 131408) fwd 5´–TGC TCC TGC AAA TTC ACA CAA–3´, rev 5´–ATC TTG GCT TTC ACA TCT GCA A–3´, product size 85 bp; zf *vegf-c* (NM 205734) fwd 5´–ATA AAC CAC CCT GCG TGT CTG TCT–3´, rev 5´–TCC TTG CTT GAC TGG AAC TGT GA– 3´, product size 132 bp; zf *flk1/kdr* (NM 001024653) fwd 5´–TCT CCA TAT CCG GGT GTG TGC ATT–3´, rev 5´–TCT GGT ATA TTT CAG GCG TGG CGT–3´, product size 103 bp; zf *hif1-α*–like protein (NM 001012371) fwd 5´–TCT GGT TCT TGA GTG CAG GGT TCT–3´, rev 5´–AGT GGC AGT AGG TGA ACG TCA TGT–3´, product size 119 bp.

2.2.8. Statistical analyses

Statistical analyses were performed using the SigmaPlot version 11 computer software package. Differences in lesion occurrence were determined using Chi–squared

analysis and Fisher exact test. The Student *t*–test was used to determine significance between mRNA levels in MTBE and control groups. The probability level for statistical significance was $p \leq 0.05$.

2.3. Results

2.3.1. MTBE mortality and dose-response studies

In the first LC50 study, embryos were exposed to 6.25, 12.5, 25, 50, 100 and 200 mM MTBE. All embryos in the 50, 100 and 200 mM treatment groups died by 24 hpf (21–somites). In 100 and 200 mM exposed embryos, mortality occurred prior to the segmental phase of development. Development of 50 mM exposed embryos ceased by the 10–somites (17 hpf), but the cranial and caudal regions, normally present at this stage, were not defined. By 120 hpf, 57% of embryos died in the 25 mM triplicates, while in both 6.25 and 12.5 mM MTBE, mortality was less than 20%. In the second LC50 study, embryos were exposed to 6.25, 12.5, 18.75, 25, and 50 mM MTBE. Again, 50 mM exposed embryos died by 10 somites, and mortality was less than 20% in 6.25 and 12.5 mM MTBE. Mortality for 18.75 and 25 mM MTBE were 31 and 49%, respectively. The calculated LC50s and confidence intervals (CI) for both studies were similar (Table 2.2): 19 mM (CI = 15.9–22.3) and 20 mM (CI= 17.9–22.7).

Dose-response studies using sub–lethal concentrations of MTBE (0.625–10 mM) were conducted to characterize the lesions associated with exposure (Table 2.3). Average mortality in both control and treatment groups over the 120 h of development was 5%. Hatching at 120 hpf was reduced in all MTBE treatment groups, but a significant decrease was observed only in the 10 mM treatment group (45% hatched as compared to

80% in control). However, no significant difference in 3 dph survival was observed in any treatment group. The lesions observed with sub–lethal MTBE treatment were consistent with the disruption of vascular development. There was a dose dependent increase in the number of embryos exhibiting pooled blood in the common cardinal vein (CCV), cranial hemorrhages, abnormal intersegmental vessel (ISV) formation, pericardial edema, and reduced circulating red blood cells (RBCs) and other blood formed elements (Table 2.3). At the lowest concentration tested, 0.625 mM, 40% of embryos exhibited at least one vascular related lesion, but was not significantly different from control (15%). However, in both 5 mM (75%) and 10 mM (95%) MTBE treatment groups, significantly ($p \leq 0.05$) more embryos exhibited lesions than in control (15%). Pooled blood in CCV occurred in 50% of embryos exposed to 5.0 mM MTBE and in 75% of embryos exposed to 10.0 mM, which was significantly more than 10% in control. Cranial hemorrhages in MTBE exposed embryos was significant ($p \leq 0.05$) at 10.0 mM, and trended toward significance in 5.0 mM ($p = 0.09$). The concentrations at which the occurrence of abnormal ISVs was significantly different from control ($p \leq 0.05$) were 5.0 and 10.0 mM. The incidence of pericardial edema also increased with dose, but was not significantly increased at any concentration. It is important to note that while 60% of embryos treated with 10 mM MTBE appeared to have a reduction or lack of circulating RBCs, this lesion was often associated with severe hemorrhages, and was considered a result of blood loss into the connective tissue, not an effect on hematopoiesis. However, because the development of endothelial and blood cells are related (Choi et al., 1998; Vogeli et al., 2006), it is possible that MTBE may have an effect on the hematopoietic branch of cardiovascular development. Further, much larger studies would need to be conducted to

determine if the reduction in circulating formed elements was a direct effect of treatment, or secondary to the severe hemorrhages that result from MTBE exposure.

The EC50 for all (total) lesions with continuous embryonic exposure to MTBE is 1.2 mM [95% CI = 0.8–1.8]. EC50s for the individual vascular lesions are reported in Table 2.2. Based on these EC50s, lesions were ranked in terms of likelihood to occur with MTBE exposure: pooled blood in the CCV, 3.2 mM [2.2–4.7] > cranial hemorrhage, 11 mM [5.9–20.5] > abnormal ISV, 14.5 mM [6.5–32.4] > pericardial edema, 20 mM [9.6–41.6].

2.3.2. Characterization of MTBE specific lesions

The predominant lesions observed following MTBE exposure were pooled blood in CCV (the ducts of cuvier), cranial hemorrhages, and abnormal ISVs. Lesions were first apparent at 48 hpf (Prim–25, Table 2.1). Formation of the major descending and ascending vessels, which occurs prior to 48 hpf, does not appear to be disrupted by MTBE. The appearance of a lesion was directly associated with the embryonic stage and phase of cardiovascular development. The MTBE induced lesions occurred at specific developmental time periods, and were often transient, except in incidences where lesions were extremely severe. The dose dependent effect of MTBE on the percentage of embryos with pooled blood in CCV on day 2 of development is presented in Fig. 2.3A. At the Prim–25 stage of zebrafish development, the CCV is a broad vessel that occupies approximately half the surface area of the yolk (Kimmel et al., 1995). Normally, blood cells exit the posterior cardinal vein laterally and flow across the yolk toward the heart in the CCV. In MTBE treated embryos, blood cells pooled in the most ventral portion of the

CCV, and cells were either stagnant or pulsated with heart contractions. Pulsation resulted in a limited number of blood cells entering the heart and therefore entering the circulation. In most individuals, this lesion was absent on day 3, even in the 5.0 mM and 10.0 mM MTBE treatment groups where 70–75% embryos exhibited pooled blood in the CCV on day 2.

Formation of microvasculature in the brain occurs primarily during the Pec Fin through the Long Pec stages of development (Table 2.1, Fig. 2.4A) on day 3 (Isogai et al., 2001). MTBE exposed embryos exhibited cranial hemorrhages as early as day 2, but the lesion occurrence was greatest on day 3, when most of the cranial vasculature was intact. The dose dependent effect of MTBE on occurrence of cranial hemorrhages on day 3 is presented in Fig. 2.3B. Cranial hemorrhages were predominantly in the forebrain/ midbrain region of the head, and the ventricles (Fig. 2.4B). Histological examination of the lesion showed RBCs extravasated into the brain tissue (Fig. 2.4C). The nucleated RBCs did not appear to be undergoing hemolysis (Fig. 2.4D).

The dorsal axial vessels between somites, ISVs, begin as sprouts off the major descending and ascending vessels early in vascular development, but these vessels are not all fully open, or patent, until the protruding mouth stage (Table 2.1) on day 4 (Isogai et al., 2001). Circulation was present through all ISVs in controls on day 4, and blood cells were visible passing through the vessel lumens with light microscopy. Under fluorescence microscopy, patent ISVs had a dim green lumenal area framed by bright green edges (Fig. 2.5A). Areas with poor or absent circulation through somites (observed under light microscopy) were associated with bright green ISVs that lacked the dim green lumen (under fluorescence microscopy). In MTBE treated embryos, circulation is not

present in all ISVs on day 4, and these embryos exhibited ISVs that appeared bright green under fluorescence (Fig. 2.5B). Furthermore, decreased or lack of circulation through the trunk resulted in abnormal formation of the somite muscles in those regions, observed in the day 4 histology of 5 mM MTBE treated embryos. Toluidine blue staining in day 4 controls revealed the characteristic chevron shaped somite, with few gaps in the muscle fibers (Fig. 2.5C). Somites of MTBE treated embryos, which exhibited decreased circulation through ISVs prior to collection on day 4, appear broader than control somites, and the muscle fibers contain regions of vacuolization (Fig. 2.5D and E).

2.3.3. Embryonic exposure to MTBE primary metabolites: TBA and formaldehyde

The vial study paradigm was repeated with equal molar concentrations of TBA or formaldehyde, the primary metabolites of MTBE (Hong et al., 1997, 1999; Le Gal et al., 2001), in order to assess whether the metabolites play a role in the appearance of MTBE specific lesions. No significant lesions were observed at any concentration tested of either metabolite. A follow up study was conducted to test whether or not concomitant exposure to both primary metabolites would induce the vascular lesions observed with MTBE exposure. Embryos were exposed to either 10 mM TBA alone, 10 mM formaldehyde alone, 10 mM TBA and 10 mM formaldehyde together, 10 mM MTBE, or control (no treatment), and observed for daily as previously described. No significant lesions were observed in the TBA alone, formaldehyde alone, or the TBA plus formaldehyde treatments as compared to control. Embryonic exposure to the primary metabolites, alone or concomitantly, did not result in the increased vascular lesions and vascular disruptions that were observed with exposure to the parent compound MTBE (Table 2.3).

2.3.4. Critical periods for embryonic MTBE exposure

Since MTBE associated lesions were not observed prior to 48 hpf and MTBE did not appear to affect the development of the major vasculature structures, the periods of cardiovascular development used for the critical period studies included 4 stages: (1) prior to angioblast migration to midline (15 hpf, 6–somites), (2) major descending/ascending blood vessel formation (24 hpf, 21–somites), (3) the commencement of circulation (30 hpf, Prim–5), and (4) after all major vascular structures are in place and patent (48 hpf, Prim–25). The percent of embryos in Study A or B (Fig. 2.2) that exhibited MTBE specific lesions on developmental days 2, 3 and 4 are presented in Tables 2.4 and 2.5, respectively. Similar to the dose-response study (Section 2.3.1), the vascular lesions occurred on specific days of treatment: pooled blood in CCV on day 2, cranial hemorrhages on day 3, and abnormal ISVs on day 4. In Study A, the embryos exposed to MTBE between 15 and 120 hpf or 24–120 hpf exhibited significantly more lesions ($p \leq 0.05$) than control embryos, while the number of lesions observed in embryos exposed to MTBE between 30 and 120 hpf or 48–120 hpf were not significantly different from controls (Table 2.4). In Study B, all embryos exposed from 0 to 30 hpf and 0–48 hpf had significantly more ($p \leq 0.05$) lesions than control embryos or than the embryos exposed from 0 to 15 hpf and 0–24 hpf (Table 2.5). Together, these studies suggest that the critical period for MTBE induced vascular disruption is between 15 and 30 hpf (the 6 somites and Prim–5 stages).

In order to directly test the proposed critical period, embryos were exposed to 10 mM MTBE from only 15 to 30 hpf (the 6 somites to Prim–5 stages). Embryos exposure during the critical period, exhibited a significant increase in vascular lesions compared to

control (Table 2.6). On developmental days 2, 3 and 4, embryos were no longer in 10 mM MTBE, but 36%, 40%, and 38% of embryos exhibited the MTBE–specific vascular lesions that were present in the embryos treated for the entire developmental period. The critical period for MTBE induced vascular disruption was determined to be between 15 and 30 hpf (the 6 somites and Prim–5 stages).

2.3.5. Expression of vascular specific genes

To determine if the vascular lesions associated with MTBE treatment were related to a disruption in the molecular regulation of angiogenesis, mRNA expression of *vegf-a*, *vegf-c*, *flk1/kdr*, and *hif1-α*–like at 21–somites was quantified by real–time PCR. The 21–somite stage was chosen because it is associated with the formation of the major descending and ascending vessels, which while not affected by MTBE, are required for microvascular angiogenesis (Kimmel et al., 1995; Isogai et al., 2001; Herbert et al., 2009) and an increase in zebrafish *vegf-a* mRNA expression (Liang et al., 1998). The 21–somite stage also corresponds to the middle of the critical period determined in the critical period study (Section 2.3.5). Expression of the primary Vegf isoform, *vegf-a*, as well as the *vegf-c* isoform, was significantly decreased ($p \leq 0.05$) in embryos treated with 5 mM MTBE when compared to controls (Fig. 2.6A and B). Expression of the primary Vegfr, flk1/kdr, was also significantly reduced (Fig. 2.6C). *Vegf-a*, *vegf-c* and *flk1/kdr* were reduced by 50%, 70% and 40%, respectively. MTBE exposure did not affect *hif1-α*–like mRNA transcript levels at 21–somites (Fig. 2.6D).

2.4. Discussion

This study is the first to characterize MTBE toxicity in the developing zebrafish, and the first to investigate the microvascular disrupting effects. All MTBE–induced lesions were related to a disruption in angiogenesis: reduced circulation of RBCs, pericardial edema, pooled blood in the CCV, cranial hemorrhages, and abnormal ISV development (Table 2.3). Chemical-induced cardiovascular toxicity is frequently observed in developing teleosts from a wide variety of compounds (Wisk and Cooper, 1990b; Spitsbergen et al., 1991; Henry et al., 1997; Dong et al., 2004; Incardona et al., 2004; Antkiewicz et al., 2005; Carney et al., 2008; Hillegass et al., 2007; Zhou et al., 2009). However, these effects involve multiple organ systems and are not attributed to a specific targeted cell or organ type. For example, three–ring PAHs caused cardiac malformation and vascular aberrations, and in addition, disrupted kidney, neural tube and cranium development in zebrafish embryos (Incardona et al., 2004). Similarly, 2,3,7,8–tetrachlorodibenzo–*p*–dioxin caused pericardial and yolk–sac edema, necrosis–associated vascular leakage in the cranium, disrupted blood flow in the trunk, decreased heart rate and cranial facial abnormalities (Henry et al., 1997; Dong et al., 2004; Antkiewicz et al., 2005). While vascular aberrations and pericardial edema occurred with MTBE exposure, the alterations in heart rate, cardiac morphology, and cranial facial structure did not. Yolk–sac edema and secondary lesions in the kidney and neural tube were also not present in MTBE treated zebrafish. Nor did the cranial histology (Fig. 2.4B and C) reveal necrosis near the site of hemorrhage. In zebrafish, MTBE specifically targeted developing microvasculature, and is therefore unique among environmental contaminants.

Environmental contamination by MTBE is well documented (Brown, 1997; Irwin, 1997; Ahmed, 2001; Post, 2001; Squillace and Moran, 2007). The LC50s previously reported for adult zebrafish and adult rainbow trout are 7.7 mM (679 mg/L) and 8.7 mM (769 mg/L) MTBE, respectively (Moreels et al., 2006a; Naddafi et al., 2008). In our study, the LC50 for MTBE at 120 hpf in the zebrafish embryo was determined to be 19–20 mM (1675–1763 mg/L) (Table 2.2). The EC50 of MTBE for total lesion occurrence in zebrafish embryos was determined to be 1.2 mM (105 mg/L) (Table 2.2), which is greater than reported MTBE surface water contamination (Irwin, 1997; Post, 2001). Due to the high solubility of MTBE (476 mM, 42 g/L), in certain spill scenarios, much higher concentrations could be obtained in surface waters, which would impact aquatic species at the site of the spill and downstream.

In our studies, neither of the putative primary metabolites, TBA and formaldehyde, resulted in vascular lesions at the same molar concentrations of MTBE that resulted in vascular lesions. MTBE metabolism in zebrafish and other aquatic organisms has not been carried out; however in mammalian systems (Fig. 2.1), TBA and formaldehyde are the primary metabolites (Hong et al., 1997, 1999; Le Gal et al., 2001). Moreels et al. (2006b) reported that exposure to 12.88 mM (955 mg/L) TBA led to an increase in catfish embryo and larval mortality, but not to the craniofacial and spinal abnormalities that were observed in catfish exposed to MTBE. In Japanese medaka, TBA was 3–4 times less toxic than MTBE, and did not inhibit vascular growth (Longo, 1995). In mammals, TBA metabolism to minor metabolites 2–methyl–1,2–propanediol and 2–hydroxyisobutyric acid occurs slowly (Fig. 2.1) (Amberg et al., 2001; Phillips et al., 2008). Formaldehyde is biotransformed to either methanol or formic acid by alcohol

dehydrogenase or aldehyde dehydrogenase, respectively (Du et al., 2005). The presence of these minor metabolites in zebrafish exposed to MTBE, TBA or formaldehyde is unknown. However, the minor metabolites are unlikely to be the cause of the vascular lesions, as they would occur in low concentrations relative to MTBE, and no toxicity was observed following treatment with TBA or formaldehyde. Therefore, the toxic effects that resulted from embryonic exposure to MTBE, were likely mediated by the parent compound, and not the primary or secondary metabolites.

The MTBE specific lesions occurred when embryos were exposed between 15 and 30 hpf (6–somites to Prim–5), which correlates to the beginning of angiogenesis (Table 2.1). In a similar stage stage specific exposure study with Japanese medaka, toxicity of 2,3,7,8–TCDD only occurs after the development of the liver (Wisk and Cooper, 1990a,b). The manifestation of lesions at different developmental periods is explained by ongoing organogenesis (Kimmel et al., 1995). In the zebrafish, the formation of the major descending and ascending blood vessels occurs around 21–somites (24 hpf) and circulation follows the initial heart contractions by Prim–5 (30 hpf). Much of the primary vascularization in the embryo is patent by Prim–25 (48 hpf), the microvasculature of the brain develops by Pec Fin (72 hpf), and the ISVs are patent by the Protruding Mouth stage (96 hpf) (Kimmel et al., 1995; Isogai et al., 2001). The disappearance of the lesions, except in severe cases, may be explained by the ability of the embryo to repair minor to moderate lesions. Hemorrhages observed at 72 hpf (Fig. 2.4) could be a result of poorly developed or delayed cell junctions in the cerebral microvasculature. Loss of the distinct chevron shape of the somite muscle at 96 hpf (Fig. 2.5) was likely a result of poor nutrient and oxygen levels due to abnormal ISVs, and

could partially explain the delayed hatch observed in 10 mM exposed MTBE embryos. The longterm ramifications of the appearance and repair of these lesions at the biochemical and functional tissue level are not known. However, it is likely that alterations in the vascularization of the brain and the muscle could be manifested in focal CNS damage and/or decreased swimming ability. In a preliminary study examining juvenile survival following embryonic exposure to 1.25 mM and 10 mM MTBE, 45 and 75% of juveniles died by 30 dph (Bonventre et al., 2009). Additionally, embryonic MTBE exposure significantly diminished larval touch response at 3 dph (5 mM) and the number of larvae swimming at 5 dph (1.25 mM and 5 mM) (Bonventre et al., 2009). Disruption of angiogenesis at an early embryonic stage impaired organ development and affected post hatch survival.

The vascular lesions resulting from embryonic exposure to MTBE parallel those observed in the vegf morpholino antisense studies. The Vegf-a morphant phenotypically exhibits pericardial edema, no or reduced circulating red blood cells, and aberrant or absent vasculature (Nasevicius et al., 2000). Bahary et al. (2007) evaluated the differences between duplicate Vegf-a genes in the zebrafish (*vegf-aa, vegf-ab*) and found that knockdown of either gene results in a similar disruption of ISVs and increased cranial hemorrhages. Knockdown of either Vegfr2 duplicated genes also results in the inhibition of ISVs (Bahary et al., 2007), a lesion that had been previously reported in a Vegfr2 mutant zebrafish (Habeck et al., 2002). Carmeliet et al. (1996) showed that the Vegf-a knockout in mice was embryonic lethal, however zebrafish morphants survive. Similarly, Vegfr2 knockout mice are embryonic lethal, lacking differentiated angioblasts and any vascular growth (Shalaby et al., 1995). There are several possible reasons for the

species differences. First, zebrafish embryos are smaller and able to diffuse oxygen into tissues from their rearing solutions. Secondly, morpholinos are transient and their ability to knockdown the gene diminishes overtime (Nasevicius and Ekker, 2000). Finally, the duplication of the zebrafish genome means that knocking down one VEGF leaves another functional gene that may compensate for the loss. However, knockdown of both Vegf-aa and Vegf-ab in zebrafish embryos was still not lethal (Bahary et al., 2007), which suggests that other Vegf isoforms, such as Vegf-c, play a greater role in compensating for the loss of Vegf-a in the zebrafish than they do in the mouse model.

The MTBE–induced phenocopy of a Vegf-a–morphant, along with the decreased mRNA of *vegf-a*, *vegf-c,* and flk1/vegfr2 (Fig. 2.6A–C) during the critical period (15–30 hpf), suggests that MTBE vascular toxicity is mediated by dysregulation of the VEGF pathway. The mechanism by which MTBE disrupts Vegf expression is unknown. Several growth factors, oncogenes, and cytokines are known to regulate Vegf expression (reviewed in Ferrara et al., 2003). Developmental pathways that promote transcription of genes involved in the regulation of embryogenesis may be involved in MTBE toxicity. For example, the Wnt canonical pathway, critical to cell growth and tumor development, up–regulates VEGF indirectly by stabilizing β–catenin, which is able to bind the VEGF promoter (Eswaran et al., 2003). β–Catenin also anchors endothelial cell junction protein VE–cadherin to the cytoskeleton, which is important to the integrity and maturation of a vessel (Lampugnani et al., 2006). HIF1 mediation of hypoxia, however, is still the most significant factor governing angiogenesis in the embryo (Ryan et al., 1998; Ramirez–Bergeron et al., 2004). Deletion of Hif1–α in knockout mice is lethal; examination of the knockouts on embryonic day 8.5 revealed a reduced vascular network in the yolk sac,

lack of cephalic vascular development, and reduced numbers of somites (Ryan et al., 1998). The fact that MTBE did not decrease *hif1-α*–like mRNA transcript levels at 21–somites does not exclude HIF1 from a role in the mechanism of MTBE vascular toxicity. Stability of the HIF1-α cytoplasmic component under low oxygen conditions, or the ability of the HIF1-α/HIF1-β heterodimer to bind to the VEGF promoter, are alternative endpoints that may be disrupted by MTBE and would result in decreased vegf expression (Ivan et al., 2001; Wang and Semenza, 1993). Further work is required to understand the underlying mechanism of MTBE disruption of vascular development in the zebrafish embryo.

2.5. Conclusions

MTBE exposure during embryonic development resulted in a unique targeting of the microvasculature angiogenesis, while other organ systems were spared. However, exposure to primary metabolites, TBA and formaldehyde, did not cause the specific vascular lesions observed with exposure to the parent compound: pooled blood in the CCV, cranial hemorrhages, and abnormal ISV development. This suggests that the sub–lethal vascular lesions were a result of MTBE and not its metabolites. Staggered exposure periods during early development demonstrated that exposure between 15 and 30 hpf (the 6–somites to Prim–5 stages) was necessary to produce the vascular lesions that were first visible at 48 hpf (long pec stage). Within the critical window, transcript levels for two isoforms of the primary regulator of angiogenesis, *vegf-a* and *vegf-c*, and the primary receptor *flk1/kdr*, were significantly reduced. MTBE exposure phenocopied the effects observed following morpholino knockdown of Vegf-a morphants (Nasevicius et al.,

2000; Bahary et al., 2007). Together, these data suggest that MTBE–induced vascular disruption of newly formed blood vessels is mediated, at least in part, by the alteration of Vegf – Vegfr regulation in the embryo.

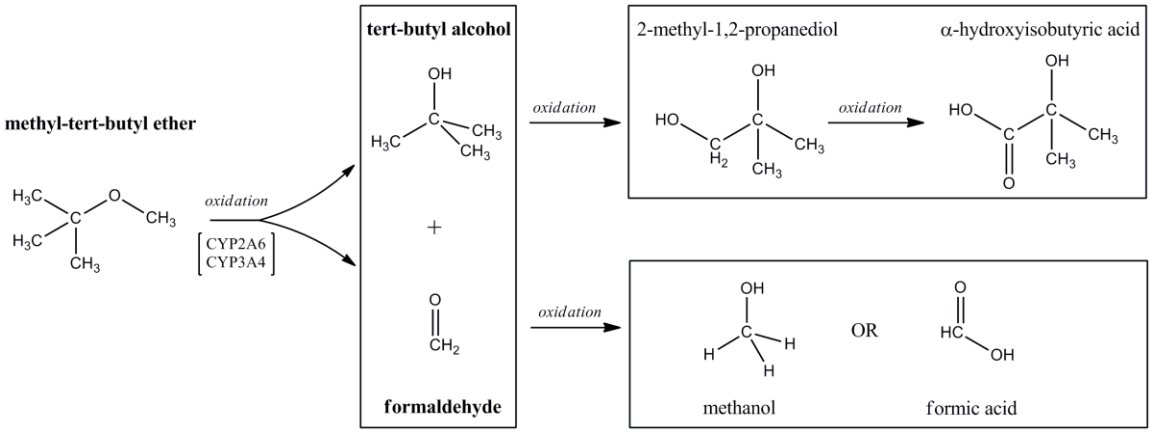

Figure 2.1. Oxidation of MTBE to known vertebrate metabolites. In mammals, MTBE is oxidized by CYP 2A6 and 3A4 to TBA and formaldehyde (Hong et al., 1999; Le Gal et al., 2001). Primary metabolites (bold faced) can be excreted or undergo further oxidation. The enzymes that oxidize TBA to 2–methyl–1,2–propanediol to α–hydroxyisobutyric acid are unknown. Formaldehyde is oxidized to methanol by alcohol dehydrogenase or to formic acid by aldehyde dehydrogenase. Based on Amberg et al. (2001) and Du et al. (2005).

Table 2.1 Developmental stages in the zebrafish embryo as described by Kimmel et al. (1995).

Hours Post Fertilization (hpf)			
28.5 °C	25 °C	Embryo Stage	Description
10	12.4	Bud	Head and tail are distinct
12	14.9	6-somite	Optic primoridium notable, Neural keel formation
14	17.4	10-somite	Rudimentary pronephros
16	19.9	14-somite	Brain subdivisions are distinguishable
19	23.6	21-somite	Angioblasts coalesce at midline to form major vessels
22	27.3	26-somite	Blood island cells differentiate
24	29.8	Prim-5	Heart beats, circulation begins
30	37.3	Prim-15	Primary vessels are patent, CCV is broad across yolk
36	44.7	Prim-25	Brain and trunk vascularization begins
42	52.2	High-pec	Liver primordial, Atrium/Ventricle are distinct in heart
48	59.6	Long-pec	Brain microvasculature is patent, CCV less prominent
60	74.5	Pec fin	Retina fully pigmented, hatching gland prominent
72	89.4	Protruding mouth	All ISVs are patent, circulation through gills begins
96	119.3	Hatch	Free of chorion, limited movement

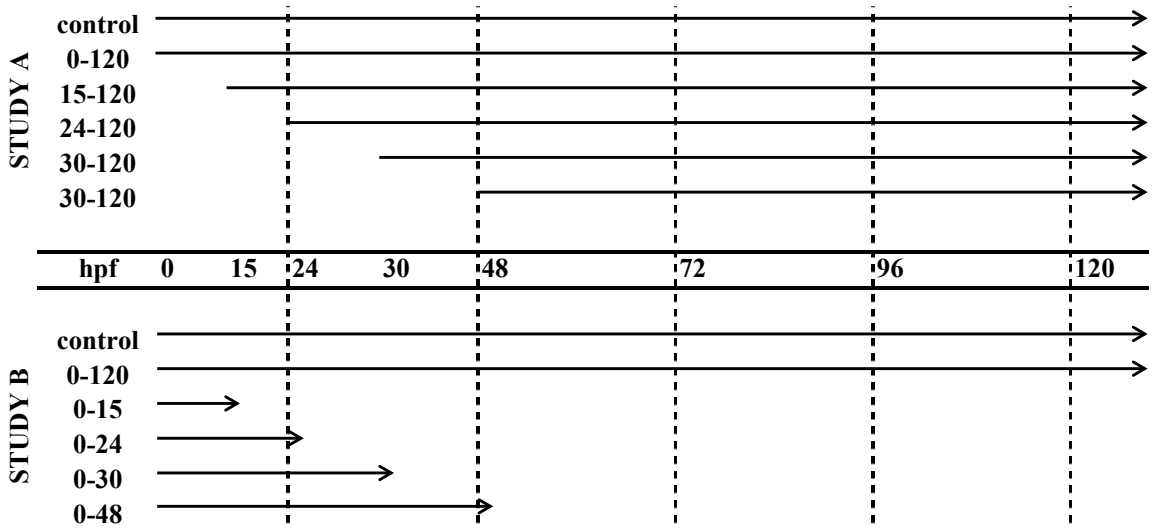

Figure 2.2. Study design schematic for MTBE critical period: Studies A and B. The arrows represent the length of treatment with 10 mM MTBE. The target time points correspond approximately to the following embryonic stages at 25 ◦C: 6–somites (15 hpf), 21–somites (24 hpf), prim–5 (30 hpf), and prim–25 (48 hpf). In Study C, not shown here, embryos were exposed to 10 mM MTBE from only 15 to 30 hpf (6–somites to prim–5).

Table 2.2. Calculated LC50s and EC50s with embryonic MTBE exposure.

	0-120h MTBE Exposure (mM)	95% CI
Mortality (LC_{50}) Study 1	19	15.9 - 22.3
Mortality (LC_{50}) Study 2	20	17.9 - 22.7
Total Lesions (EC_{50})†	1.2	0.8 - 1.8
Individual Lesions (EC_{50})†		
Pericardial Edema	20	9.6 - 41.6
Pooled Blood in CCV	3.2	2.2 - 4.7
Cranial Hemorrhage	11	5.9 - 20.5
Abnormal ISV	14.5	6.5 - 32.4

†Data determined by averaging the three individual MTBE dose-response vial studies

Table 2.3. Percent of embryos exhibiting lesions with MTBE, TBA or formaldehyde exposure.

	Control	0.625mM MTBE	1.25mM MTBE	2.5mM MTBE	5.0mM MTBE	10.0mM MTBE	10.0mM TBA	10.0mM CH_2O	10.0mM TBA+CH2O
All Lesions	15 (± 10)	40 (± 13)	45 (± 8)	45 (± 12)	75 (± 22)*	95 (± 9)*	10 (± 3)	25 (± 15)	20 (± 4)
Death (by 120hpf)	5 (± 6)	5 (± 3)	5 (± 8)	5 (± 3)	5 (± 3)	5 (± 6)	5 (± 6)	5 (± 3)	5 (± 4)
Hatch (at 120hpf)	80 (± 3)	75 (± 26)	60 (± 28)	60 (± 20)	65 (± 24)	45 (± 6)*	60 (± 13)	55 (± 9)	65 (± 11)
3dph Survival	90 (± 5)	85 (± 3)	85 (± 3)	85 (± 0)	85 (± 9)	90 (± 5)	70 (± 13)	80 (± 14)	85 (± 4)
Reduced Circulating RBCs	5 (± 10)	0 (± 0)	5 (± 5)	15 (± 12.5)	45 (± 30)*	60 (± 37.5)*	5 (± 3)	0 (± 0)	5 (± 4)
Pericardial Edema	5 (± 5)	5 (± 5)	5 (± 5)	5 (± 5)	15 (± 10)	35 (± 15)*	5 (± 8)	0 (± 0)	5 (± 7)
Pooled Blood in CCV	10 (± 10)	15 (± 5)	15 (± 5)	20 (± 15)	50 (± 5)*	75 (± 20)*	0 (± 0)	5 (± 5)	5 (± 0)
Cranial Hemorrhage	5 (± 5)	10 (± 5)	15 (± 15)	25 (± 5)	30 (± 5)	45 (± 5)*	5 (± 9)	10 (± 8)	5 (± 0)
Abnormal ISVs	5 (± 5)	15 (± 10)	15 (± 10)	20 (± 10)	35 (± 5)*	60 (± 5)*	5 (± 3)	10 (± 13)	5 (± 7)

Values in the table are percentages ± standard deviation based on the average number of embryos in each category from replicate studies. (N=20)
*Significantly different from control ($P \leq 0.05$).

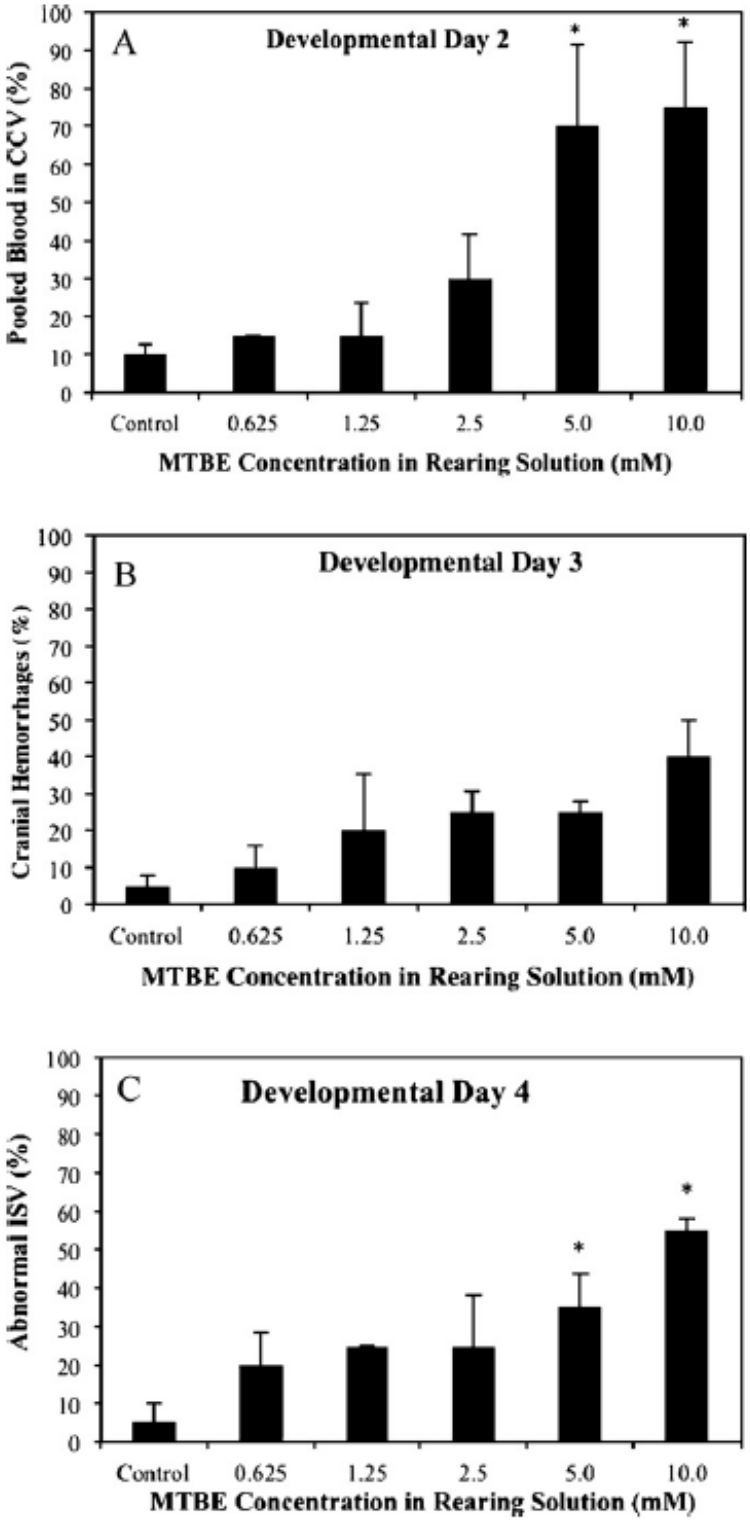

Figure 2.3. Dose dependent effects of MTBE on the percent of embryos exhibiting a specific vascular lesion. (A) Developmental Day 2 begins with the High Pec stage of embryo development. At this stage the CCV is a broad vein across the yolk. With MTBE treatment, blood cells pool in the lower portion of the CCV. The percent of embryos exhibiting this lesion is the higher on day 2 than on other days. (B) Developmental Day 3 begins with the Long Pec stage of embryo development. At this stage the microvasculature of the brain becomes patent. Embryos exposed to MTBE trend toward a dose dependent increase in cranial hemorrhages. (C) By Developmental Day 4, most of the vasculature in the embryo is formed and patent. MTBE treated embryos exhibit a dose dependent increase in abnormal development of ISVs, located between the dorsal somite muscles. *Significantly different from control ($p \leq 0.05$). Data represents the average of three independent MTBE dose-response vial studies.

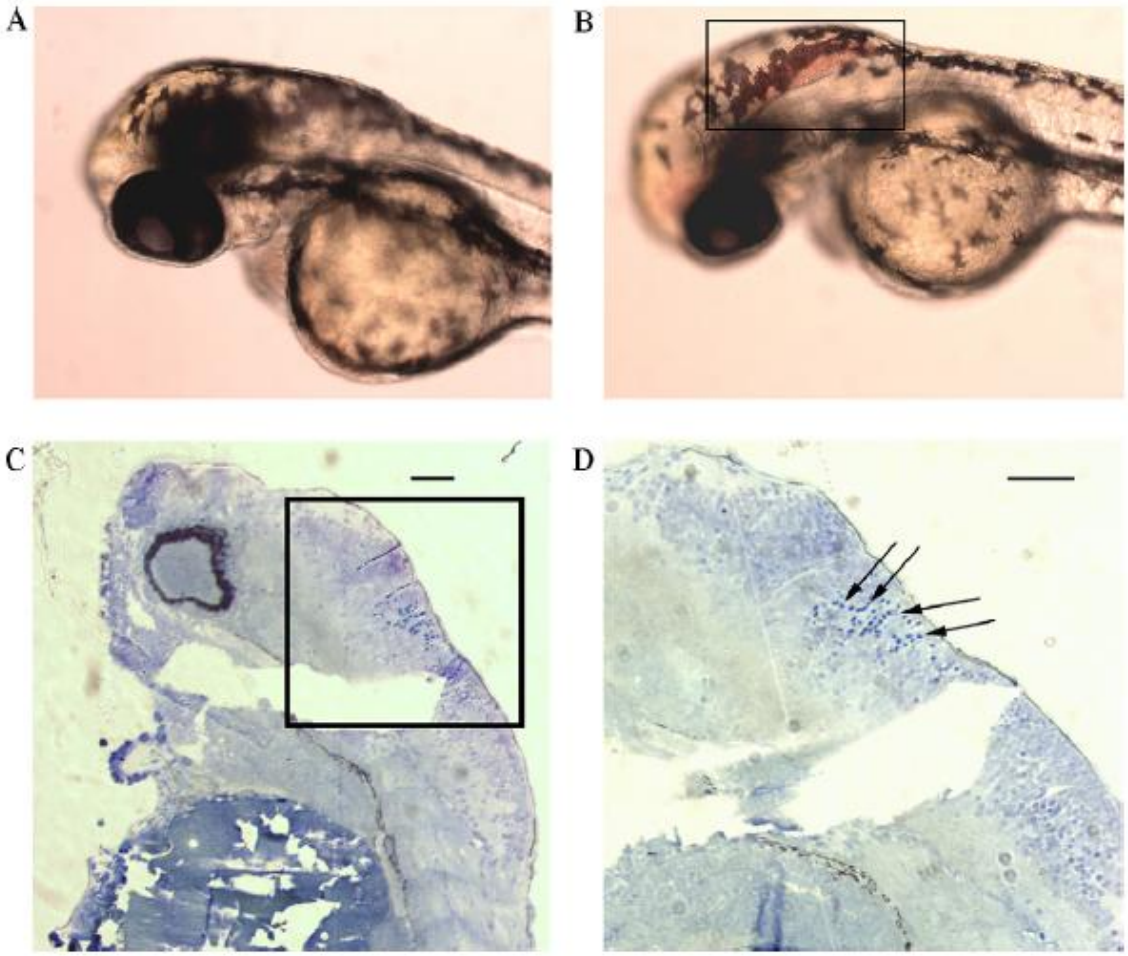

Figure 2.4. Developmental Day 3 (long pec) embryos with (A) normal cranial vascular flow or (B) a cranial hemorrhages in a zebrafish exposed to 10 mM MTBE. Cranial hemorrhages are predominantly present in the forebrain/midbrain region of the head, and the ventricles (10×); black box. (C) Toluidine blue staining in a 72 hpf embryo revealed nucleated RBCs extravasated into the brain tissue (10×); black box. (D) Red blood cells did not appear to be undergoing hemolysis (20×); arrows. Scale bar = 100 µm.

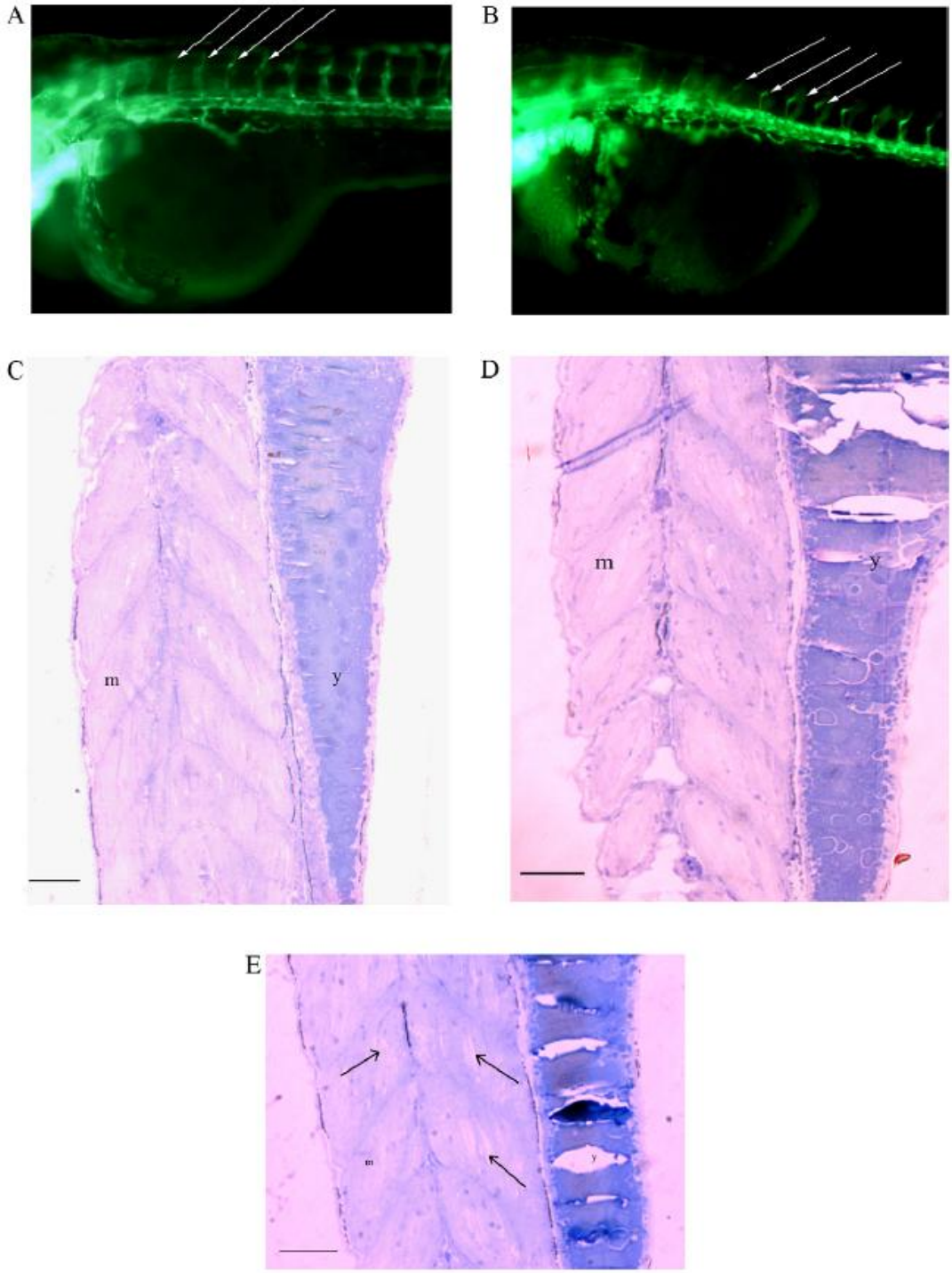

Figure 2.5. Developmental Day 4 (protruding mouth) embryos with (A) fully patent ISVs that appear as bright green edged tubes with a dim green lumenal area in controls (10×) – white arrows; or (B) abnormal ISV which lack proper circulation and appear as bright green vessels lacking a dim lumen in 10 mM MTBE treated embryos (10×) – white arrows. (C) Toluidine blue staining of day 4 control embryos reveals chevron shaped somite muscles; light blue stained tissue above dark blue yolk (20×). (D) Somites in MTBE treated embryos appear rounder and broader than in controls (20×) and (E) muscle fibers appear more disorganized (40×) – black arrows. Scale bar = 100 µm.

Table 2.4. Percent of embryos exhibiting specific lesions on different developmental days in critical period: Study A.

	Duration of Exposure					
Day 2 Lesions	Control	0-120hpf	15-120hpf	24-120hpf	30-120hpf	48-120hpf
Reduced Circulating RBCs	-	16	-	-	-	-
Pericardial Edema	-	-	-	-	-	-
Pooled Blood in CCV	-	44*	36*	32*	16	16
Cranial Hemorrhage	-	-	-	-	-	-
Abnormal ISVs	-	-	-	-	-	-

	Duration of Exposure					
Day 3 Lesions	Control	0-120hpf	15-120hpf	24-120hpf	30-120hpf	48-120hpf
Reduced Circulating RBCs	-	-	4	-	-	-
Pericardial Edema	-	4	-	4	4	-
Pooled Blood in CCV	-	4	-	-	-	-
Cranial Hemorrhage	-	36*	44*	32	28	16
Abnormal ISVs	-	-	-	-	-	-

	Duration of Exposure					
Day 4 Lesions	Control	0-120hpf	15-120hpf	24-120hpf	30-120hpf	48-120hpf
Reduced Circulating RBCs	-	4	4	12	8	4
Pericardial Edema	-	-	-	4	16	-
Pooled Blood in CCV	-	-	-	-	-	-
Cranial Hemorrhage	-	12	12	20	20	12
Abnormal ISVs	-	44*	48*	44*	24	12

Values in table are percentages (N = 25)
*Significantly different from control ($P \leq 0.05$)

Table 2.5. Percent of embryos exhibiting specific lesions on different developmental days in critical period: Study B.

	Duration of Exposure					
Day 2 Lesions	Control	0-120hpf	0-15hpf	0-24hpf	0-30hpf	0-48hpf
Reduced Circulating RBCs	-	8	-	-	4	8
Pericardial Edema	-	-	-	-	-	-
Pooled Blood in CCV	-	32*	-	16	8	24*
Cranial Hemorrhage	-	-	-	-	-	-
Abnormal ISVs	-	-	-	-	-	-

	Duration of Exposure					
Day 3 Lesions	Control	0-120hpf	0-15hpf	0-24hpf	0-30hpf	0-48hpf
Reduced Circulating RBCs	-	4	-	-	4	4
Pericardial Edema	-	8	-	-	-	-
Pooled Blood in CCV	-	4	-	-	4	4
Cranial Hemorrhage	-	36*	12	12	16	28*
Abnormal ISVs	-	-	-	-	-	-

	Duration of Exposure					
Day 4 Lesions	Control	0-120hpf	0-15hpf	0-24hpf	0-30hpf	0-48hpf
Reduced Circulating RBCs	-	8	-	-	4	8
Pericardial Edema	-	4	-	-	-	-
Pooled Blood in CCV	-	-	-	-	-	-
Cranial Hemorrhage	-	8	12	8	16	4
Abnormal ISVs	-	48*	4	20	44*	60*

Values in table are percentages (N = 25)
*Significantly different from control ($P \leq 0.05$)

Table 2.6. Percent of embryos exhibiting lesions in critical period: Study C.

	Day 2 Lesions	Day 3 Lesions	Day 4 Lesions	Total Lesions
Control	6 (± 2)	10 (± 6)	6 (± 6)	12 (± 6)
0-120hpf	68 (± 16)*	54 (± 6)*	50 (± 2)*	74 (± 20)*
15-30hpf	36 (± 4)*	40 (± 12)*	38 (±62)*	60 (± 11)*

Embryos were exposed to 10 mM MTBE during the time period indicated by the hpf.
Values in table are percentages ± range (N = 25). Study repeated twice.
*Significantly different from control ($P \leq 0.05$)

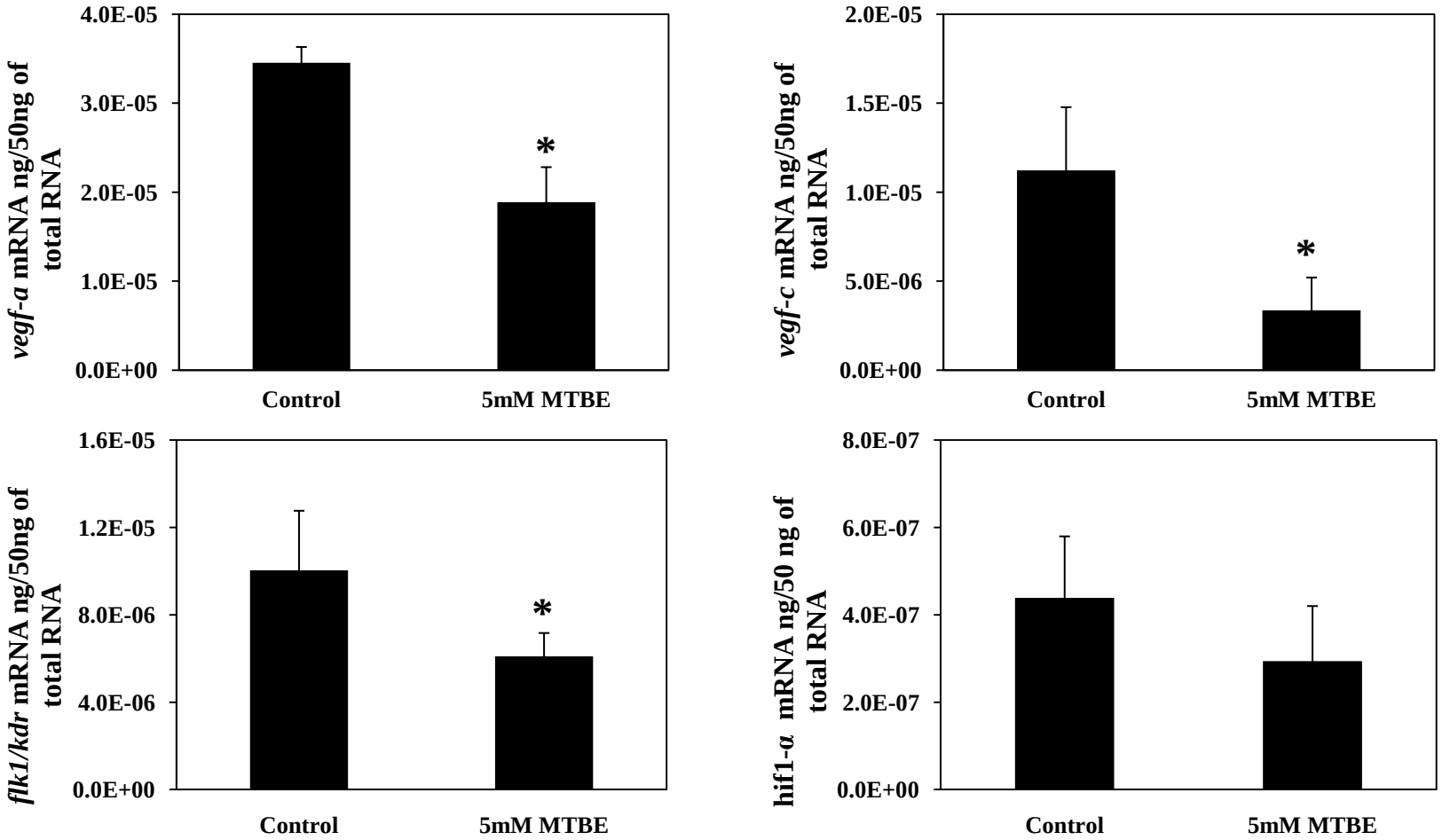

Fig. 2.6. Average mRNA expression of (A) *vegf-a* (B) *vegf-c* (C) *flk1/kdr/vegfr-2* and (D) *hif1*–α–like were determined for zebrafish embryos exposed to 5 mM MTBE at the 512–cell stage and collected for mRNA at 21–somites (N = 3). The graphs are representative of 3 individual experiments. Error bars indicate standard deviation. *Significantly different from control ($p \leq$

CHAPTER 3

Craniofacial abnormalities and altered *wnt* and *mmp* mRNA expression in zebrafish embryos exposed to gasoline oxygenates ETBE and TAME

Josephine A. Bonventre[a,b], Lori A. White[a,b], Keith R. Cooper[a,b]

[a]Rutgers, The State University of New Jersey, Joint Program in Toxicology, United States
[b]Rutgers, The State University of New Jersey, Department of Biochemistry and Microbiology, United States

This manuscript appeared in: Aquatic Toxicology, 2012. In press
Reprinted with permission from the publisher, Elsevier B.V. (License #2923630292700)

Abstract

Gasoline additives ethyl tert butyl ether (ETBE) and tertiary amyl methyl ether (TAME) are used world wide, but the consequence of developmental exposure to these hydrophilic chemicals is unknown for aquatic vertebrates. The effect of ETBE and TAME on zebrafish embryos was determined following OCED 212 guidelines, and their toxicity was compared to structurally related methyl tert-butyl ether (MTBE), which is known to target developing vasculature. LC50s for ETBE and TAME were 14 mM [95% CI = 10 to 20] and 10 mM [CI = 8 to 12.5], respectively. Both chemicals caused dose dependent developmental lesions (0.625 to 10 mM), which included pericardial edema, abnormal vascular development, whole body edema, and craniofacial abnormalities. The lesions were suggestive of a dysregulation of WNT ligands and matrix metalloproteinase (MMP) protein families based on their roles in development. Exposure to 5 mM ETBE significantly ($p \leq 0.05$) decreased relative mRNA transcript levels of *mmp-9* and *wnt3a,* while 2.5 and 5 mM TAME significantly decreased *wnt3a* and *wnt8a*. TAME also significantly decreased *mmp-2* and *-9* mRNA levels at 5 mM. ETBE and TAME were less effective in altering the expression of *vascular endothelial growth factor-a* and *-c,*

which were the only genes tested that were significantly decreased by MTBE. This is the first study to characterize the aquatic developmental toxicity following embryonic exposure to ETBE and TAME. Unlike MTBE, which specifically targets angiogenesis, ETBE and TAME disrupt multiple organ systems and significantly alter the mRNA transcript levels of genes required for general development.

3.1 Introduction

Gasoline oxygenates were originally added to gasoline as octane enhancers following the removal of lead in the 1970s (Ancillotti and Fattore, 1998). Later, oxygenates were used to meet the standards of the Clean Air Act in 1990 (Ahmed, 2001; US EPA, 1990). Methyl tert butyl ether (MTBE) [$CH_3OC(CH_3)_3$] was a popular additive due to its blending properties and storage stability. Two structurally related chemicals, ETBE [$CH_3CH_2OC(CH_3)_3$] and TAME [$CH_3OC(CH_3)_2CH_2CH_3$], are also used as fuel oxygenates. Despite similarities in chemical characteristics (Table 3.1), the limitations put on the use of MTBE in the United States did not extend to ETBE and TAME, which are still used today (Coons, 2009; van Wezel et al., 2009). Neither ETBE nor TAME have been extensively studied for their potential as developmental toxicants.

We previously reported MTBE induces vascular lesions in developing *Danio rerio*, including pooled blood in the common cardinal vein (CCV), cranial hemorrhages, and abnormal intersegmental vessels (ISV), while other tissues appear to develop normally (Bonventre et al., 2011). The vascular lesions occur following an exposure during the 6-somites to prim-25 stages of development, and are associated with a decrease in mRNA transcripts of *vascular endothelial growth factor* (*vegf*) -*a* and -*c* and

vascular endothelial growth factor receptor 2 (*vegfr2*) at the 21-somite stage. Disruption of *vegf* and *vegfr* during development is detrimental to embryogenesis, as it results in dysregulation of angiogenesis, the growth of blood vessels (Carmeliet et al., 1996; Ferrara et al., 1996; Shalaby et al., 1995). The available aquatic toxicity data on ETBE and TAME are limited to acute toxicity studies on fish, daphnia and algae. The MSDS for ETBE reports the LC50 for adult *Cyprinodon variegatus* as >2500 mg/L (24.5 mM), as no published studies have provided the data to establish a true 96 hr LC50 for ETBE (Chevron Philips, 2010). Huttunen et al. (1997) reported no toxic effects to *Oncorhynchus mykiss* treated up to 100 mg/L [0.97 mM] TAME, whereas the American Petroleum Institute (1995) reported the LC50 for adult *Oncorhynchus mykiss* to be 580 mg/L (5.7 mM) TAME. Characterization of ETBE and TAME toxicity to developing aquatic models has not been previously reported.

In mammalian systems, developmental toxicity studies report similar concentrations for effects with MTBE, ETBE, and TAME. Gestational exposure to MTBE via inhalation showed increased fetal resorption in rats and mice at 2500 ppm (28.4 moles/m^3 air), with no effect on the dam (Conaway *et al.*, 1985). In another study, mice exposed to 4000 ppm (45.4 moles/m^3 air) and 8000 ppm (90.8 moles/m^3 air) MTBE exhibited a significant increase in fetal toxicity, post implantation loss, altered sex ratio, craniofacial abnormalities, and skeletal variations, with mild maternal toxicity, even though similar effects were not observed in rabbits (Bevan *et al.*, 1997). Finally, gavaged doses of 500-1500 mg/kg (5.7-17 moles/kg) of MTBE to pregnant Sprague Dawley rats did not result in treatment-related effects in the pups (Kozlosky et al., 2012). Developmental inhalation studies for ETBE have not been published. However, rat and

rabbit developmental studies report no adverse effects to fetuses exposed prenatally up to 1,000 mg/kg/day (9.8 moles/kg/day) ETBE (Asano et al., 2011, reviewed in de Peyster, 2010). TAME gestational inhalation studies reported NOAELs to be 1500 ppm (14.7 moles/m^3 air) for rat fetuses and 250 ppm (2.5 moles/m^3 air) for mice fetuses (Welsh et al, 2003). The mice in this study exhibited significantly reduced fetal body weights, increased cleft palate and enlarged lateral cerebral ventricles when exposed to 1500 ppm (14.7 moles/m^3 air) and 3500 ppm (24.2 moles/m^3 air) TAME. A direct comparison between the developmental effects of the three gasoline oxygenates is complicated due to the various paradigms used and the lack of any study designed to directly compare the three oxygenates.

The aims of the present studies were to: (1) characterize developmental lesions associated with ETBE and TAME exposure in the zebrafish embryos, (2) compare and contrast the toxicity of MTBE to that of the replacement oxygenates, ETBE and TAME and (3) examine gene transcript levels of *vegf*, as well as multiple isoforms from the *wnt* and *mmp* families. WNT signaling plays a major role in early embryogenesis in the form of axis orientation, embryonic stem cell pluripotency, germ layer formation, cell fate specifications, and organogenesis (reviewed in Sokol et al., 2011). WNT ligands bind to cell surface receptors and activate signal transduction pathways that result in targeted gene activation. Matrix metalloproteinases (MMPs), in contrast, are a family of zinc-dependent proteins that cleave extracellular matrix (ECM) components, including collagen, laminin, gelatin, and elastin, to allow for tissue restructuring (reviewed in Zitka et al., 2010). Both WNTs and MMPs are important to normal embryonic development. We hypothesized that structurally related chemicals ETBE and TAME would have

similar toxic effects on the zebrafish embryo due to similarities in chemical structure and characteristics. Our results demonstrate that although MTBE, ETBE, and TAME differ by only one methyl group, they caused significantly different developmental lesions and targeted different genes in normal embryogenesis pathways.

3.2 Methods

3.2.1 Animal Handling

Transgenic zebrafish *fli1*-EGFPs (Fli1s), which express enhanced green fluorescent protein in all vascular endothelial cells (Lawson and Weinstein, 2002), were used for all experiments in order to visualize the developing vascular structures. Fli1s were obtained from the Zebrafish International Resource Center. Breeding stocks were housed in an Aquatic Habitat recirculating system under a 14:10 hour light:dark cycle. Water quality was maintained at <0.05 ppm nitrite, <0.2 ppm ammonia, pH between 7.2 and 7.7, and temperature between 26 and 28°C. Husbandry (#03-014) and embryonic exposure protocols (#08-025) were approved by the Rutgers University Animal Care and Facilities Committee. During exposures, embryos were incubated at 25 °C as previously described, and all embryos were selected at the same stage at the beginning of each experiment (Bonventre *et al.* 2011).

3.2.2 Chemicals

All chemicals were obtained from Sigma Aldrich: ethyl tert-butyl ether (ETBE) [purity 97.0 %], tertiary amyl methyl ether (TAME) [purity 97.0 %], and methyl tert-

butyl ether (MTBE) [purity 99.9 %]. All chemical solutions were made the day of treatment with aerated egg water (60 µg/ml Instant Ocean in double distilled H_2O).

3.2.3 LC50 Studies

Exposures were performed in triplicate at nominal concentrations of 2.5, 5.0, 7.5, 10.0, 12.5, 15.0, 20.0, 25.0, 30.0, and 40.0 mM ETBE or TAME in sealed glass scintillation vials to avoid volatilization of the chemical (N = 3 vials per concentration, 15 embryos each vial). Exposure began at approximately 3 hours post fertilization (hpf) (approximately the 512 cell stage) and embryos were observed daily for mortality until 120 hpf (day 5 of development). ETBE and TAME LC50 studies were carried out separately and were repeated twice. LC50 and 95% confidence intervals were calculated at 120 hpf using the Litchfield-Wilcoxon method (Litchfield and Wilcoxon, 1949).

3.2.4 Dose-Response Vial Studies

Following OECD 212 guidelines, embryos were exposed individually (N = 20 per treatment) in sealed 4 ml glass vials to static, non-renewal concentrations of 0.625, 1.25, 2.5, 5, and 10 mM nominal concentrations of ETBE or TAME. The concentrations used for the dose-response studies were based on sub-lethal concentrations of MTBE (0.625 - 10 mM) established in Bonventre *et al*. (2011). Embryos were observed under light and fluorescence microscopy daily for the 5 day developmental period characteristic of development at 25°C, and eleutheroembryos (sac-fry) survival was observed at 3 day post hatch (dph). On day 3 and 5 (approximately the Pec Fin and Protruding Mouth stages of development), heart rate was measured for each embryo by manually counting the

number of beats for one minute. Since heart rate was not measured in the original MTBE dose-response studies, 20 embryos were exposed individually in vials to 10 mM MTBE, and the heart rate was measured as previously described. EC50 and 95% confidence intervals for lesion occurrence were determined using the Litchfield-Wilcoxon method (Litchfield and Wilcoxon, 1949). ETBE and TAME dose-response studies were each performed twice.

3.2.5 Alcian Blue stain for cranio-facial abnormalities

Embryos (N=10) were exposed as described in the dose-response vial studies and were collected at hatch (5 days post fertilization). Alcian Blue staining and measurements were carried out as described in Hillegass *et al.* (2008). Briefly, embryos were fixed in paraformaldehyde and then incubated in 30% peroxide to decrease pigmentation. Alcian Blue staining was performed overnight and destained in acidified ethanol before being transferred through a gradient of glycerol, up to 100% glycerol, for craniofacial measurements. Pictures were of each embryo taken with a Scion camera, and craniofacial measurements were performed using Adobe Photoshop and converted to μm.

3.2.6 Analysis of mRNA expression by Quantitative Polymerase Chain Reaction (qPCR)

The effect of ETBE or TAME on the relative mRNA transcript levels of key genes involved in early development was determined with qPCR. In order to directly compare these studies with the previously published MTBE zebrafish studies (Bonventre et al., 2011), embryos were exposed to 5 mM ETBE or TAME. Due to the lower LC50 for TAME, an additional concentration of 2.5 mM TAME was also used for the mRNA

expression studies. Embryos were exposed to a static non-renewal treatment of 0 (control) or 5 mM ETBE, 2.5 mM TAME, or 5 mM TAME until 24 hpf (21-somites) in glass scintillation vials. Three individual samples were set up for each treatment group (3 biological replicates), and each sample consisted of approximately 50 pooled embryos. The experiment was repeated three separate times for each chemical (3 experimental replicates). Studies for the different chemicals were performed independently, each with its own control at the time of the experiment.

QPCR sample preparation was carried out as described in Bugel et al. (2010). Briefly, mRNA was isolated using TRIzol® Reagent (Invitrogen), checked for quality (A260/280), and DNase treated with the DNA-*free*™ kit (Ambion®). Reverse transcription to produce cDNA was performed with iScript™ (Bio-Rad) and real-time PCR was performed with SYBER green qPCR methods from Bio-Rad. Primer sets were selected to work with the same qPCR protocol: 35 cycles of 95°C for 15 sec and 60°C for 1 minute. All genes were normalized to the housekeeping gene, 28s ribosomal RNA (Delaunay et al., 2000), and the relative mRNA levels were determined using standard curves. The primer sets for *mmp-2* and *mmp-9* were previously published in Hillegass et al. (2008), and for mmp-13 in Hillegass et al. (2007). Primer sets for *vegf-a* and *vegf-c* were previously published in Bonventre et al., (2011). Primer sets for *wnt3a* and *wnt8a* were created using IDT Primer Quest. All the primer sets are listed in Table 3.2.

3.2.8. Statistical analyses

Statistical analyses were performed using the SigmaPlot version 11 computer software package. Differences in lesion occurrence were determined using the Chi–

Squared Analysis and Fisher Exact Test. The effect of treatment on heart rate at each time point was determined with a One-way Analysis of Variance (ANOVA) with the Holm-Sidak post hoc for ETBE or TAME, and a t-test for 10 mM MTBE. Differences in craniofacial structures were determined using a One-way ANOVA with the Holm-Sidak post hoc or an ANOVA on the Ranks with the Dunn's post hoc test when equal variance was not achieved. Outliers were removed using Grubbs Test for Detecting Outliers on GraphPad. The Student *t*–test was used to determine significance between relative mRNA levels in treatment and control groups for each experimental replicate for MTBE and ETBE. Since the two concentrations of TAME were run concurrently, a One-way ANOVA with the Holm-Sidak post hoc was used to analyze the difference between control and treatments. The probability level for statistical significance was $p \leq 0.05$ for all studies.

3.3. Results

3.3.1 ETBE and TAME Mortality Studies

The calculated LC50s and confidence intervals for ETBE and TAME were based on nominal test concentrations. Embryos were exposed to 2.5, 5.0, 7.5, 10.0, 12.5, 15.0, 20.0, 25.0, 30.0, 40.0 mM of either ETBE or TAME to establish LC50s for each compound. The LC50 studies were repeated twice for each compound and an LC50 was determined for each study separately (Table 3.3). The percentages presented here are the average percent of embryos dead in each treatment group from both LC50 studies. By day 1, (24 hrs post exposure), 100% of embryos were dead in the 30 and 40 mM treatments of ETBE. Development in 30 mM ETBE terminated development at the bud

stage, while embryos in the 40 mM treatment terminated earlier than that, as indicated by total cell necrosis. At the end of a 5 day exposure to ETBE, the average percent of embryos that died in the 5.0 and 7.5 mM treatments was 20%, 30-35% in 10 and 12.5 mM, 40% in 15mM, greater than 60% in 20 mM, and 100% in 25, 30 and 40 mM ETBE. Less than 10% of embryos died in 2.5 mM ETBE by day 5. The lesions that were observed during the LC50 studies with ETBE included enlarged hearts, cranial hemorrhages, and yolk dysmorphogenesis. The calculated LC50s and confidence intervals (CI) for both studies were similar (Table 3.3): 16 mM (CI = 14.9 – 17.2) and 12 mM (CI= 10.9 – 13.2).

The same concentration range was used for the TAME LC50 studies. By day 1, 100% of embryos exposed to 25, 30 and 40 mM TAME were dead. Seventy-five percent of embryos exposed to 20 mM TAME were dead by day 1 and 100% were dead by day 3. At the end of 5 days, less than 10% of the embryos died in 2.5 and 5 mM, 20% in 7.5 mM, 58% in 10 mM, 80% in 12.5 mM, 91% in 15 mM, and 100 % in 20, 25, 30 and 40 mM TAME. The lesions that were observed during the TAME LC50 studies included stage delay (beginning at 10 mM), craniofacial abnormalities, no circulating blood cells, serpentine body structure, decreased pigmentation, and yolk dysmorphogenesis. The calculated LC50s and confidence intervals (CI) for both studies were similar (Table 3.3): 11.2 mM (CI = 10.2 – 12.3) and 8.7 mM (CI= 8.1 – 9.3).

3.3.2 ETBE and TAME Dose-Response Studies

The purpose of the dose-response studies was to compare the toxicity of ETBE and TAME to developing zebrafish to the previously reported toxicity of MTBE

(Bonventre et al. 2011). Embryos were exposed to 0.625 - 10 mM ETBE or TAME, and the lesions associated with exposure were characterized and reported in Tables 3.3 and 3.4. Both ETBE and TAME caused a significant increase ($p \leq 0.05$) in mortality at 5 days post fertilization (dpf) in the 10 mM treatments with an average of 30.8% and 45%, respectively. Significant increases in lesion occurrence began at 1.25 mM for both ETBE (42.5%) and TAME (45%). The EC50 for all (total) lesions with continuous embryonic exposure is 1.7 mM [95% CI = 1.1 – 2.5] ETBE and 1.6 mM [1.1-2.3] TAME (Table 3.3).

Hatching by day 5 was significantly decreased at 10 mM ETBE where only 22.9% of embryos were hatched, compared to 97.5% hatched in control (Table 3.4, 3.5). All concentrations of TAME decreased hatching, but the decrease was statistically significant at both 5 mM (67.5%) and 10 mM (0%). Three day post hatch survival, based on the control hatch time, was significantly reduced with 10 mM of both ETBE (2.6%) and TAME (0%). Embryos exposed to 10 mM TAME did not hatch by 3 dph (8 dpf), the last day of observation. These embryos were severely edematous, dysmorphic, and 90% and showed no signs of circulating red blood cells in the blood (Fig. 3.1f). Exposure to 10 mM TAME also caused a significant stage delay in 100% of the embryos. At 24 hpf, when untreated embryos were at the 21-somite stage, embryos exposed to 10 mM TAME were at the 12-somites, and as a result, were smaller and underdeveloped over the entire development period (5 days). Embryos exposed to 10 mM ETBE also exhibited a significant increase in edema (55% at 10 mM) and a reduction in circulating red blood cells (65%).

Other common lesions induced by ETBE and TAME included pericardial edema (PE), pooled blood in CCV, cranial hemorrhages, abnormal ISVs, and dysmorphic yolks (Table 3.4, 3.5). Embryos exposed to 10 mM ETBE exhibited significantly more PE than controls, 52.5% verses 2.5% (background control). TAME caused a significant increase in PE at 5 mM (40%) and 10 mM (72.5%) as compared to control embryos. Both ETBE and TAME caused a significant increase in the pooling of blood in the CCV, which occurs on 2 dpf (Bonventre et al., 2011). Cranial hemorrhages occurred in at least 20% of the embryos exposed to any concentration of ETBE, but was significantly increased in 5 mM (55%). TAME caused a significant increase of cranial hemorrhages (40%) at 2.5 mM. Effects on the heart were also observed with ETBE and TAME, including a significant decrease in heart rate on day 3 and 4 of development. On day 3, average heart rate was significantly reduced by ETBE (5 and 10 mM) and TAME (1.25 – 10 mM). On day 4, average heart rate was similarly reduced by ETBE (5 and 10 mM) and TAME (1.25, 5 and 10 mM). Embryos treated with 10 mM MTBE had a significantly reduced average heart rate as compared to control on day 3, but by day 4, average heart rate in MTBE animals was no longer significantly different from control. In addition to an effect on heart rate, 10-30% of the embryos in 10 mM treatments of ETBE or TAME exhibited tube hearts or enlarged hearts, but the effect were not significant. Morphological abnormalities of the heart were not observed with MTBE treatment. ETBE also caused an increase, though not significant, in hemorrhages in locations other than the common cardinal vein and the cranium, specifically in different regions of the tail (Fig. 3.1e).

3.3.3 Craniofacial Abnormalities

Abnormal craniofacial structures were observed in the higher concentrations (5 and 10 mM) of the ETBE and TAME dose-response studies. In order to quantify the observation, cartilaginous structures in the embryo were stained with Alcian Blue, and the lengths of three cranial structures were measured: interocular distance, long jaw length, and ceratohyal cartilage length. Since craniofacial abnormalities were not observed with MTBE, only 10 mM MTBE treated embryos were stained and measured for comparison. Both ETBE and TAME caused a significant change in the lengths of the long jaw and ceratohyal cartilage (Table 3.6). In 10 mM TAME treated animals, the formation of both structures was almost completely impeded, with embryos exhibiting only rudimentary and incomplete formation of long jaws and ceratohyal cartilages (Fig. 3.2d). Both structures were also shorter in embryos exposed to 5 mM TAME when compared to controls. At 0.625 mM TAME, embryos exhibited significantly longer ceratohyal cartilage as well as longer long jaws, though the length of the long jaw was not significantly different from control. TAME also significantly decreased interocular distance at 10 mM. ETBE significantly decreased the lengths of the long jaw and the ceratohyal cartilage at both 5 and 10 mM, though to a lesser degree than TAME (Fig. 3.2c). The distribution of the CCL measurements for ETBE and TAME are presented in Fig. 3.3a and b. MTBE did not have an effect on the formation of any of the cartilaginous cranium endpoints used in this study.

3.3.4 Gene expression

At the 21-somites stage, 5 mM TAME induced a statistically significant decrease in *vegf-c* transcript levels (1.94 fold change from control). Although not significant, 5 mM ETBE reduced mRNA transcript levels of *vegf-a* (1.42 fold change from control) and *vegf-c* (1.69 fold), and 5 mM TAME decreased *vegf-a* (1.64 fold). Conversely, 2.5 mM TAME increased both *vegf -a* and *-c* transcript levels (1.74 and 1.30 fold), though not significantly. In comparison, 5 mM MTBE significantly decreases both isoforms greater than 2 fold (Table 3.7). ETBE decreased both *wnts* and all three *mmps*, but statistically decreased transcript levels of *mmp-9* (2.78 fold) and *wnt3a* (4.07 fold). The expression of both *wnt* isoforms was significantly decreased by both 2.5 and 5.0 mM TAME. Both *mmp-2* and *mmp-9* were significantly decreased more than 3.5 fold by 5.0 mM TAME. All three *mmps* were decreased by 2.5 mM TAME, but none significantly (Table 3.7). MTBE did not significantly alter the transcript levels of any of the *wnt* or *mmp* genes tested. MTBE exposure decreased *mmp-9* greater than 2.5 fold, but the effect was not significant (P = 0.081 for all three replicates).

3.4 Discussion

Historically, chemicals with similar structures were presumed to have similar toxic effects. The hypothesis that ETBE and TAME would be toxic to developing vasculature of zebrafish embryos was based on the characterization of MTBE toxicity in both piscine and mammalian model systems (Longo, 1995; Bonventre *et al.*, 2011; Kozlosky *et al.*, 2012). MTBE, ETBE, and TAME are chemically similar (Table 3.1), and on a concentration basis, did not have vastly different LC50s in zebrafish embryos. The

toxicity of the gasoline oxygenates differed in sublethal effects and target tissues. ETBE and TAME are four times more lipophilic than MTBE, and therefore have the potential to be more readily taken up by the embryo. However, the calculated LC50 for ETBE and TAME were one third and one half that of MTBE, respectively. The greater toxicity observed with ETBE and TAME was due to more than their lipophilicity alone. Similarly, different lesions observed at the same concentrations indicated that the toxicities of the three chemicals resulted from different biochemical mechanisms.

We are the first to report developmental LC50s and effects for ETBE and TAME in an aquatic finfish. The LC50s of MTBE, ETBE, and TAME are within the same range, but TAME had the lowest LC50 and the steepest mortality curve. Based on LC50s alone (Table 3.3 and Bonventre *et al.*, 2011), TAME (~9.5 mM) and ETBE (~14.2 mM) were more toxic than MTBE (~19.5 mM). While vascular lesions commonly induced by MTBE were observed with ETBE and TAME exposure, other non-vascular lesions were also present (Table 3.4, 3.5). ETBE and TAME significantly induced whole body edema, craniofacial abnormalities, and both had a greater effect on cardiac development, based on occurrence of pericardial edema and decreased heart rate. The effective concentrations at which the three chemicals caused the various developmental lesions observed with the different studies are shown in Table 3.8. Most of the lesions represented within the table were not observed with MTBE in the range of concentrations tested, and were therefore represented as >10 mM MTBE. Based on the calculated LC50s and the effective concentrations, ETBE toxicity was more similar to MTBE, than was TAME. ETBE exposed embryos exhibited dose dependent vascular lesions similar to those of MTBE exposed embryos (Table 3.3). However, ETBE hemorrhages occurred in parts of the

body that were not observed in MTBE exposed embryos, specifically in the medial caudal region (Fig. 3.1e). Furthermore, all the lesions present in TAME exposed embryos, but not with MTBE (edema, yolk dysmorphogenesis, craniofacial abnormalities), were also present with ETBE exposure, though generally at higher concentrations of ETBE.

Reduced circulating red blood cells (RBCs) was the only lesion in which MTBE, ETBE, and TAME were equally effective at inducing (5 mM). However, since a reduction in circulating formed elements in the blood can be caused by decreased RBC production, increased RBC depletion, and hemorrhages that remove cells from circulation, the physiological mechanism by which all three induce this lesion may differ, making it a less specific lesion from which to draw conclusions. In contrast, cardiac-specific lesions, including tube hearts and decreased heart rates, were more severe in ETBE and TAME than in MTBE, which only caused a decrease in heart rate on day 3. The effect on the heart development may be a consequence of the severe edema observed with ETBE and TAME. Alternatively, ETBE and TAME may induce a direct affect on cardiac development which could then lead to edema or other secondary effects, as has been previously reported with dioxin (Antkiewicz et al., 2005) and PAHs (Incardona et al., 2004).

The lesion unique to TAME in our studies was developmental delay. TAME significantly delayed embryogenesis at 10 mM, while ETBE and MTBE did not. Coupled with the fact that TAME induces all the observed lesions at one-half and one-quarter the concentrations of ETBE and MTBE, and has an LC50 approximately one-half that of MTBE, the conclusion is that TAME is significantly more toxic to developing embryos

and poses a potentially greater risk in a spill scenario. The data for the LC50 and dose-response studies suggest the order of toxicity to developing zebrafish embryos for the three oxygenates to be TAME > ETBE > MTBE.

TAME induced craniofacial abnormalities in zebrafish embryos at a lower concentration than MTBE or ETBE (Table 3.6). In the zebrafish, 10 mM MTBE did not cause craniofacial abnormalities (Table 3.8). It is possible that higher concentrations of MTBE could result in effects on craniofacial development, although based on the morphological observations reported in Bonventre et al. (2011), MTBE did not induce cranial structures deformities in treatments as high as 25 mM MTBE (Bonventre et al., 2011). Craniofacial abnormalities, including cleft palate, were previously reported for mammalian developmental models with MTBE and TAME exposure, but not with ETBE (Bevan et al., 1997, Welsh et al., 2003; Asano et al., 2011). The craniofacial structures measured in our study are similar to cleft palate formation in mammals in that they involve comparable molecular mechanisms, specifically the involvement of both WNTs and MMPs.

The bimodal effect of TAME on long jaw and ceratohyal cartilage lengths in the embryos, significantly increased at 0.625 mM and significantly decreased at 5 mM, suggests multiple mechanisms or targets of TAME in the developing embryo (Table 3.6, Fig. 3.3b). The inhibition of growth by TAME at 5 and 10 mM may be mediated, at least in part, by the significant down regulation of *wnt3a* and *wnt8a* by both 2.5 and 5 mM TAME at 21-somites (Table 3.7). While WNTs play multiple roles in development, WNT signaling in the development of the palate well known. Palatopathogenesis has been associated with WNT inhibition, knockouts, and mutations in rodent and human studies.

Brugmann *et al.* (2007) and Mani et al. (2010) identified a role for WNT signaling in the development of vertebrate facial structures by mapping out the regions of WNT activity in the snout of Wnt-reporter TOPgal and BATgal mice. Correlations between single nucleotide polymorphisms (SNPs) in different WNT isoforms and cleft palate in Brazilian, Chinese, and Polish populations have been reported (Mostowska et al. 2012; Menezes et al., 2010; Yao et al., 2010; Chiquet, et al. 2008). Both ETBE and TAME significantly decrease *wnt3a*, which has been shown in multiple SNP studies to be associated with cleft palate formation.

The decreased mRNA transcripts of *mmp-9* by ETBE and both *mmp-2* and *mmp-9* by 5 mM TAME may also play a role in the cranial cartilage defects. The temporospatial distribution of MMPs, including MMP-2, MMP-9, and MMP-13, has been shown to play a critical role in secondary palate formation during gestational day 12, 13, and 14 in mice (Morris-Wiman et al., 2000). In zebrafish, craniofacial defects induced by glucocorticoids were associated with altered expression and activity of MMP-2, MMP-9, and MMP-13 (Hillegass et al., 2008; Hillegass et al., 2007). Furthermore, the interaction between WNT and MMP pathways may also affect cranial facial formation in the presence of ETBE or TAME. WNT3a protein was shown to upregulate the expression of *MMP-2* mRNA in a human cell culture invasion model, a relationship that may be compromised in an embryo exposed to ETBE or TAME, both of which significantly decrease mRNA levels of *wnt3a* (Planutiene et al. 2011).

While MTBE significantly decreases both *vegf-a* and *vegf-c* expression, neither mRNA transcript level was significantly reduced by ETBE, and TAME significantly reduced only *vegf-c*. These results further support MTBE's specific toxicity, and suggest

the gasoline oxygenates act via different mechanisms. VEGF is essential to the formation of blood vessels and lymphatic vessels. Multiple splice variants and homologous proteins bind to extracellular portions of tyrosine kinase receptors, VEGFRs (Habeck *et al*., 2002; Bahary, *et al.*, 2007; Covassin, *et al.*, 2006). All VEGF ligands and receptors are required in assorted combinations for endothelial cell differentiation and migration, but each has varying capacities as factors in vessel growth. VEGF-c is known to play an important role in lymphangiogenesis (Enholm et al., 2001). The significant reduction in *vegf-c* transcripts at 5 mM TAME, along with the severe edema observed in these animals, may indicate a disruption in lymphangiogenesis. Further studies would be necessary to determine if a direct relationship between TAME and the lymphatic system exists beyond an effect on VEGF-c.

3.5 Conclusions

In summary, short term embryo-sac fry toxicity studies (OECD 212) with nominal concentrations of ETBE and TAME (0.625 mM to 10 mM) yielded a dose-response relationship for multiple developmental lesions. At equal molar concentrations, ETBE and TAME were more toxic than MTBE based on the calculated LC50s and EC50s. MTBE toxicity is specific to angiogenesis (Bonventre et al., 2011), while ETBE and TAME toxicity disrupted the development of multiple organ systems, including the heart, skeletal system, and water regulation. ETBE and TAME were less effective in altering the mRNA expression of *vegf-a* and *vegf-c* compared to MTBE, which significantly decreases the expression of both genes (Bonventre et al., 2011). The significant decrease of *wnts* and *mmps* by ETBE and TAME, but not by MTBE, suggests a possible

mechanism for the general developmental dysfunction observed with ETBE and TAME, and further supports the specificity of MTBE as an anti-angiogenic compound. Although the addition of a methyl group does not drastically alter the chemical characteristics between MTBE, ETBE and TAME (Table 3.1), the toxicity of the three oxygenates on developing zebrafish was different. While MTBE, ETBE and TAME elicit some of the same vascular lesions, the addition and placement of a methyl group in ETBE and TAME resulted in more toxic compounds with different target organ systems. MTBE remains unique in its ability to specifically target the developing vasculature, even when compared to two structurally related chemicals.

Table 3.1: Chemical Properties of Gasoline Oxygenates MTBE, ETBE and TAME.

Chemical	Structure	Molecular Formula	Molecular Weight (g/mol)	Boiling/Melting Point (C°)	Vapor Pressure (mm Hg)	Solubility (per 100g of H20)
Methyl *tert*-butyl ether (MTBE)	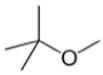	$C_5H_{12}O$	88.15	55/-108	245	4.8g
Ethyl *tert*-butyl ether (ETBE)	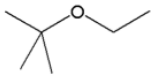	$C_6H_{14}O$	102.18	73/-94	130	1.2g
Tertiary amyl methyl ether (TAME)	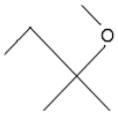	$C_6H_{14}O$	102.18	85/-80	75	1.2g

Table 3.2 Primer sequences used for real-time PCR

Gene	Accession #	Sequences	Product size	Reference (if applicable)
vegf-a	NM_131408	fwd 5'-TGCTCCTGCAAATTCACACAA-3' rev 5'-ATCTTGGCTTTCACATCTGCAA-3'	85 bp	Bonventre et al., 2011
vegf-c	NM_205734	fwd 5'- ATAAACCACCCTGCGTGTCTGTCT-3' rev 5' - TCCTTGCTTGACTGGAACTGTGA - 3'	132 bp	Bonventre et al., 2011
wnt3a	NM_001007185	fwd 5' – ATGGTGTCCCGAGAGTTTGCTGAT- 3' rev 5'- AAGCCCGTGACACTTGCATTTCAG -3'	134 bp	
wnt8a	BC164176	fwd 5' – GGACTACATGGAACTGAAGG -3' rev 5'- CTGTCTCAATCCTCCTCTCTT – 3'	130 bp	
mmp-2	NM_198067	fwd 5'-AGCTTTGACGATGACCGCAAATGG -3' rev 5'-GCCAATGGCTTGTCTGTTGGTTCT-3'	224 bp	Hillegass et al., 2008
mmp-9	NM_213123	fwd 5'-AACCACCGCAGACTATGACAAGGA-3' rev 5'-GTGCTTCATTGCTGTTCCCGTCAA-3'	89 bp	Hillegass et al., 2008
mmp-13	BC065591	fwd 5'-ATGGTGCAAGGCTATCCCAAGAGT-3' rev 5'-GCCTGTTGTTGGAGCCAAACTCAA-3'	289 bp	Hillegass et al., 2007

Table 3.3 Calculated LC50 and EC50s for ETBE and TAME

	0-120 hpf ETBE Exposure (mM)	95% CI	0-120 hpf TAME Exposure (mM)	95% CI
Mortality (LC_{50}) Study 1[¥]	16	14.9 - 17.2	11.2	10.2 - 12.3
Mortality (LC_{50}) Study 2[¥]	12	10.9 - 13.2	8.7	8.1 - 9.3
Total Lesions (EC_{50})[♯]	1.7	1.1 - 2.5	1.6	1.1 - 2.3
Individual Lesions (EC_{50})[♯]				
Pericardial Edema	9.5	6.1 - 14.8	6	4.1 - 8.8
Pooled Blood in CCV	4.2	2.9 - 6.1	4.1	3.1 - 5.5
Cranial Hemorrhage	10	4.9 - 20.6	4.8	2.8 - 8.2
Abnormal ISV	8.5	5.4 - 13.3	3.8	2.2 - 6.4
Edema	7.5	5.1 - 11.1	9	5.9 - 13.8

¥ Group exposure: N =15, 3 replicates per concentration

♯ Individual exposure: Average of 2 individual studies, N=20 for each concentration

Table 3.4 Percent of embryos exhibiting lesions with ETBE exposure.

	Control	0.625mM ETBE	1.25mM ETBE	2.5mM ETBE	5.0mM ETBE	10.0mM ETBE
All Lesions	10 (± 5)	25 (± 15)	42.5 (± 2.5)*	56.3 (± 3.7)*	90 (± 10)*	85 (± 15)*
Death (by 120hpf)	0 (± 0)	0 (± 0)	5 (± 5)	5 (± 0)	7.5 (± 2.5)	30.8 (± 0.8)*
Hatch (at 120hpf)	97.5 (± 2.5)	95 (± 0)	90 (± 10)	95 (± 2.5)	90 (± 0)	22.9 (± 7.1)*
3dph Survival	97.5 (± 2.5)	96 (± 0)	91 (± 10)	97.5 (± 2.5)	90 (± 0)	2.6 (± 2.6)*
Reduced Circulating RBCs	0 (± 0)	0 (± 0)	2.5 (± 2.5)	10 (± 0)	37.5 (± 7.5)*	65 (± 25)*
Pericardial Edema	2.5 (± 2.5)	0 (± 0)	0 (± 0)	10 (± 5)	27.5 (± 17.5)	52.5 (±7.5)*
Pooled Blood in CCV§	2.5 (± 2.5)	5 (± 5)	10 (± 10)	25 (± 5)	55 (± 25)*	72.5 (± 22.5)*
Cranial Hemorrhage§	2.5 (± 2.5)	20 (± 15)	20 (± 5)	22.5 (± 2.5)	52.1 (± 17.5)*	30 (± 5)*
Abnormal ISVs§	2.5 (± 2.5)	0 (± 0)	10 (± 5)	15 (± 5)	17.5 (± 12.5)	65 (± 10)*
Edema	2.5 (± 2.5)	2.5 (± 2.5)	15 (± 10)	30 (± 10)	27.5 (±17 5)	55 (± 0)*
Yolk Dysmorphogenesis	0 (± 0)	0 (± 0)	0 (± 0)	0 (± 0)	15 (± 10)	65 (± 5)*

Values in the table are percentages (± range) based on the average number of embryos in each category from replicate studies. (N=20)
*Significantly different from control ($P \leq 0.05$). § MTBE-induced vascular lesion

Table 3.5 Percent of embryos exhibiting lesions with TAME exposure.

	Control	0.625mM TAME	1.25mM TAME	2.5mM TAME	5.0mM TAME	10.0mM TAME
All Lesions	7.5 (± 7.5)	20 (± 15)	45 (± 15)*	70 (± 5)*	92.5 (± 2.5)*	90 (± 10)*
Death (by 120hpf)	2.5 (± 2.5)	0 (± 0)	2.5 (± 2.5)	2.5 (± 2.5)	7.5 (± 7.5)	45 (± 35)*
Hatch (at 120hpf)	92.5 (± 2.5)	87.5 (± 2.5)	85 (± 10)	82.5 (± 7.5)	67.5 (± 2.5)*	0 (± 0)*
3dph Survival	97.5 (± 7.5)	87.5 (± 7.5)	87.5 (± 7.5)	92.5 (± 2.5)	67.5 (± 2.5)	0 (± 0)*
Reduced Circulating RBCs	0 (± 0)	2.5 (± 2.5)	10 (± 0)	25 (± 10)	65 (± 15)*	90 (± 10)*
Pericardial Edema	0 (± 0)	2.5 (± 2.5)	12.5 (± 2.5)	12.5 (± 2.5)	40 (± 7.5)*	72.5 (± 27.5)*
Pooled Blood in CCV[§]	2.5 (± 2.5)	7.5 (± 2.5)	17.5 (± 2.5)	27.5 (± 2.5)	72.5 (± 2.5)*	27.5 (± 22.5)
Cranial Hemorrhage[§]	2.5 (± 2.5)	10 (± 5)	25 (± 10)	40 (± 10)*	32.5 (± 5)*	7.5 (± 7.5)
Abnormal ISVs[§]	0 (± 0)	12.5 (± 2.5)	20 (± 5)	32.5 (± 12.5)*	65 (± 5)*	15 (± 15)
Yolk Edema	0 (± 0)	0 (± 0)	5 (± 0)	10 (± 0)	50 (± 0)*	90 (± 10)*
Yolk Dysmorphogenesis	0 (± 0)	0 (± 0)	0 (± 0)	0 (± 0)	92.5 (± 7.5)*	62.5 (± 37.5)*

Values in the table are percentages (± range) based on the average number of embryos in each category from replicate studies. (N=20)
*Significantly different from control ($P \leq 0.05$). § MTBE-induced vascular lesion

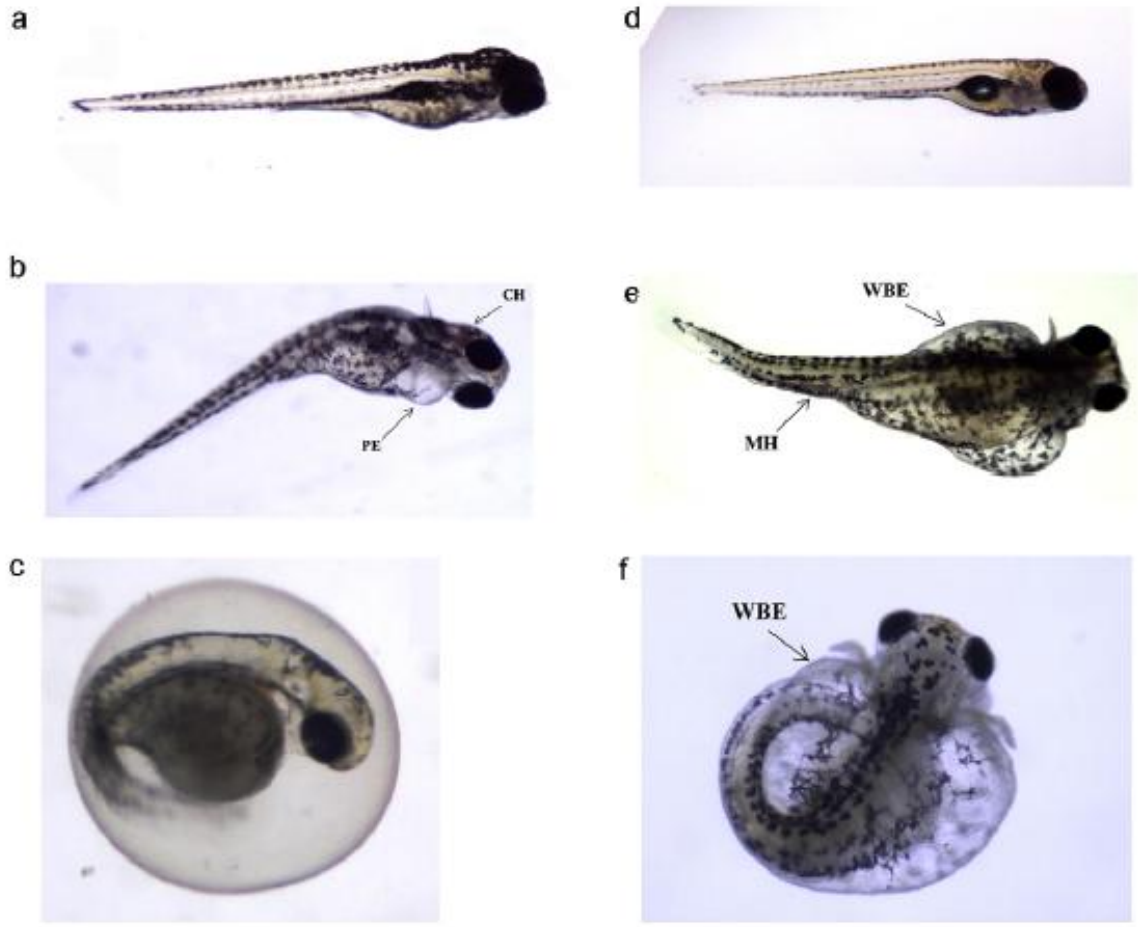

Figure 3.1 The effect of ETBE and TAME on morphological endpoints in zebrafish embryos. A-C: Representative pictures of embryos at 120 hpf for control (A), 10 mM ETBE (B), and 10 mM TAME (C). D-F: Representative pictures of embryos at 3 dph for control (D), 10 mM ETBE (E), and 10 mM TAME (F). PE = Pericardial Edema, CH = Cranial Hemorrhage, WBE = Whole Body Edema, MH = Miscellaneous Hemorrhage.

Table 3.6 Exposure to ETBE or TAME results in craniofacial abnormalities in zebrafish

	mM	Interocular Distance	Long Jaw Length	Ceratohyal Cartilage Length
Control	0	156.5 (± 21.4)	480.3 (± 20.9)	294.8 (± 26.6)
MTBE	10.0	157.8 (± 24.9)	479.6 (± 32.2)	315.3 (± 31.7)
ETBE	0.625	151.0 (± 11.3)	462.8 (± 8.9)	292.3 (± 17.4)
	1.25	145.5 (± 7.7)	466.6 (± 15.6)	297.0 (± 8.3)
	2.5	145.6 (± 5.3)	463.5 (± 6.2)	289.7 (± 13.3)
	5.0	148.4 (± 6.0)	433.3 (± 12.6)*	265.3 (± 8.2)*
	10.0	156.6 (± 10.6)	309.3 (± 33.1)*	170.6 (± 36.3)*
TAME	0.625	172.1 (± 31.2)	506.0 (± 40.5)	342.4 (± 21.2)*
	1.25	152.7 (± 18.9)	480.4 (± 25.3)	308.5 (± 25.6)
	2.5	164.8 (±16.5)	483.8 (± 24.5)	318.1 (±18.0)
	5.0	154.0 (± 24.8)	379.7 (± 59.3)*	227.7 (± 46.6)*
	10.0	95.0 (± 44.7)*	n.a.	n.a.

Numbers represent the average length of the structure (μm) from an N of 10. Significance determined by ANOVA ($p \leq 0.05$). *Significantly different from control. LJL and CCL for 10 mM TAME are represented as n.a. because the structures were not formed in the embryos and could therefore not be measured.

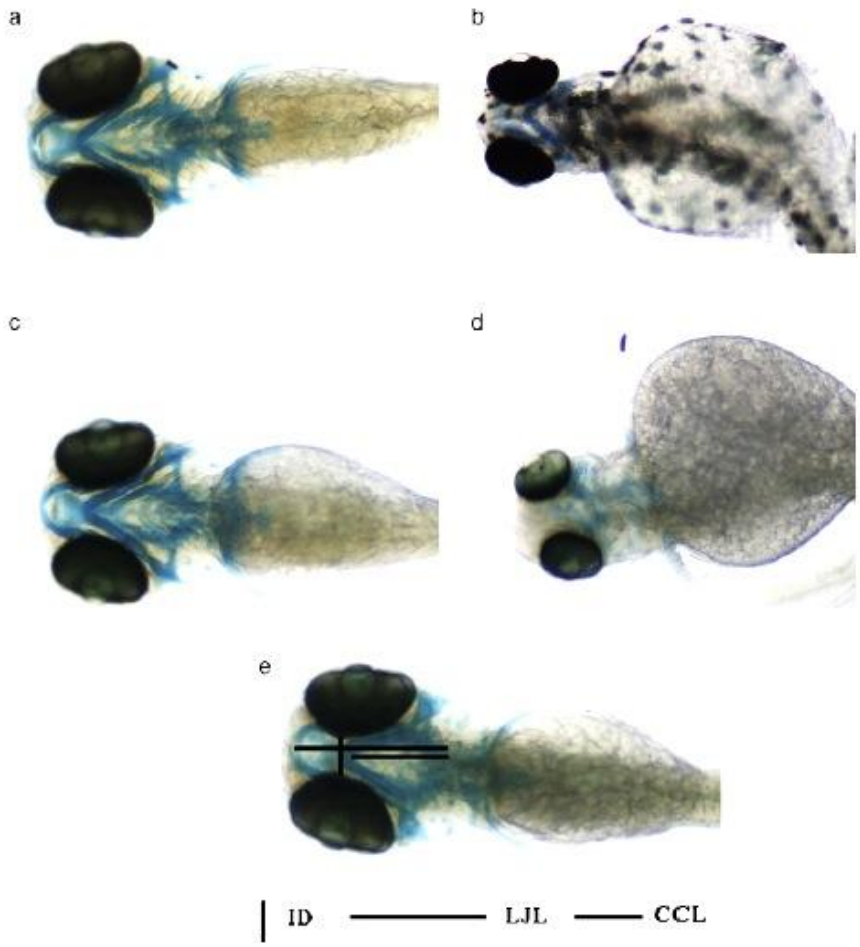

Figure 3.2 Alcian blue stain of craniofacial structures in the 5 dpf embryo. A-D: Representative pictures of embryos at 5 dpf for control (A), 10 mM ETBE (B) 10 mM MTBE (C), and 10 mM TAME (D). Craniofacial measurement description in panel E.

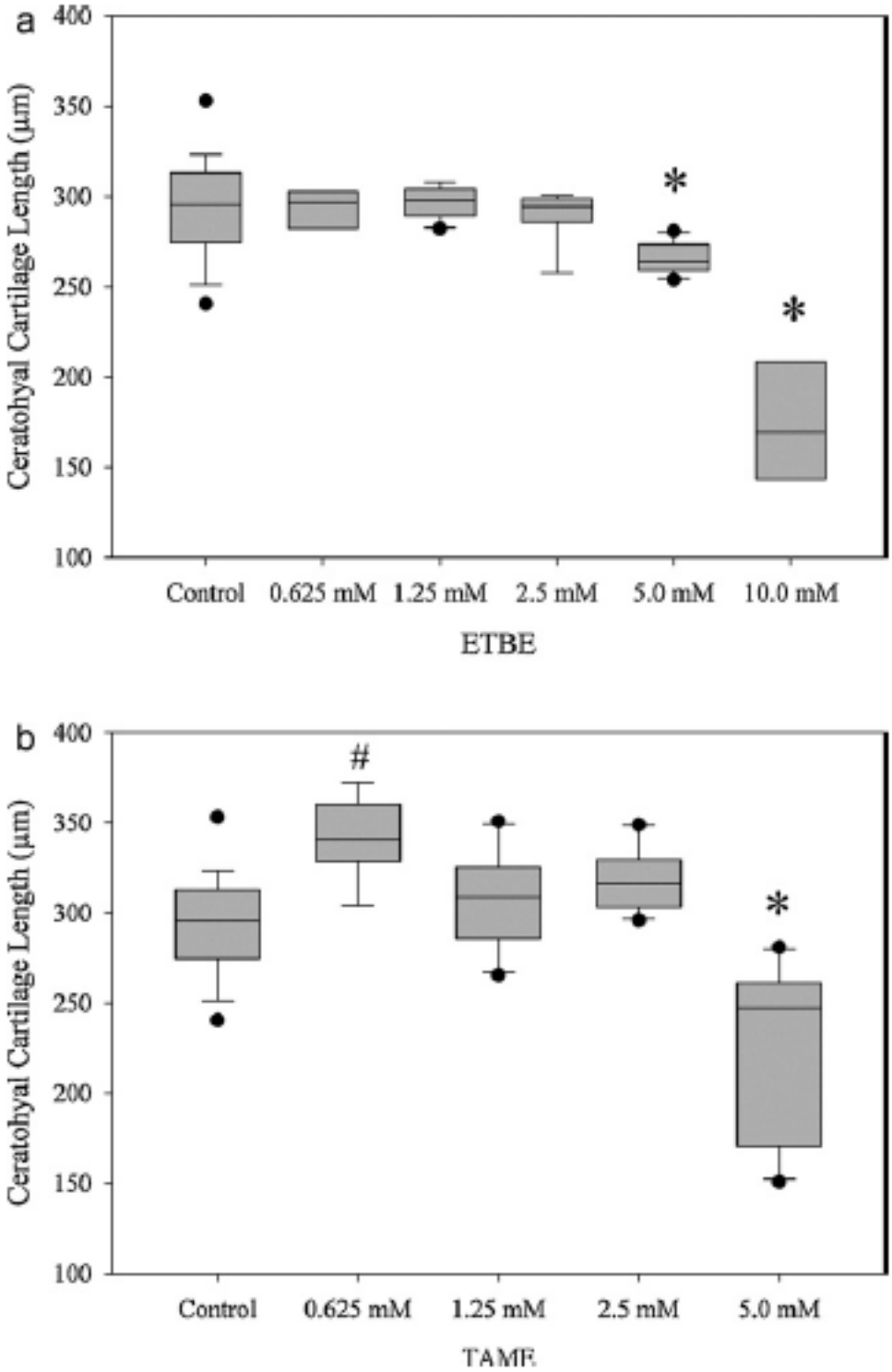

Figure 3.3 Box plot of the ceratohyal cartilage lengths of all doses measured for (A) ETBE and (B) TAME. * denotes significantly decreased from control, # denotes significantly increased from control.

Table 3.7 Comparison of the relative fold changes from control at 21-somites.

	5 mM MTBE	5 mM ETBE	2.5 mM TAME	5 mM TAME
vegfa	↓2.14*	↓1.42	↑1.74	↓1.64
vegfc	↓2.21*	↓1.69	↑1.30	↓1.94*
wnt3a	↓1.90	↓4.07*	↓2.29*	↓2.27*
wnt8a	↓1.86	↓1.75	↓3.80*	↓3.66*
mmp-2	1.03	↓1.83	↓1.74	↓3.72*
mmp-9	↓2.54	↓2.78*	↓1.29	↓3.54*
mmp-13	↓1.35	↓1.89	↓1.54	↓1.45

Values in the table are averaged fold changes from 3 studies. Each study consisted of 3 to 4 biological replicates. Arrows indicate an increase or decrease of expression at 21-somites. * Significantly different from control.

TABLE 3.8 Concentrations at which the gasoline oxygenates induced significant lesions at the doses tested (0.625 to 10 mM)

	MTBE (mM)	ETBE (mM)	TAME (mM)
Developmental Delay	> 10	> 10	10
Delayed Hatch (by 120 hpf)	> 10	10	10
Survival to 3 days post hatch	> 10	10	5
Reduced Circulation	5	5	5
Pericardial Edema	10	10	5
Heart Rate at 72hpf (beats/min)	10	5	1.25
Heart Rate at 96hpf (beast/min)	>10	5	1.25
Pooled Blood in CCV	5	5	5
Cranial Hemorrhages	10	5	2.5
Abnormal ISVs	5	10	2.5
Edema	> 10	10	5
Yolk Dysmorphogenesis	> 10	10	5
Craniofacial Abnormalities	> 10	5	0.625, 5[#]

Based on data from dose-response studies. # At 0.62 5mM TAME there was a significant increase in craniofacial abnormalities, while at 5 mM TAME there was a significant decrease.

CHAPTER 4

Microarray analysis of global gene expression during early stages of vascular development in the zebrafish

4.1 Introduction

Zebrafish embryos have emerged as a useful vertebrate toxicological model, largely due to their capacity for high-throughput experimentation, rapid development, and increasing availability of molecular techniques (Hill et al., 2005). Although there are species-specific genes, many pathways are conserved between lower and higher vertebrates, allowing for exploratory investigations into xenobiotic effects of the initiation of toxicity and the subsequent downstream events. Gene array analysis, when used to explore developmental toxicity in the zebrafish, provides a large volume of data from which hypotheses may be generated to direct further studies into the mode or mechanism of action of a chemical of interest. In a large-scale study encompassing 11 chemicals, 3 stages of exposure, and multiple doses, Yang et al. (2007) demonstrated the sensitivity, specificity, and reproducibility with which the zebrafish genome responds to chemical exposures. The study identified altered transcriptional expression of genes in known chemical/gene relationships (i.e. TCDD/*cyp1a1*), as well as new genes of potential interest. The abundance of transgenic zebrafish provides an opportunity to look at different populations of cells within the embryo. Flow cytometry can be used to separate fluorescently labeled cells in transgenics, and the differential gene expression in the different cell populations can be used to explore pathways regulating specific developmental processes (Dickmeiss et al., 2004). Zebrafish microarrays have also been successfully used to explore transcriptional changes during physiological states, including hypoxia (Ton et al., 2003). Consistent with what is known of hypoxia's effect on cellular

regulation, gene transcripts of enzymes associated with the glycolytic pathway were up regulated, while those associated with the cell cycle were repressed. Demonstrating the utility of this technique to shed light on physiologic targets of toxicants in the zebrafish embryo model.

The use of gene arrays for early time points in developing zebrafish can be complicated by the rate at which the embryo develops. Based on the temporal sequence and developmental stage data provided in Kimmel et al. (1995), growth in the zebrafish is linear in the first 36 hours (Fig. 4.1). Between 16 and 30 hours post fertilization (hpf) (14hrs or 840 minutes), the zebrafish embryo grows 1.6 mm (1600 μm) in length. The embryo, therefore, grows an average of 28.6 μm every 15 minutes between 16 and 30 hpf. If the total length of an embryo at hatch is 3.5 mm (at 72 hpf, 28.5°C), then 1.6 mm is approximately 45 % of the embryo's total growth in length, and this growth in length occurs over approximately 19 % of the total development time. During this period of rapid growth, significant changes in gene and protein expression occur (Mathavan et al., 2005; Leng Tay et al., 2006). As a result, a difference of 15 minutes in the developmental timing (e.g. between control and treatments or of embryos within a treatment) may result in substantial global gene expression changes that could confound the identification of altered expression between untreated and treated embryo samples. An alternative approach to treatment-based hypothesis generation from global gene expression changes occuring in a rapidly developing whole embryo model is to look at developmental pathways activated in the untreated embryos at different time points. The networks created by examining fold changes in gene expression between different stages of normally developing embryos represent the pathways that are activated during that period

of development. This information can, in turn, be used as a resource to generate hypotheses for a chemical's mode or mechanism of action with a known molecular target that resides within a network.

Due to our interest in angiogenesis, the time points used in these studies were designed to focus on the early developmental period surrounding the formation of blood vessels. The microarray study presented in this chapter was designed to meet two different aims: 1) to identify pathways activated at early time points in developing zebrafish, and 2) to identify cellular networks altered by methyl tert butyl ether (MTBE) during the critical period for MTBE toxicity in the embryo. The hypothesis for this study was that specific genes or pathways of interest would be identified using gene chip analysis during the critical period on non-treated zebrafish, as well as in embryos treated with MTBE. The data demonstrated that the hypothesis was too simplistic to be applied to a rapidly developing organism. The whole organism approach to determine a cellular response verses single organ or cell type further complicated the analysis of the data. However, when coupled, the gene array data with Ingenuity Pathway Analysis (IPA)®, supported the pivotal role of the HIF/VEGF pathway in MTBE anti-angiogenesis, and identified other pathway connections that could be examined in the future.

4.2 Methods

4.2.1 Animal Handling

Transgenic zebrafish *fli1*-EGFPs (Fli1s), which express enhanced green fluorescent protein in all vascular endothelial cells (Lawson and Weinstein, 2002), were obtained from the Zebrafish International Resource Center and were used for all

experiments. Breeding stocks were housed in an Aquatic Habitat recirculating system under a 14:10 light:dark photoperiod. Water quality was maintained at <0.05 ppm nitrite, <0.2 ppm ammonia, pH between 7.2 and 7.7, and temperature between 26 and 28°C. During exposures, embryos were incubated at 25 °C as previously described in Bonventre et al. (2011), and all embryos were selected at the same stage at the beginning of each experiment. All of the husbandry and embryonic exposure protocols were approved by the Rutgers University Animal Care & Facilities Committee.

4.2.2 MTBE Exposure and Global Gene Expression During Early Vascular Development

Staged embryos (1k cell stage) were randomly selected and assigned to one of three time points: 6-somites (approximately 15 hpf at 25 °C), 21-somites (approximately 24 hpf), or Prim-5 (approximately 30 hpf) shown in Figure 4.2. To determine the effect of MTBE on global gene expression during early vascular development, three concentrations were chosen: 5.0 mM MTBE (causes a significant increase in vascular lesions), 0.625 mM MTBE (does not cause significant vascular lesions, NOAEL), and 0.00625 mM MTBE (100-fold lower than NOAEL) (Bonventre et al., 2011). MTBE was obtained from Sigma Aldrich [purity 99.9%]. All chemical solutions were made the day of treatment with aerated egg water (60 µg/ml Instant Ocean in double distilled H_2O). Three biological replicates, each containing 15 gang (group) housed embryos, were prepared in scintillation vials for each of the three developmental time point and MTBE treatment groups. Untreated embryos served as the control for MTBE exposure and were used for the analysis of gene expression during early vascular development.

4.2.3 Microarray analysis

Total RNA extraction, hybridization to the Affymetrix Zebrafish Genome Array GeneChip®, and data acquisition were performed by the Bionomics Research and Technology Center in the Environmental Health & Occupational Sciences Institute in Piscataway, NJ. All the data were analyzed using the GeneSpring GX® software package. The effect of developmental stage (time) on global gene expression was determined with a One-way Analysis of Variance (ANOVA) with a $p \leq 0.01$ cut off and a Student-Newman-Keuls (SNK) post hoc test. The Benjamin-Hochberg procedure was applied to the data to limit the false discovery rate. The effect of MTBE treatment on development within each stage was analyzed similarly. In the case where treatment was not significant, normalized log2 data were transformed to fold changes, and a 1.5 fold cut off was applied to the data for further analysis in IPA.

4.2.4 Ingenuity Pathway Analysis

For the developmental stage study, genes that were significantly different from the previous stage were entered into IPA software to determine the functional networks activated at each stage. To demonstrate how the pathways identified in the analysis of untreated embryos can be used to direct studies for developmental toxicants with unknown targets, gasoline oxygenates ethyl tert-butyl ether (ETBE) and tert-amyl methyl ether were. For the MTBE exposure study, genes that had a greater than 1.5 fold change from control were entered into the IPA software since gene alterations were not found to be significantly different between control and treated embryos. The pathways and

networks created in IPA are based on gene connections published in peer-reviewed literature.

4.3 Results

4.3.1 Global gene expression during early vascular development

Time had a significant ($p \leq 0.01$) effect on changes in global gene expression. Of the 14,900 genes on the zebrafish GeneChip, 1001 genes were significantly different from 6-somites to 21-somites, and 706 genes were significantly different from 21-somites to Prim-5 (Table 4.1). For 6-somites to 21-somites, 534 significantly up regulated genes and 197 significantly down regulated genes had a greater than 2-fold change in expression. For 21-somites to Prim-5, 543 significantly up regulated genes and 190 significantly down regulated genes had a greater than 2-fold change in expression.

The data set of significantly altered genes were uploaded to IPA and analyzed using the Core Analysis function. The resulting networks are listed in Tables 4.2A and B. The top two networks for 6-somites to 21-somites included “cell cycle, cellular development, connective tissues development and function” and “cellular compromise, cellular assembly and organization, cardiovascular system development and function”. The top three networks for the differences between 21-somites and Prim-5 all include “skeletal and muscular system development and function” and “tissue morphology”. The top genes (molecules) up or down regulated between 6-somites and 21-somites or 21-somites to Prim-5, along with the function and fold change, are listed in Tables 4.3A, B and 4 A, B. Among the top molecules were skeletal and cardiac muscle components,

transcription factors, structural elements, hemoglobins, and members of the WNT and frizzled families.

To demonstrate how the pathways identified in this study can be used to generate hypothesis for developmental toxicants, ETBE and TAME were used as example toxicants. Both chemicals were shown to significantly decrease mRNA transcript levels of matrix metalloproteinases (MMPs) and Wnts at 21-somites (Bonventre et al., 2012). Members of both MMP and Wnt families were significantly differentially expressed from 6- to 21-somites in untreated embryos, and many of the top networks included members of one or both famiies. In Figure 4.3, two of the networks that included MMPs and Wnts were selected as example networks that can be used to design future experiments exploring the toxicity of each chemical.

4.3.2 The effect of MTBE on global expression during early vascular development

Treatment did not significantly alter the expression of any genes at any stage stage at $p < 0.05$. Therefore, the analysis of the effect of MTBE on global gene expression was based on fold changes alone. The number of genes differentially expressed meeting the 1.5 fold cut was determined for each concentration of MTBE at each stage (Table 4.5). The stage with the greatest number of gene changes in all three treatment groups was 21-somites, followed by 6-somites. At Prim-5, fewer than 5 genes were altered with any concentration of MTBE. The total number of altered genes independent of MTBE concentration, and the number of those genes common to all three MTBE concentrations was determined (Table 4.6). Both 6-somites and 21-somites had a

similar number of genes altered by MTBE exposure, however 57 out of 59 total genes were altered by all three concentrations of MTBE at 21-somites.

The 21-somite data set was uploaded to IPA and analyzed. Based on fold change up or down, the top 10 genes altered by each concentration of MTBE were identified and listed in Tables 4.7 A-C. With the exception of Cathepsin b (CTSB) in the 0.625 mM MTBE, all of the top 10 molecules had a greater than 1.5 fold change, however, they were not all regulated in the same direction. Table 4.8 shows the top molecules in common to the three concentrations of MTBE. The molecules were categorized into different either general cell responses including, cell stress (CTSB, CTSS, NPC2, OCM2, and SERPINA1) or energy/metabolism (ACP5, APOA1, FBP1, MTHFD1), or more specific cell functions including, blood clotting (FGG), iron homeostasis (TF), oxygen sensing (EGLN3), innate immunity (CFI), and steroid synthesis (CYP11A1). ACP5, CFI, CTSS, FBP1, MTHFD1, NPC2, and TF were all up regulated by each concentration of MTBE at 21-somites. SERPINA1 was the one gene of the top 10 to be down regulated by each concentration. APOA1, CTSB, CYP11A1, EGLN3, and OCM2 were all upregulated with 0.00625 mM MTBE, but downregulated with 5 mM MTBE. FGG was downregulated with both 0.00625 and 5 mM MTBE, but upregulated 2 fold with 0.625mM MTBE. The 14 molecules were entered into IPA for a “custom list” data analysis, and 2 networks were created based on the relationships between the molecules: “Cancer, Cardiovascular System Development and Function, Tumor Morphology” and “Lipid Metabolism, Small Molecule Biochemistry, Carbohydrate Metabolism” (Fig. 4.4 A, B). Most of the molecules (10/14) were present in the first network, which included a relationship to VEGF.

4.4 Discussion

The studies presented in this chapter were designed to generate hypotheses from global gene expression changes that occur early in zebrafish embryo development. The three embryonic stages selected for the Zebrafish Affymetix GeneChip® experiment corresponded to both early cardiovascular development in the zebrafish and to the critical period of MTBE-induced vascular toxicity (Bonventre et al., 2011). By analyzing the global gene expression of untreated embryos at the three different stages, 6-somites, 21-somites and Prim-5, we identified pathways activated early in development, which can be used to direct studies on how chemicals of unknown targets disrupt development. The effect of MTBE on gene expression at each stage presented new evidence that MTBE targets components involved in cardiovascular development, while identifying new pathways to pursue in future studies.

Previous studies with zebrafish embryos have demonstrated that time (stage) has a significant effect on global gene expression in the embryo (Mathavan et al., 2005; Leng Tay et al., 2006). The pathways upregulated in the data set corresponded to the known developmental processes occurring in the embryo at these stages (Table 4.2 A and B). From 6-somites to 21-somites, the major pathways upregulated involved general cell growth (1, Table 4.2A), cardiovascular system development (2, Table 4.2A), and nervous system development (3, Table 4.2A). In contrast, from 21-somites to Prim-5, the top three major pathways upregulated involved to processes of overall growth and development (Table 4.2B). The switch from specific organ system development to general growth paralleled the graph of zebrafish development depicted in figure 4.1, where growth is linear from 16 hpf (approximately 6-somites) to 30 hpf (approximately Prim-5), and

changes to shallow slope. Once embryos reach Prim-5, many of the major organ systems have lain down rudimentary or primordial tissues, indicating the goal of the embryo from this point forward is to simply grow (Kimmel et al., 1995).

Using single gene endpoints for developmental toxicity studies provides a limited scope of a chemical's toxicity. Understanding the networks that are involved in early development can help to identify possible target pathways vulnerable to chemical insult, and may be used to direct future studies. Among the pathways developed by IPA for the untreated zebrafish, two were selected for future studies with ETBE and TAME (Fig. 4.3). ETBE and TAME disrupt normal development in zebrafish embryos causing edema, decreased heart beat, craniofacial abnormalities, and delayed development (Bonventre et al., 2012). Both chemicals were shown to significantly decrease mRNA transcript levels of MMPs and Wnts at 21-somites. Since the protein families associated with the ETBE or TAME lesions are involved in multiple developmental pathways, determine the underlying mechanisms of action for ETBE or TAME by targeting a pathway is challenging. However, since members of both MMP and Wnt families were significantly differentially expressed from 6- to 21-somites in the analysis of untreated embryos, pathways including MMPs or Wnts could be pursued to more mechanistic studies (Fig. 4.3). For example, over expression studies could be carried out to rescue protein levels of MMPs or Wnts, and the consequence of over expression on other molecules in the networks may indicate targets of ETBE or TAME in the developing zebrafish. Alternative networks from this data set could be used to develop hypotheses for other chemicals, known to disrupt development and alter mRNA expression in early time points, but where target pathways are unclear.

The critical period of MTBE anti-angiogenesis in zebrafish is early in development, and precedes the appearance of vascular lesions by 1 day (Bonventre et al., 2011). Embryos exposed to MTBE prior to 6-somites or after Prim-5 stages did not exhibit MTBE pooled blood in the common cardinal vein, cranial hemorrhages, or abnormal intersegmental vessels. While the MTBE treatments did not result in any statistically significant gene changes, based on the number of genes altered at each time point, 21-somites was identified as an important stage for MTBE toxicity. More genes changed at 21-somites (Table 4.5), the middle of the critical period, and that stage had the most number of altered genes common to all three concentrations of MTBE (Table 4.6). This time period is also important to cardiovascular development in the zebrafish embryo, as it represents the time period in which the major blood vessels are formed within the embryo (Kimmel et al., 1995; Isogai et al., 2001). Therefore, while statistical significance was not achieved, the data of the microarray is consistent with our previous studies.

Quantitative PCR (qPCR) studies demonstrated that 5 mM MTBE significantly decrease mRNA transcript levels of *vegf-a*, *vegf-c*, and *vegfr2* (Bonventre et al., 2011), however, these genes were not among the list of genes altered by at least 1.5 fold in any treatment data set. A possible explanation for this observation is that qPCR is more sensitive than microarrays. This does not, however, diminish utility of the technique, as the goal of a gene-array studies are not to necessarily identify specific targets, but rather groups of genes with a common physiological goal or directive. Messenger RNA transcripts of some genes upregulated in cells at sites of localized hypoxia may not achieve concentrations detectable by microarrays. Hypoxia did not alter the expression of

either *erythropoietin* or *vegf* gene expression in a previous zebrafish microarray study (Ton et al., 2003). Identifying effects on specific proteins may be confounded by the specificity of MTBE for a cell type or pathway. Our studies used whole embryo lysate at a period of rapid development. The reduced sensitivity of the microarray platform, combined with whole embryo lysate at a period of rapid development and a toxicant that targets a cell type that composes a small portion of the total mass of an embryo may be the reason for the lack of significant differential gene expression in our treatment studies. This suggests that, while global gene expression provides a wealth of information, samples of a single organ or cell type would be a better study design to obtain more statistically significant findings.

The cardiovascular system was the first network created by the list of MTBE-altered genes entered into IPA (Fig. 4.3 A). Therefore, despite the lack of significantly altered genes in the microarray analysis, the genes that changed the most were related to primarily cardiovascular system. The second network created by IPA from the list of molecules included the “small molecule biochemistry” pathway (Fig. 4.3 B). The same network was identified in a previous zebrafish Affymetrix gene-chip study, which analyzed genes differentially regulated by a zebrafish Vegf-Aa morpholino (Bahary et al., 2007). The similarity between the networks associated with the Vegf-Aa morphant and the networks identified with the MTBE treatments supports the hypothesis that MTBE toxicity is Vegf-A dependent.

Gene-array analysis of MTBE-treated embryos was also carried out to identify alternative pathways implicated in MTBE toxicity. Hypoxia inducible factor (HIF) activation is not limited to regulation of angiogenesis and erythropoiesis. The

hypothesized role of HIF in the toxicity of MTBE suggested other pathways might be altered with exposure to the chemical, specifically those involved in energy utilization or cell survival (reviewd in Nordgren and Tavassoli, 2011; Goda and Kanai, 2012). Under normoxic conditions, aerobic respiration occurs in the cell. However, in the absence of oxygen, the electron transport chain and preceding TCA cycle are inhibited, and anaerobic respiration (glycolysis) takes over. A lack of oxygen also stabilizes HIF-α subunits in the cytoplasm, as prolyl-4-hydroxylase domain (PHD)s require oxygen and 2-oxoglutarate (TCA cycle) to function. In addition to the cardiovascular system, many of altered molecules were associated with signs of cell stress and cellular energy homeostasis (Table 4.8). It is possible that the signs of cell stress resulted from exposure to the putative primary metabolites of MTBE, tert-butyl acohol (TBA) and formaldehyde. While exposure to TBA or formaldehyde did not induce vascular lesions, there was a decrease, though not significant, in embryo hatch by 5 days and survival to 3 days post hatch. These effects may be a result of altered cell stress pathways in the embryo. Further studies would be necessary to determine if exposure to TBA or formaldehyde contributed to the gene expression changes of CTSB, CTSS, NPC2, OCM2, and SERPINA1 (Table 4.8) or other markers of cell stress. The MTBE-induced altered expression of molecules associated with metabolism and energy production also provides an interesting area of study as these pathways (glycolysis, lipid metabolism, gluconeogenesis) are often altered in tumors due to the increased hypoxia often associated with rapid growth (Hamanaka and Chandel, 2012). As an anti-angiogenic with little toxicity to tissues other than vasculature, a role for MTBE could be found in anti-tumor treatments in conjunction with

other therapies. The potential for MTBE to alter energy metabolism within a cell would be important to understand prior to use to combat solid-tumors.

The lowest concentration of MTBE chosen for the studies discussed in this chapter, 0.00625 mM MTBE, was 100 fold lower than the previously reported NOAEL, and approximately 10 fold higher than the drinking water standards established by the EPA (Bonventre et al., 2011; Post 2001). It was interesting to see that although lesions are not observed in the zebrafish with 0.00625 and 0.625 mM MTBE, many of the same genes were altered in all three concentrations of MTBE at 21-somites (Table 4.7 A-C). However, the genes were not all regulated in the same manner. One notable gene of interest, *egl nine homolog 3 (egln3)*, was regulated differently by the lowest (+2.07) and highest (-1.78) concentrations of MTBE (Table 4.8). EGLN3, also know as PHD3, is part of the cellular oxygen sensing system, responsible for regulating HIF1-α levels in the cytoplasm. Under hypoxic conditions, PHDs are not active, HIF1-α accumulates and translocates into the nucleus, where it binds to HIF1-β and activate hypoxia compensatory functions (reviewed in Keith et al., 2012). EGLN3 is also upregulated by HIF activation (Berra et al., 2003; Marxsen et al. 2004). If MTBE exposure in developing zebrafish decreases Vegf-a as hypothesized, then it is possible that a decrease of the angiogenic protein by low levels of MTBE (0.00625 mM) may result in stimulation of Hif activity. The ability of the embryo to compensate for the hypothesized decreased circulating Vegf-a may be lost at higher concentrations of MTBE where the system is swamped. Therefore, the data from the microarray, support to the hypothesis that there is a relationship between MTBE toxicity and the Hif-Vegf pathway.

4.5 Conclusions

Zebrafish microarray analyses identify pathways of interest from changed in global gene expression provide an abundant data set from which to create hypothesis designed to better understand developmental processes. Pursuing specific gene and protein expression studies are important to uncovering mechanisms of toxicity when a targeted organ system is known. However, global changes in gene expression broaden the understanding of how a chemical disrupts multiple pathways in the process of toxicity. Microarrays enable the scientist to look at questions 'outside the box' of the standard uni-directional studies. Rather than focus only upstream or downstream of a protein of interest, the networks created with IPA, or other pathway analysis programs, aid in visualization of pathways as they exist in the cell: intersecting and overlapping. Studies of global changes are important to identifying alternative modes of action for a toxiciant are because disease states are generally a result of multiple toxic endpoints.

MTBE can be considered a unique toxicant in that all the data support the hypothesis that MTBE toxicity is specific to developing vasculature, and may be particularly targeted at the microvasculature (Bonventre et al., 2011; Kozlosky et al., 2012). To better understand the effect of MTBE on global gene expression, a study designed to specifically examine differential changes within endothelial cells, rather than a whole organism homogenate, would be beneficial. The lack of significance within the treated samples notwithstanding, the data provided in this chapter can be used to form hypotheses and design future experiments both for further studies to determine how MTBE targets the developing vascular system, and for pursuing other chemicals with unknown target systems, such as ETBE and TAME. The data from the gene-array

analysis support our hypothesis that MTBE toxicity results from a dysregulation of the Vegf pathway and present alternative pathways that are altered by exposure. Further analysis of the data sets, both untreated controls and MTBE, could provide additional useful information to be used to design future studies.

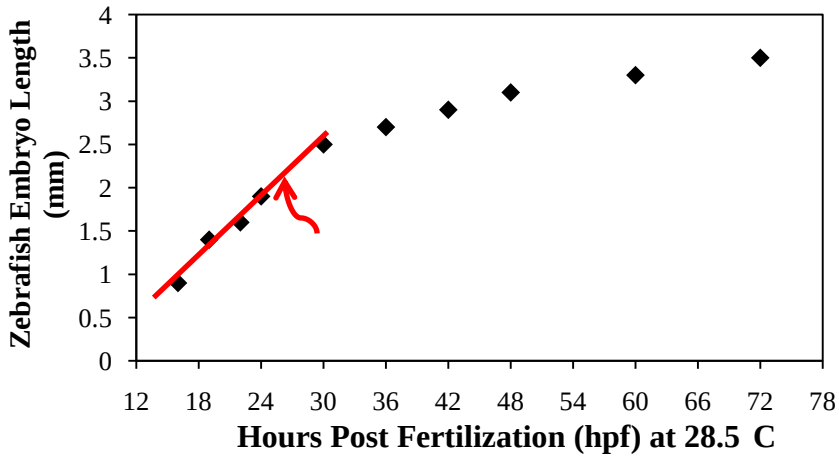

Figure 4.1. Embryonic development in a zebrafish is linear for the first 30 hours of development. At 28.5°C, the zebrafish embryo grows approximately 1600 µm) in length between 16 and 30 hpf, which is an average of 28.6 µm every 15 minutes. Approximately 45% of the embryo's total growth in length (about 3.5 mm) occurs over approximately 19% of the total development time. Rate determination based on stage characterization and lengths in Kimmel et al., 1995.

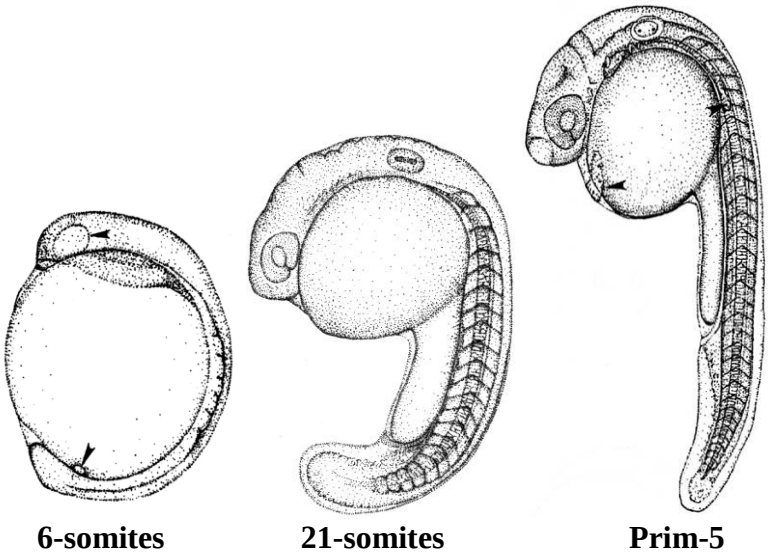

Figure 4.2. Stages of embryonic development used for the microarray studies. The time points selected for these studies were designed to focus on the developmental period surrounding the formations of the earliest vessels. They also correspond to the critical period established for MTBE-induced vascular lesions (Bonventre et al., 2011).

Table 4.1. The number of significantly different gene alterations between early developmental stages.

	Total # genes (out of ~14,900*)	Genes with ≥ 2 fold Δ
6-somites vs. 21-somites	1001	↑ 534 ↓ 197
21-somites vs. Prim-5	706	↑ 543 ↓ 190

*Affymetrix Zebrafish Gene-Chip has ~14,900 zebrafish gene sequences on the chip

Table 4.2A. Top 5 Functional Networks Activated between 6-somites and 21-somites

1.	Cell Cycle, Cellular Development, Connective Tissues Development/Function
2.	Cellular Compromise, Cellular Assembly/Organization, Cardiovascular System Development/Function
3.	Nervous System Development/Function, Tissue Morphology, Cellular Growth/Proliferation
4.	Developmental Disorder, Gastrointestinal Disease, Cancer
5.	Skeletal & Muscular System Development/Function, Tissue Morphology, Skeletal/Muscular Disorder

Table 4.2B. Top 5 Functional Networks Activated between 21-somites and Prim-5

1.	Skeletal & Muscular System Development/Function, Tissue Morphology, Developmental Disorder
2.	Skeletal & Muscular System Development/Function, Tissue Morphology, Skeletal/Muscular Disorder
3.	Skeletal & Muscular System Development/Function, Tissue Morphology, Gene Expression
4.	Cellular Development, Embryonic Development, Tissue Development
5.	Cellular Development, Tissue Development, Cell Cycle

Table 4.3A. Top 10 molecules upregulated from 6-somites to 21-somites

Molecule	Name	Function	Exp. Value
LCP1	Lymphocyte cytosolic protein 1	Actin binding protein, role in T-cell response to costimulation	+6.820
WNT8A	Wingless type, MMTV integration site family 8 A	Involved in development, cell fate and patterning, ligand for frizzled	+4.842
NR6A1	Nuclear receptor subfamily 6, group A, 1	Orphan receptor, involved in neurogenesis, germ cell development	+4.367
DUSP2	Dual specificity phosphatase 2	Regulates mitogenic signal transduction of MAPK-ERK1 and ERK2	+4.174
RAX	Retina anterior neural fold homeobox	Required for retinal cell fate determination and eye development	+3.968
FZD8	Frizzled family receptor 8	Receptor for WNT proteins	+3.801
ZP3	Zona pellucida glycoprotein 3	An extracellular matrix that surrounds the oocyte and early embryo	+3.739
GATA2	GATA binding protein 2	Transcriptional activator, regulates endothelin-1 gene expression	+3.508
GATA3	GATA binding protein 3	Transcriptional activator, regulates T-cell receptor α and δ genes	+3.486
GSC	Goosecoid homeobox	Transcription factor involved in craniofacial development	+3.433

Table 4.3B. Top 10 molecules downregulated from 6-somites to 21-somites

Molecule	Name	Function	Exp. Value
MYL1	Myosin light chain 1	Component of the myosin hexamer	-88.282
ATP2A1	ATPase (calcium transporting) 2A1	Catalyzes hydrolysis of ATP, Ca2+ sequestration	-69.535
HBE1	Hemoglobin epsilon 1	Normally expressed in the embryonic yolk sac	-29.566
SYT4	Synaptogamin IV	May be involved in Ca^{2+}-dependent exocytosis of secretory vesicles	-25.034
MYLPF	Myosin light chain phosphorylatable (fast twitch)	Calcium binding change in the myosin hexamer	-23.663
COL1A1	Collagen alpha-1(I) chain precursor	Fibril-forming collagen found in most connective tissues	-22.662
MYH7	Myosin heavy chain (cardiac muscle)	Involved in muscle contraction with actin creating contractile force	-18.080
POSTN	Periostin osteoblast specific factor	Binds to heparin, induces cell attachment, cell adhesion	-16.843
TNNC2	Troponin C type 2	Central regulatory protein of striated muscle contraction	-15.780
MAFA	musculoaponeurotic fibrosarcoma oncogene homolog	Transcription factor, activates insulin gene expression	-14.423

Table 4.4A. Top 10 molecules up regulated from 21-somites to Prim-5

Molecule	Name	Function	Exp. Value
MSGN1	Mesogenin 1	Formation and segmentation of paraxial mesoderm	+3.928
CDX4	Caudal type homeobox 4	Transcription factor	+3.853
UOX	Urate oxidase, pseudogene	Catalyzes the oxidation of uric acid to allantoin	+2.508
FN1	Fibornectin	Cell adhesion, cell motility, opsonization, maintenance of cell shape	+2.284
DACT2	Dapper, antagonist of beta-catenin, homolog 2	Negatively regulates the Nodal signaling pathway	+2.186
EFEMP2	EGF containing fibulin-like extracellular matrix protein2	Necessary for elastic fiber formation, connective tissue development	+2.167
EPPK1	Epiplakin 1	Associated with junction complexes and the cytoskeleton	+2.006
ZP3	Zona pellucida glycoprotein 3	Extracellular matrix that surrounds the oocyte and early embryo	+1.954
FST	Follistatin	inhibits follicle-stimulating hormone release	+1.947
CA8	Carbonic anhydrase related protein 8	putatively involved in nerve function	+1.805

Table 4.4B. Top 10 molecules down regulated from 21-somites to Prim-5

Molecule	Name	Function	Exp. Value
TNNI2	Troponin 1 type 2	Inhibitory subunit of troponin	-28.787
TNNT3	Troponin T type 3	Tropomyosin-binding subunit of troponin	-14.455
AQP1	Aquaporin 1	Water channel in plasma membranes of RBCs, proximal tubules	-6.020
HBZ	Hemoglobin, zeta	Synthesized in the yolk sac of the early embryo	-5.146
CKM	Creatine kinase muscle	Catalyzes the transfer of phosphates, energy homeostatis	-4.718
IGFN1	Immunoglobulin-like and fibronectin type III domain-containing protein 1	Muscle specific protein associate with filamin C, kyphoscoliosis peptidase	-4.441
GCHI	GTP cyclohydrolase	Positively regulates nitric oxide synthesis	-4.415
MYLPF	Myosin light chain, phosphorylatable, (fast twitch)	Calcium binding change in the myosin hexamer	-4.413
HBE1	Hemoglobin epsilon 1	Normally expressed in the embryonic yolk sac	-3.709
ANKH	Progressive ankylosis protein homolog	Regulates intra- and extracellular levels of inorganic pyrophosphate	-3.584

Table 4.5. Number of genes differentially expressed with 1.5 fold cut off for all treatments and stages

MTBE (mM)	6-somites	21-somites	Prim 5
0.00625	51	41	2
0.0625	24	32	2
5.0	15	32	1

Table 4.6. Number of genes differentially expressed with 1.5 fold cut off within each stage

Stage	Total number of altered genes	Altered genes common to all [MTBE] within stage
6-somites	57	4
21-somites	59	57
Prim 5	5	0

Table 4.7A. Top 10 molecules differentially regulated between Control and 0.00625 mM MTBE at 21-somites

Molecule	Name	Function	Exp. Value
CTSB	Cathepsin B	intracellular degradation and turnover of proteins	+2.90
ACP5	Acid Phosphatase	converts orthophosphoric monoester to alcohol and orthophosphate	+2.32
CTSS	Cathepsin S	degrades antigenic proteins to peptides for MHC II presentation	+2.28
OCM2	Oncomodulin 2	high affinity calcium ion binding	+2.16
CYP11A1	Cytochrome p450 11A1	converts cholesterol to pregnenolone	+2.11
CFI	Complement factor 1	regulates thZe complement cascade	+2.10
EGLN3	Egl Nine Homolog 3	cellular oxygen sensor, targets HIF1-α for proteosomal degradation	+2.07
FGG	Fibrinogen Gamma Chain	fibrin precursor, required for blood clotting and platelet aggregation	-1.99
NPC2	Niemann-Pick disease	lysosomal storage disorder	-1.93
SERPINA1	Serine Proteinase inhibitor	Inhibitor of serine proteases, including elastase plasmin & thrombin	-1.92

Table 4.7B. Top 10 molecules differentially regulated between Control and 0.625 mM MTBE at 21-somites

Molecule	Name	Function	Exp. Value
CTSS	Cathepsin S	degradation of antigenic proteins to peptides for MHC II presentation	+2.49
ACP5	Acid Phosphatase	converts orthophosphoric monoester to alcohol and orthophosphate	+2.19
FGG	Fibrinogen Gamma Chain	fibrin precursor required for blood clotting and platelet aggregation	+2.03
OCM2	Oncomodulin 2	high affinity calcium ion binding	-1.95
SERPINA1	Serine Proteinase inhibitor	Inhibitor of serine proteases, including elastase plasmin and thrombin	-1.83
CYP11A1	Cytochrome p450 11A1	converts cholesterol to pregnenolone	-1.82
MTHFD1	Methylenetetrahydrofolate dehydrogenase	redox cycling, participates in glycolate and dicarboxylate metabolism	-1.78
APOA4	Apolipoprotein	major component of HDL and chylomicrons, lipid metabolism	+1.75
TF	Transferrin	transports iron	-1.74
CFD	Complement factor D	humoral suppression of infectious agents, associated with adipose	-1.74

Table 4.7C. Top 10 molecules differentially regulated between Control and 5.0 mM MTBE at 21-somites

Molecule	Name	Function	Exp. Value
CTSS	Cathepsin S	degradation of antigenic proteins to peptides for MHC II presentation	+2.24
ACP5	Acid Phosphatase	converts orthophosphoric monoester to alcohol and orthophosphate	+2.14
CFI	Complement factor 1	regulation of the complement cascade	+1.92
OCM2	Oncomodulin 2	high affinity calcium ion binding	-1.91
APOA4	Apolipoprotein	major component of HDL and chylomicrons, lipid metabolism	-1.87
SERPINA1	Serine Proteinase inhibitor	Inhibitor of serine proteases, including elastase plasmin and thrombin	-1.86
FGG	Fibrinogen Gamma Chain	fibrin precursor required for blood clotting and platelet aggregation	-1.82
EGLN3	Egl Nine Homolog 3	cellular oxygen sensor, targets HIF1-α for proteosomal degradation	-1.78
CYP11A1	Cytochrome p450 11A1	converts cholesterol to pregnenolone	-1.77
FBP1	Fructose-1,6-bisphosphatase	gluconeogenesis regulatory enzyme	-1.74

Table 4.8. Comparison of the top molecules altered by MTBE at 21-somites

Molecule	Name	Function	0.00625 mM	0.625 mM	5.0 mM
ACP5*	Acid Phosphatase	Energy/Metabolism	+2.32	+2.19	+2.14
APOA1*	Apolipoprotein	Energy/Metabolism	+1.59	+1.75	-1.87
CFI	Complement factor 1	Innate Immunity	+2.10	+1.69	+1.92
CTSB	Cathepsin B	Cell Stress	+2.90	<1.50	+1.66
CTSS*	Cathepsin S	Cell Stress	+2.28	+2.49	+2.24
CYP11A1*	Cytochrome p450 11A1	Steroid Synthesis	+2.11	-1.82	-1.77
EGLN3	Egl Nine Homolog 3	Oxygen Sensing	+2.07	-1.63	-1.78
FGG*	Fibrinogen Gamma Chain	Blood Clotting	-1.99	+2.03	-1.74
FBP1	Fructose-1,6-bisphosphatase	Energy/Metabolism	+1.87	+1.61	+1.74
MTHFD1	Methylenetetrahydrofolate dehydrogenase	Energy/Metabolism	+1.84	+1.73	+1.57
NPC2	Niemann-Pick disease	Cell Stress	-1.93	-1.72	-1.60
OCM2*	Oncomodulin 2	Cell Stress	+2.16	-1.95	-1.91
SERPINA1*	Serine Proteinase inhibitor	Cell Stress	-1.92	-1.82	-1.86
TF	Transferrin	Iron Homeostasis	-1.79	-1.74	-1.66

*Indicates the molecules in the top 10 of all three MTBE treatment group

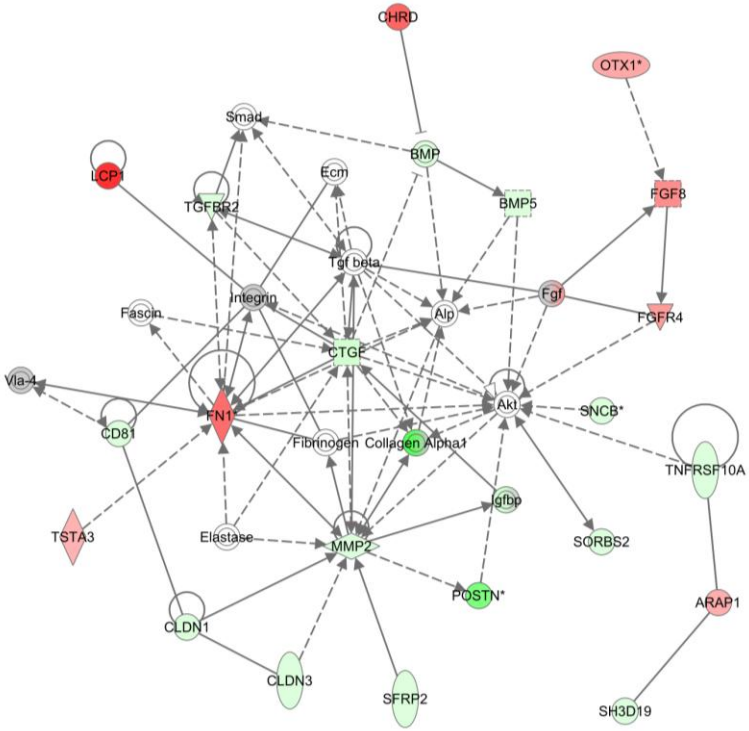

A: Connective Tissue Development/Function; Skeletal and Muscular System Development/Function; Tissue Development

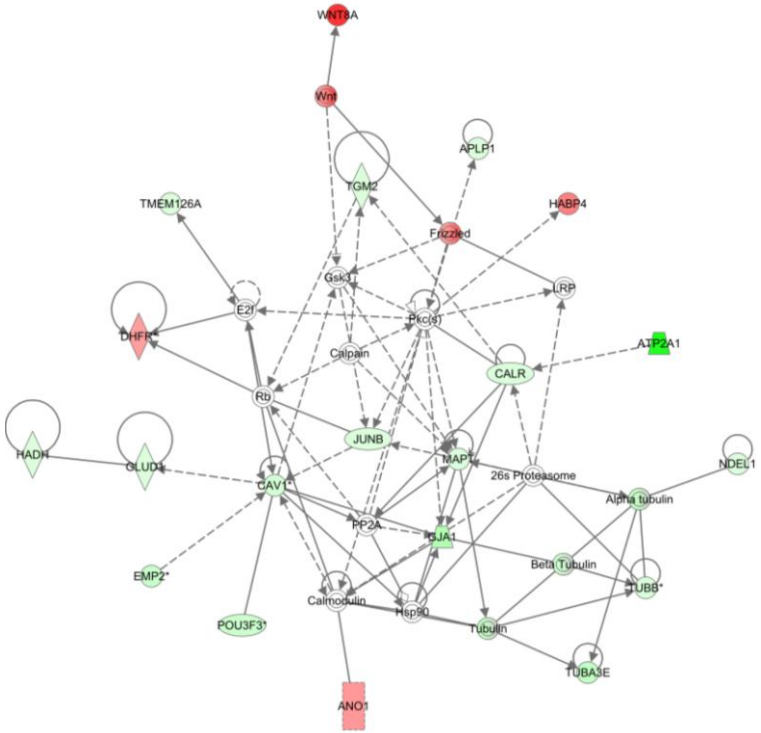

B: Cellular Assembly and Organization; Cellular Function and Maintenance; Cellular Compromise

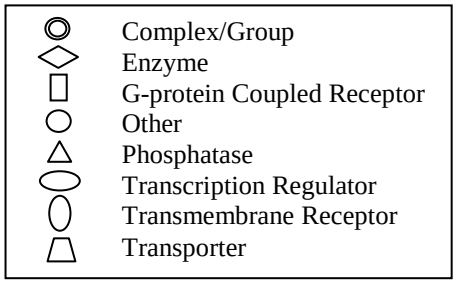

Figure 4.3. Networks activated at 21-somites involving MMPs and Wnts. Both ETBE and TAME disrupt MMP and Wnt mRNA transcript levels at 21-somites. Networks A and B could be used to generate hypotheses or drive experiments to identify target pathways of ETBE or TAME toxicity. Red molecules are upregulated from 6-somites, green molecues are downregulated from 6-somites.

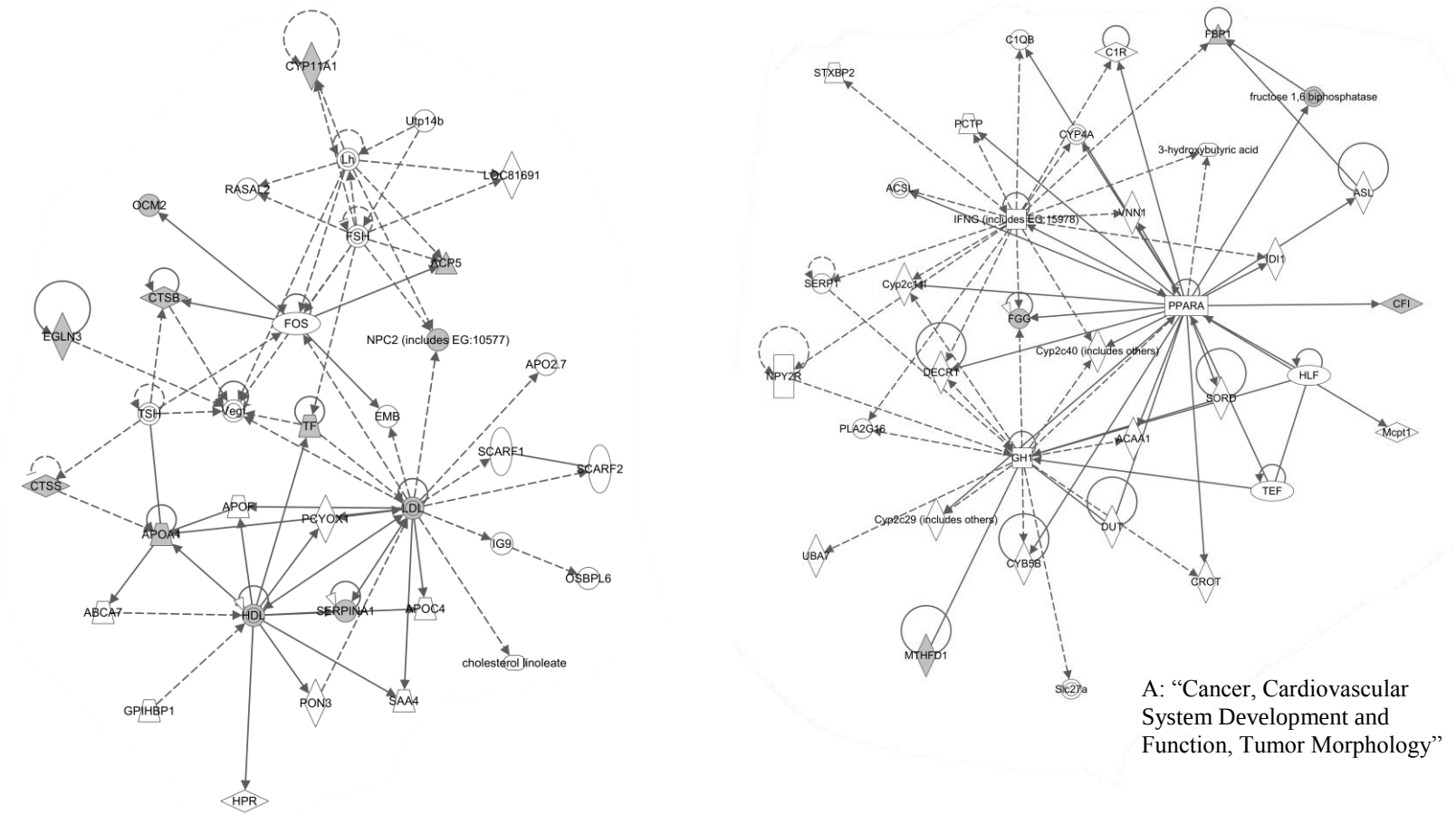

A: "Cancer, Cardiovascular System Development and Function, Tumor Morphology"

Figure 4.4. Neworks created by Ingenuity Pathway Analysis with a list of the top most differentially expressed genes by MTBE at 21-somites. The relationships between molecules that were altered with exposure to MTBE (shaded gray) are depicted in the networks. Network A contains 10/14 molecules: ACP5, APOA1, CTSB, CTSS, CYP11A1, EGLN3, OCM2, NPC2, SERPINA1, and TF. Network B contains 4/14 molecules: CFI, FBP1, FGG, and MTHFD1. The solid lines indicate a direct relationship while dashed lines indicate an indirect relationship.

CHAPTER 5

Over expression of *vascular endothelial growth factor-a* and forced accumulation of hypoxia inducible factor rescues MTBE-induced vascular lesions.

5.1 Introduction

Hypoxia inducible factor 1 (HIF1), a heterodimeric transcription factor composed of cytoplasmic HIF1-α and nuclear HIF1-β, is responsible for the regulation of hypoxia compensatory mechanisms in all cells (Forsythe *et al.*, 1996; Adelman *et al.*, 1999). Under hypoxic conditions, HIF1α translocates into the nucleus, dimerizes with HIF1-β, and bind to DNA at HIF response elements (HRE) to activate genes (Wang and Semenza, 1993) (Fig. 5.1). One such gene is vascular endothelial growth factor (VEGF), a protein that is essential to the vasculogenesis, angiogenesis, and hematopoiesis. HIF1 increases *VEGF* mRNA transcription and stabilization in hypoxic conditions. Hypoxia is the primary inducer of angiogenesis in the developing embryo (Ryan et al. 1998, Ramirez-Bergeron et al., 2004). During vertebrate development, the relationship between HIF1 and VEGF is essential to promote angiogenesis and, therefore, to organogenesis.

Under conditions of abundant molecular oxygen, cytoplasmic HIF1-α is degraded and therefore unable to activate HREs (Fig. 5.1). Prolyl-4-hydroxylase domain (PHD) proteins are the oxygen sensors of the system and function to hydroxylate two conserved proline residues in the oxygen-dependent degradation domain of cytoplasmic HIF1-α, which ultimately targets HIF-α for ubiquitination and proteasomal degradation (Ivan et al., 2001; Jaakkola et al., 2001). The hydroxylation of prolines 402 and 564 by PHD requires not only O_2, but also 2-oxoglutarate and Fe^{2+}, and altered levels of either may disrupt the hypoxia response system. An excess of 2-oxoglutarate drives HIF1-α hydroxylation, and therefore decreases angiogenesis and VEGF expression, while 2-

oxoglutarate mimics, i.e., N-oxaloylglycine or dimethyloxaloylglycine, competitively inhibit PHD activity (Matsumoto et al., 2006; Wirthner et al., 2007; van Rooijen et al., 2009). Iron chelators have been shown up-regulate angiogenic growth factors (Gleadle et al., 1995). Somewhat paradoxically, both PHD2 and PHD3, also known by their original names egl nine homolog (EGLN) 1 and 2, respectively, are upregulated by HIF1 activation, providing a mechanism for HIF1-dependent autoregulation of the cell's hypoxic response (Berra et al., 2003; Marxsen et al. 2004).

Hydroxylation of the oxygen-dependent degradation domain on HIF1-α by PHD allows for von Hippel-Lindau (VHL) protein to bind and promote the ubiquitination and trafficking of HIF1-α to the proteasome (Maxwell, et al., 1999; Ohh et al., 2000; Ivan et al., 2001). VHL can only bind to HIF1-α in the presence of hydroxylated prolines (Kim et al. 2006). VHL serves as the recognition element in an E3 ubiquitin ligase complex that includes elongin b, elongin c, and cullin-2 (Kibel et al., 1995; Lonergan et al., 1998; Iwai et al., 1999).

The von Hippel-Lindau syndrome, the disease from which the protein derives its name, is characterized by sporadic clear cell renal carcinomas and is associated with loss of function of the VHL, the result of either missense mutations in exon 2 or germline deletions of exon 2 (Gnarra et al., 1994; reviewed in Chew 2005). VHL inactivation in tumors leads to increased stabilization of HIF1-α, and the over-expression of HIF responsive genes, i.e., VEGF-A. VHL knockout mice models die between embryonic day 10.5 and 12.5 due to vascular aberrations of the placenta (Gnarra et al., 1997). The zebrafish transheterozygote ($vhl^{hu2117}/vhl^{hu2081}$) mutant embryo model, with two mutations in the Hif1-α binding domain, develop polycythemia, dilated blood vessels,

aberrant intersegmental vessel sprouts, and increased Vegf-a/Vegfr2 signaling (van Rooijen et al., 2009; van Rooijen et al., 2010). Despite the importance of Vhl to development, the mutants survive to 11 days post fertilization due to their size and ability to transfer oxygen from their environment, at which point they succumb to systemic hypoxia.

The lesions described in the zebrafish Vhl mutant are opposite to the vascular lesions induced by embryonic exposure to methyl tert-butyl ether (MTBE) in zebrafish, which include pooled blood in the common cardinal vein (CCV), cranial hemorrhages, abnormal intersegmental vessels (ISV), decreased circulating red blood cells, and pericardial edema (Bonventre et al., 2011). MTBE exhibits anti-angiogenic properties in both piscine and mammalian model systems while other tissues appear to develop normally (Longo, 1995; Bonventre et al., 2011; Kozlosky et al., 2012). In Japanese medaka (*Oryzias latipes*) embryos, exposure to 29.5 mM (2600 mg/L) MTBE completely inhibited vascular growth (Longo, 1995). *In vitro* rodent and human endothelial cell cultures developed fewer, thinner, and shorter capillary-like tubes in the presence of MTBE, while Matrigel plugs containing the chemical displayed fewer vascular invasions in a mouse model (Kozlosky et al., 2012). The vascular lesions in zebrafish are associated with a significant decrease in mRNA transcript levels of *vegf-a*, *vegf-c* and *vegfr2*, as well as decreased *hif1-α* and *mmp-9* at the 21-somite stage (Bonventre et al., 2011; Bonventre et al., 2012). Disruption of VEGF and VEGFR during development results in dysregulation of angiogenesis and abnormal vascular growth in the embryo (Carmeliet et al., 1996; Ferrara et al., 1996; Shalaby et al., 1995).

To test the hypothesis that MTBE induces anti-angiogenesis by targeting the HIF1-VEGF pathway, three rescue studies were conducted in an attempt to reverse MTBE induced vascular lesions (Fig. 5.2). In the first study, a zebrafish *vegf-a* expression construct (p-zfVEGF) was injected into single cell embryos to over-express the critical vascular protein, which was previously found to be downregulated following MTBE exposure (Bonventre et al., 2011). In the second study, a 2-oxoglutarate mimic and competitive inhibitor, N-oxalylglycine (NOG), was used to chemically inhibit PHD hydroxylation of Hif1-α, and thus stabilize Hif1-α and promote a localized hypoxic response. In the third study, a morpholino was designed to knockdown functional protein levels of VHL (VHL-MO) and block HIF1-α ubiquitination. The results of the rescue studies demonstrate that MTBE disrupts the HIF1-VEGF pathway. Manipulating the components of the pathway rescued different MTBE-induced vascular lesions, which provides insight into the mechanism of toxicity and indicates differential roles for HIF and VEGF in vascular system development.

5.2 Methods

5.2.1 Animal Handling

Transgenic zebrafish *fli1*-EGFPs (Fli1s), which express enhanced green fluorescent protein in all vascular endothelial cells (Lawson and Weinstein, 2002), were used for all experiments. Fli1s were obtained from the Zebrafish International Resource Center (Eugene, OR). Breeding stocks were housed in an Aquatic Habitat recirculating system under a 14:10 light:dark cycle. Water quality was maintained at <0.05 ppm nitrite, <0.2 ppm ammonia, pH between 7.2 and 7.7, and temperature between 26 and 28°C.

Husbandry (#03-014) and embryonic exposure protocols (#08-025) were approved by the Rutgers University Animal Care and Facilities Committee. During exposures, embryos were incubated at 25 °C as previously described in Bonventre et al. (2011), and all embryos were selected to be at the same stage at the beginning of each experiment.

5.2.2 Chemicals

Methyl tert butyl ether (MTBE) was obtained from Sigma Aldrich [purity 99.0 %]. N-oxalylglycine was obtained from Enzo Laboratories (Farmingdale, NY). All exposure solutions were made the day of treatment with aerated egg water (60 µg/ml Instant Ocean in ddH_2O).

5.2.3 Zebrafish vegf-a containing plasmid

The $pCS2^+$ vector containing zebrafish vegf-a sequence was obtained from Dr. Ruowen Ge at the National University of Singapore, Singapore 119260, Singapore (Liang et al., 2001). The vector was transfected into DH5-alpha competent *E. coli* cells (Protein Express) and amplified under ampicillin selection. Sequencing reactions using an SP6 forward primer and M13 reverse primer were performed to verify the *vegf-a* sequence. A pCS2+ vector control without the insert (empty vector) was also prepared by restriction digestion with EcoRI, followed by re-ligation of the empty backbone. Based on previously reported VEGF rescue studies in zebrafish (Habeck et al., 2002; Bahary et al., 2007), 80 pg of gel purified plasmid (QIAGEN Gel Extraction kit), with or without insert, was injected into each embryo at the 1-4 cell stages for the gene rescue experiments. The total injection volume was 8 nl.

5.2.4 *N-oxalylglycine*

A dose finding study was performed to determine an appropriate concentration of NOG to use for the rescue study since this is the first study using NOG in the zebrafish embryo model. The first concentrations tested were based on the published in vitro studies: 10-50 μM for cell lystate studies and 500-1000 μM for cell culture studies (Jaakkola et al., 2001; Wirthner et al., 2007). Embryos were first exposed to 20, 60, 100, 500, and 2500 μM starting at the 512-cell stage in sealed glass scintillation vials with 10 embryos per concentration, and observed for 5 days for developmental defects. Based on the results of the dose finding a study, a 2 hr incubation with 50, 200, 500 μM NOG was performed at 21-somites to determine the ability of NOG to alter the expression of *vegf-a, vegf-c, vegfr2, hif1-α, mmp-9,* and *elgn3* at those concentrations. The length of the incubation was chosen to be enough time to induce mRNA changes. Ultimately 200 μM NOG was chosen for the chemical rescue studies.

5.2.5 von Hippel-Lindau protein morpholino

An antisense morpholino to zebrafish von Hippel-Lindau protein (VHL-morpholino oligonucleotide [MO]), designed to target the intron 1-exon 2 splice site on the pre-mRNA sequence, was obtained from Gene Tools, LLC (Philomath, OR). The sequence of the VHL-MO was 5'-TGTCCTGACAGAACAGGAAAAACA-3', and was designed to delete exon 2, known to be associated with the VHL disease syndrome in humans (Gnarra et al., 1994). A standard control morpholino (CoMO) sequence from the Gene Tools was used as a control, and the sequence was previously published in Hillegass et al. (2007). A dose finding study to observe embryonic survival and possible

VHL-MO phenotypes was performed using 12.5, 25, 50, 100, 200, and 400 μM of the VHL-MO. Embryos were injected at the 1-4 cells stage with a total injection volume of 8 nl of the morpholino and observed daily. Based on the dose finding study, 8 nl of 25 μM VHL-MO or 50 μM of CoMO were used for the morpholino rescue experiments.

5.2.6 Morphological Rescue Studies

Following OECD 212 guidelines, embryos were exposed individually in sealed 4 ml glass vials to static, non-renewal concentrations 10 mM MTBE (nominal concentration). Due to the increased death that results from injection at the 1-2 cell stages, 40 embryos were set up for all injected embryo groups (empty vector and p-zfVEGF, or CoMO and VHL-MO, both with and without MTBE). Uninjected controls untreated and treated with 10 mM MTBE were set up for each study (N = 20). For NOG studies, 25 embryos per treatment group were used, and embryos were exposed to either 5 or 10 mM MTBE in the presence or absence of 200 μM NOG. Untreated and NOG only treatments served as controls. Treatment of NOG began at the same time as the MTBE treatment, at approximately the 512 cell stage. Embryos were observed under light and fluorescence microscopy daily over the 5 day developmental period characteristic of zebrafish development at 25°C. The occurrence of MTBE specific vascular lesions, pooled blood in the CCV, cranial hemorrhages, and abnormal ISVs was recorded.

5.2.7 mRNA rescue of MTBE altered genes

The effect of *vegf-a* over expression, NOG, or VHL knockdown on rescuing the MTBE altered gene expression at 21-somites was determined with qualitative polymerase chain reaction (q-PCR). Embryos were exposed to a static non-renewal treatment of 0 (control) or 5 mM MTBE in 20 ml glass scintillation vials from approximately the 512 cell stage and harvested at 21-somites. Approximately 50 embryos were used per treatment and each treatment was performed in duplicate in a nested study design. Q-PCR sample preparation was carried out as described in Bonventre et al. (2012). Primer sets were selected to work with the same qPCR protocol: 35 cycles of 95°C for 15 sec and 60°C for 1 minute. All CTs were normalized to the housekeeping gene, 28s ribosomal RNA (Delaunay et al., 2000), and the relative mRNA levels were determined using standard curves. The primer sets for *vegf-a*, *vegf-c*, *vegfr2*, *hif1-α*, and *mmp-9* were previously published (Bonventre et al., 2011; Hillegass et al. 2008). The primer set for zebrafish *egln3* (BC066699) was developed using IDT PrimerQuest software: fwd 5'-GGA TTG CTG AGG ATC TTT CC- 3', rev 5'- GAT TCC TTC GAT CTG ACC AG-3'.

5.2.8 Statistical analyses

Statistical analyses were performed using the SigmaPlot version 11. Differences in lesion occurrence within the individual morphology rescue studies were determined using a Chi-square test for the categorical data. A two-way analysis of variance (ANOVA) test was used to analyze the replicate morphology studies. The results from both the Chi-square and the ANOVA were the same. Transcript levels were analyzed

using a two way ANOVA within each experimental replicate. The Holm-Sidak post hoc test was used where data were significant. The probability level for statistical significance was $p \leq 0.05$ for all studies.

5.3 Results

5.3.1 Over-expression of zebrafish *vegf-a*

5.3.1.1 Morphology rescue

Embryos were injected with a plasmid containing the zebrafish *vegf-a* gene to determine if over-expression of the gene would rescue MTBE induced vascular lesions. Injections of the plasmid with or without the insert did not result in any significant vascular or other developmental lesions among untreated embryos. Exposure to 10 mM MTBE induced a significant increase in the occurrence of pooled blood in CCV (at the Prim-25 stage), cranial hemorrhages (at Pec Fin stage), and abnormal ISVs (at Protruding Mouth stage) in empty vector injected embryos as well as the non-injected positive (MTBE) controls, consistent with Bonventre et al. (2011). There was no significant difference in the percent of animals exhibiting pooled blood in the CCV as a result of MTBE exposure between empty vector controls or p-zfVEGF injected embryos (Fig. 5.3A). There was a significant difference in the percent of embryos exhibiting cranial hemorrhages following MTBE exposure between empty vector injected embryos as compared to p-zfVEGF injected embryos (Fig. 5.3B). Over-expression of *vegf-a* resulted in a 46 (± 5.5)% rescue of animals exhibiting MTBE induced cranial hemorrhages. Similarly, there was a significant difference between empty vector and p-zfvegf injected

embryos exhibiting abnormal ISVs following MTBE exposure (Fig. 5.3C), where over-expression resulted in 35 (± 5.8)% fewer embryos exhibiting the lesion.

5.3.1.2 mRNA rescue

Embryos were injected with a plasmid containing the zebrafish *vegf-a* gene and exposed to MTBE until 21-somites to determine if over-expression of the gene would rescue MTBE suppression of angiogenesis related genes. Exposure to 5 mM MTBE resulted in decreased transcript levels at 21-somites of *vegf-a*, *vegf-c*, *vegfr2*, *hif1-α*, *mmp-9*, and *egln3* in the empty vector injected embryos, with at least a 1.5 fold change (Table 5.1A). These values were consistent with previously reported studies (Bonventre et al., 2011; Bonventre et al., 2012). When embryos injected with p-zfVEGF were treated with MTBE, the transcript levels of all 6 genes were greater than in treated embryos injected with the empty vector (Table 5.1B). The differences between transcript levels of MTBE-treated empty vector compared to treated p-zfVEGF were not significant, despite the greater than 2 fold change for *hif1α*, *mmp9*, and *egln3*.

In untreated embryos, *vegf-a* over-expression resulted in a relative increase in mRNA transcripts of all the genes of interest at 21-somites. Notably, over-expression of *vegf-a* resulted in a statistically significant 4.25 fold increase in *mmp-9* transcript levels. However, following treatment with MTBE, *mmp-9* transcript levels significantly decreased from p-zfVEGF untreated embryos and back down to control levels (Fig. 5.4).

5.3.2 Chemical inhibition of PHDs by NOG

5.3.2.1 Dose finding studies

Embryos were first exposed to 20, 60, 100, 500, and 2500 μM NOG at the 512 cell stage to establish a concentration that would not elicit toxicity under the conditions required for the morphology studies. Embryos exposed to 2500 μM NOG were dead within minutes of treatment. At 24 h post treatment, greater than 20 % of the embryos exposed to 500 μM NOG were dead, while the remainder appeared opaque and showed signs of morbidity. No morphological defects were observed in the embryos exposed to 20, 60 or 100 μM NOG.

The 2 hr incubation study at the 21-somite stage was performed to determine the ability of a non-lethal concentration of NOG to alter the expression of HIF1-α related genes in our *in vivo* embryo model system. The effect of NOG on *vegf-a, vegf-c, vegfr2, hif1-α, mmp-9,* and *elgn3* is shown in Figure 5.5A-F. The trend in expression was the same for all 6 genes: 50 μM NOG had virtually no effect on expression, while 200 μM NOG increased expression the most, and at 500 μM NOG, expression either decreases from 200 μM NOG or was about the same. The difference in expression between 200 and 500 μM NOG was greatest for *egln3*. Based on the results of these studies, 200 μM NOG was chosen for the rescue studies.

5.3.2.2 Morphology rescue

Embryos were treated with a competitive inhibitor of PHDs to determine if forced accumulation of Hif1-α and stimulation of hypoxia pathways would rescue MTBE induced vascular lesions. Treatment with 200 μM NOG alone did not result in any

significant lesions. There was a significant increase in the incidence of pooled blood in CCV, cranial hemorrhages, and abnormal ISVs in the embryos treated with only 5 or 10 mM MTBE (positive control), consistent with Bonventre et al. (2011). Co-exposure of embryos to 5 mM MTBE and NOG resulted in 24 (± 6.0) % fewer embryos exhibiting pooled blood in CCV, a significant decrease from exposure to 5 mM MTBE alone (Fig. 5.6A). The percent of embryos exhibiting cranial hemorrhages or abnormal ISVs was also decreased for 5 mM MTBE plus NOG, but the decrease was not significant for either lesion (Fig. 5.6B and C). Similarly, co-exposure to 10mM MTBE and NOG resulted in decreased occurrence of all three lesions when compared to embryos exposed to 10mM MTBE only; however, the difference was only significant for cranial hemorrhage occurrence (32 ± 3.9 %).

5.3.2.3 mRNA rescue

Embryos were treated with a competitive inhibitor of PHDs to determine if forced accumulation of Hif1-α and stimulation of hypoxia pathways would rescue MTBE suppression of angiogenesis-related genes. Exposure to 5 mM MTBE decreased mRNA transcripts for *vegf-a*, *vegf-c*, *vegfr2*, *hif1-α*, *mmp-9*, and *egln3* at 21-somites. Co-exposure with 200 μM NOG altered the effect of MTBE on the expression for all but *egln3* (Table 5.2). Embryos co-treated with MTBE and NOG had a greater than 2 fold increase of *vegf-a* (2.35 fold), *vegfr2* (2.40 fold), and *mmp-9* (2.65 fold), as compared to embryos exposed to 5 mM MTBE alone. Co-treated embryos expressed 1.75 fold increase in *vegf-c*, and only a 1.22 fold increase in *hif1-α*, as compared to MTBE alone. Despite the differences, the statistical analyses were not significant

5.3.3 Antisense morpholino to zebrafish von Hippel-Lindau protein

5.3.3.1 Dose finding studies

Since VHL is critical for normal development, embryos were injected with a wide range of VHL-MO to determine a concentration where a knock-down of the protein would not be lethal. Approximately 100 embryos were injected with 12.5, 25, 50, 100, 200, or 400 μM of the VHL-MO and observed for 5 days. Mortality and lesion occurrence in the embryos were qualitatively assessed. Injection of both 200 and 400 μM VHL-MO resulted in greater than 90% mortality in the embryos by day 5, with 100% of the remaining embryos exhibiting classic morpholino toxicity, including shortened body structure, gnarled tail, and small head and eyes (Bedell et al., 2011). Morpholino toxicity was apparent in more than 75% of the embryos injected with 100 μM VHL-MO, and in approximately 50% of embryos injected with 50 μM. However, observation of 50 μM injected embryos with fluorescence microscopy revealed a number of embryos exhibiting addition aberrant vascular structures associated with the ISVs (Fig. 5.7 B, C). Embryos injected with 12.5 or 25 μM VHL-MO appeared to develop normally. Therefore, despite the extra vessels observed with 50 μM, 25 μM VHL-MO was used for the rescue studies since it was the highest concentration tested that did not cause morpholino toxicity in the embryos.

5.3.2.2 Morphology rescue

Embryos were injected with the VHL-MO to determine if blocking Hif1-α degradation would rescue MTBE induced vascular lesions. Morpholino injections of

either 50 μM Co-MO or 25 μM VHL-MO resulted in no significant lesions among untreated embryos. MTBE induced a significant increase of pooled blood in CCV, cranial hemorrhages, and abnormal ISVs in Co-MO injected embryos as well as non-injected positive controls, consistent with Bonventre et al. (2011). VHL morphants had a significant 35 (± 4.5)% decrease in embryos exhibiting pooled blood in CCV following exposure to MTBE when compared to exposed Co-MO injected embryos (Fig. 5.8A). A similar trend was observed for MTBE induced cranial hemorrhages, however the results were not significant (Fig. 5.8B). VHL-MO injection did not significantly change the percent of embryos exhibiting MTBE induced abnormal ISVs when compared to Co-MO injected animals (Fig. 5.8C).

5.3.2.3 mRNA rescue

Embryos were injected with the VHL-MO to determine if blocking Hif1-α degradation would rescue MTBE induced suppression of angiogenesis-related genes. Exposure to 5 mM MTBE resulted in decreased transcript levels at 21-somites of *vegfa* (-1.53), *vegf-c* (-1.69), *hif1-α* (-1.20), *mmp-9* (-1.31), and *egln3* (-3.19) in the Co-MO injected embryos (Table 5.3A). When VHL-MO injected embryos were treated with MTBE, the transcript levels of all 6 genes were greater than in Co-MO embryos treated with MTBE (Table 5.3B). The differences between transcript levels of MTBE-treated Co-MO verses treated VHL-MO were not significant, despite the greater than 2 fold change for *vegf-c, vegfr2, mmp-9,* and *egln3*.

5.4 Discussion

The relationship between Hif1 and Vegf is critical to normal embryogenesis. In murine knockout studies, a loss of either gene causes aberrant vascularization in the embryo and lethality (Ryan et al., 1998; Carmeliet et al., 1996; Ferrara et al., 1996). Morpholino knockdown of vegf-a or vegfr2 in the zebrafish causes vascular lesions in the cranium and dorsal segmental vessels (Nasevicius *et al.*, 2000; Bahary et al., 2007). Exposure of zebrafish to MTBE during development results in similar vascular lesions and a decrease in mRNA transcript levels of *vegf-a*, *vegf-c*, and *vegfr2* (Bonventre et al., 2011). Here, we rescued MTBE-induced vascular lesions in zebrafish by manipulating the Hif1-Vegf pathway through over-expression of zebrafish *vegf-a* and forced accumulation of Hif1-α.

Pooling of blood in the CCV is the first MTBE induced vascular lesion observed in developing zebrafish (Bonventre et al., 2011). Both co-exposure to NOG and morpholino knockdown significantly rescued the appearance of this lesion, while over expression of zebrafish *vegf-a* via p-zfVEGF did not (Figs. 5.3A, 5.6A, and 5.8A). The CCV begins as paired branches from the posterior caudal vein that form across the center of the yolk directing red blood cells through a broad vessel to the heart. As the embryo grows, the CCV shrinks in size and width as additional veins develop to bring deoxygenated red blood cells to the heart (Kimmel et al., 1995; Isogai et al., 2001). The pooled blood in the CCV induced by MTBE exposure occurs when the CCV is still a broad vessel, during the Prim-25 stage of development. Red blood cells accumulate in the lower (caudal) portion of the CCV, and circulation toward the heart does not occur in the severest forms of the lesion (Bonventre et al., 2011). MTBE is not the only toxicant

known to disrupt normal CCV formation. TCDD inhibits CCV growth and regression in zebrafish embryos in an aryl hydrocarbon receptor-2 (AHR2)-dependent manner (Bello et al., 2004). Both Hif-α and AHR are known to bind to Hif-β, known also as the aryl hydrocarbon receptor nuclear transporter. Multiple isoforms of Hif-α and Hif-β exist in both zebrafish and higher vertebrates, but regulation by PHDs and VHL is similar for each of the known Hif-αs (reviewed in Keith et al., 2012). Therefore, NOG and VHL knockdown have the potential to force the accumulation of all three Hif-α isoforms, and increase the availability of Hif-αs to bind to Hif-βs. In contrast, over-expression of *vegf-a* does not directly stimulate Hif-α/Hif-β activation. Together, the TCDD study and our MTBE-rescue studies, via different mechanisms, suggest an important role for Hif-β activity in the formation of the CCV in zebrafish embryos.

Both cranial hemorrhages and abnormal ISVs were rescued by over-expression of *vegf-a* (Figs. 5.3B and C). Following MTBE exposure, cranial hemorrhages and the ISV lesion occur predominately at the Pec Fin and Protruding Mouth stages, respectively (Bonventre et al., 2011). These lesions are similar to those described in embryos injected with a vegf-a morpholino (Nasevicius et al., 2000; Bahary et al., 2007). Much like embryonic exposure to MTBE, the initial establishment of the axial vasculature was not affected in the vegf-a morphant. In contrast, the development of the cranial vasculature and ISVs is vegf-a dependent (Nasevicius et al., 2000; Bahary et al., 2007). Vegfr2 is also important in ISV formation in zebrafish as both mutants and morpholinos have demonstrated (Habeck et al., 2002; Bahary et al., 2007). Over-expression of *vegf-a* did not, however, rescue the lack of ISV in vegfr2 mutant embryos, indicating normal ISV development is dependent upon vegfr2 signaling (Habeck et al. 2002). Since over

expression of *vegf-a* rescues MTBE induced ISV abnormalities, MTBE does not directly effect Vegfr2, but rather its ligand, Vegf-a.

Co-exposure to NOG also rescued MTBE-induced cranial hemorrhages (Fig. 5.6B), but not the ISV lesion (Fig. 5.6C), demonstrating a role for Hif1-α in cranial vasculature development, most likely through upregulation of Vegf-a. A different 2-oxoglutarate mimic has been previously used in zebrafish embryos to simulate systemic hypoxia. However, embryonic exposure to dimethyloxalylglycine (DMOG) prior to 3 days post fertilization was lethal (van Rooijen et al., 2009). Embryos exposed to DMOG from 3 to 7 days post fertilization exhibited an increase in expression of *egln3*, *vegf-a*, and *erythropoietin* mRNA compared with the controls. The 2-hour incubation with NOG also increased transcript levels of *egln3* and *vegf-a*, in addition to other angiogenesis related genes (Fig. 5.5A-F). However, alterations in gene expression were not apparent at the 21-somites, following 24 hrs of exposure to NOG alone. This is likely due to the fact that by that time point NOG was metabolized to a concentration that no longer alters the mRNA transcript levels. The short incubation experiment demonstrated that exposure to 200 μM NOG altered the expression of hypoxia related genes at some point during the co-exposure with MTBE. NOG was toxic to embryos above 200 μM when exposed from 3 hours post fertilization onward. The ability of the chemical to completely ameliorate the MTBE lesions may have been limited by the concentration used in the experiments. Due to the critical period of MTBE in zebrafish (6-somites to Prim 5 stages of development) and the experimental design (static, non-renewal in sealed glass vials), it was necessary to use a concentration of NOG that was not lethal under these conditions. As a result, only the CCV and cranial hemorrhage lesions were rescued significantly with NOG, despite

the fact that forced accumulation of Hif-α should have resulted in increased Vegf-a and rescued treated embryos from MTBE-induced vascular lesions, as demonstrated by the p-zfVEGF rescue study. In addition, NOG is a competitive inhibitor and therefore it does not completely prevent PHD activity unless the concentration of NOG exceeds that of the endogenous substrate, 2-oxoglutrate. The difference in survival between 200 and 500 μM NOG could be explained by incomplete inhibition of PHD activity by 200 μM NOG, which would suggest some Hif1-α hydroxylation occurs in rescue studies.

Similarly, VHL knockdown only significantly rescued MTBE-induced pooled blood in the CCV. This may have resulted from the necessity to use a very low concentration of VHL-MO so as to not induce morpholino toxicity in the embryos (Bedell et al., 2011). When higher concentrations of the morpholino were used (Fig. 7B, 7C), extra blood vessels were observed in the ISVs similar to those reported in the VHL mutant zebrafish (van Rooijen et al., 2010). Like NOG, the VHL-MO should have resulted in an indirect increase of Vegf-a by forcing an accumulation of Hif1-α, however, because the VHL-MO only transiently knocked down VHL protein, and therefore ubiquitination of Hif1-α, it did not block hydroxylation of Hif1-α by PHD, and does not preclude the possibility that hydroxylated Hif1-α may be degraded by some other mechanism hitherto unknown. The change in concentration of the Vegf-a by either the chemical or morpholino at the concentrations tested was unable to completely override the mechanism by which MTBE induces vascular lesions.

Due to MTBE's specificity to developing vasculature, the hypothesis was that MTBE acted through a VEGF-dependent mechanism. Indeed, MTBE significantly decreases mRNA transcripts of *vegf-a* and *vegf-c* at 21-somites (Bonventre et al. 2011).

The expression of all of our genes of interest were increased from the 5 mM MTBE treated experimental control by both p-zfVEGF and VHL-MO, and all but *egln3* were increased by co-exposure with NOG. While these increases were not statistically significant, they suggest a possible mode of action by which the morphological lesions were rescued. The lack of significance may be due to variability in embryonic stage at a period of rapid growth (see Chapter 4, Fig. 4.1), variability in injection volume, or timing, as the mRNA expression of genes was sampled at only one stage.

Finally, the effect of MTBE on the relationship between Vegf-a and Mmp-9 expression was also demonstrated in the *vegf-a* over-expression study. Over-expression of *vegf-a* caused a statistically significant increase in *mmp-9* transcript levels at 21-somites (Fig. 5.4). The significant increase in *mmp-9* mRNA was lost when p-zfVEGF injected embryos were exposed to 5 mM MTBE. These data provide two important points of information: 1) injection of p-zfVEGF resulted in an increase in Vegf-A as *mmp-9* transcription is induced by VEGF-A through the VEGFR2 signaling cascade (Wang and Keiser, 1998; Pufe et al., 2002; Hollborn et al., 2007), and 2) MTBE disrupts a known function of Vegf-A. Exposure to MTBE was shown to decrease *mmp-9* in zebrafish greater than 2 fold at 21-somites (Bonventre et al., 2012). In mice, a deficiency in MMP-9 resulted in increased vascular permeability (Kolaczkowska et al., 2006). Perhaps the increased cranial hemorrhages observed with the MTBE treatment result from an Mmp-9-induced vascular permeability that results from the decrease in *vegf-a* mRNA. Further studies would be needed to better understand how this disruption occurs.

5.5 Conclusions

The hypothesis tested in this chapter was that MTBE induced anti-angiogenesis resulted from a dysregulation of the HIF1-VEGF pathway. Our data support this hypothesis (Table 4). Over expression of zebrafish *vegf-a* significantly reduced the occurrence of cranial hemorrhages (46%) and abnormal ISV (35%) in MTBE exposed embryos, but did not rescue the pooled blood in the CCV lesion. Co-exposure to NOG significantly rescued the CCV lesion (24%) and cranial hemorrhages (32%), while the VHL-MO rescued only the CCV lesion (35%). Manipulating components of the pathway rescued different MTBE induced vascular lesions, which provides insight into differential roles for Hif and Vegf in the development of different vascular structures. Furthermore, it was demonstrated that MTBE does in fact disrupt Vegf-a activity as 5 mM MTBE inhibited an increase in *mmp-9* mRNA induced by *vegf-a* over-expression. However, exactly how MTBE inhibits Vegf-a is still unclear. Studies investigating MTBE's effect on *vegf-a* promoter activity, mRNA stability and protein concentrations, as well as studies identifying the activity and stability of Hif1-α, would provide further insight into the mechanism by which MTBE inhibits Vegf-a and disrupts angiogenesis.

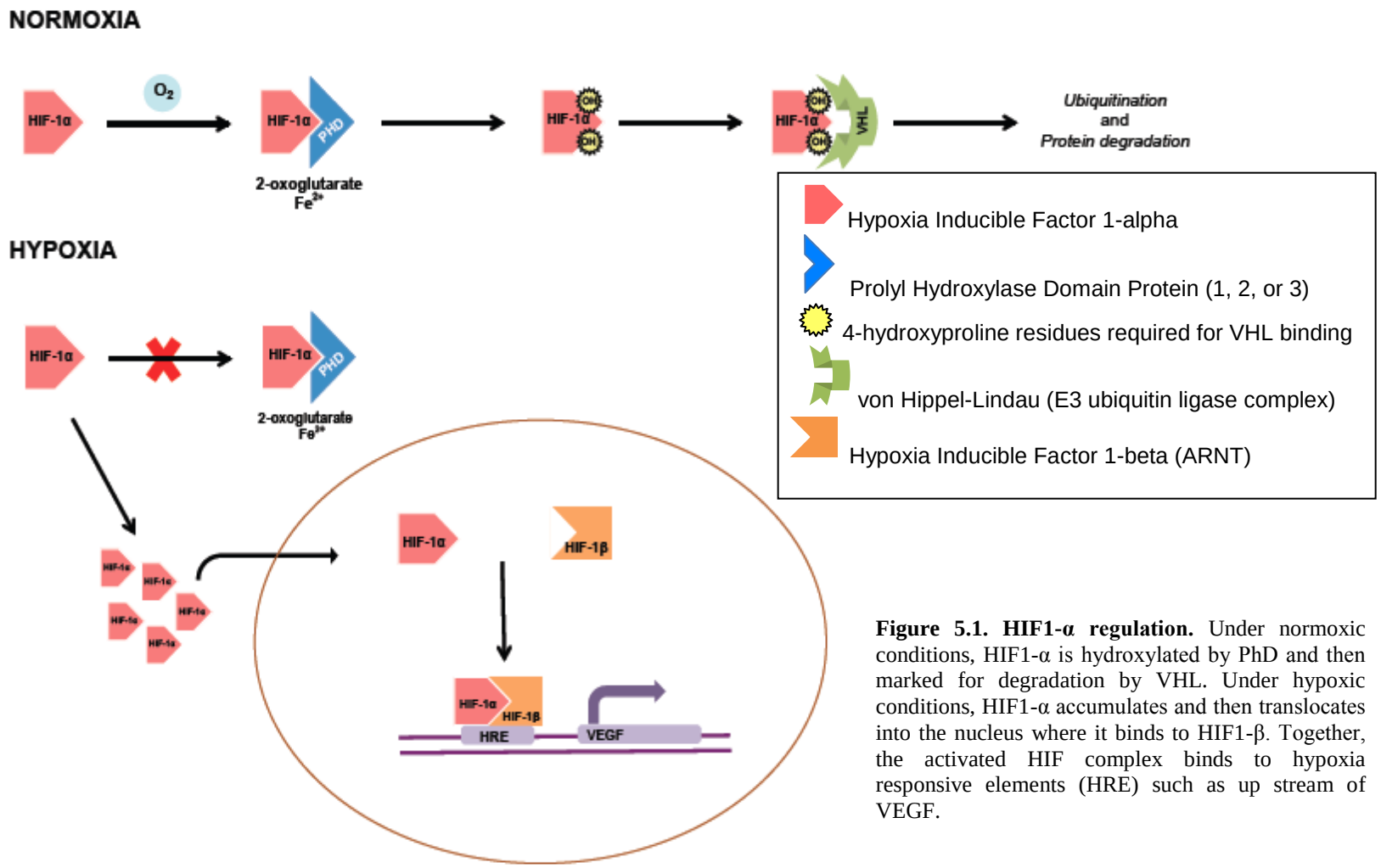

Figure 5.1. HIF1-α regulation. Under normoxic conditions, HIF1-α is hydroxylated by PhD and then marked for degradation by VHL. Under hypoxic conditions, HIF1-α accumulates and then translocates into the nucleus where it binds to HIF1-β. Together, the activated HIF complex binds to hypoxia responsive elements (HRE) such as up stream of VEGF.

150

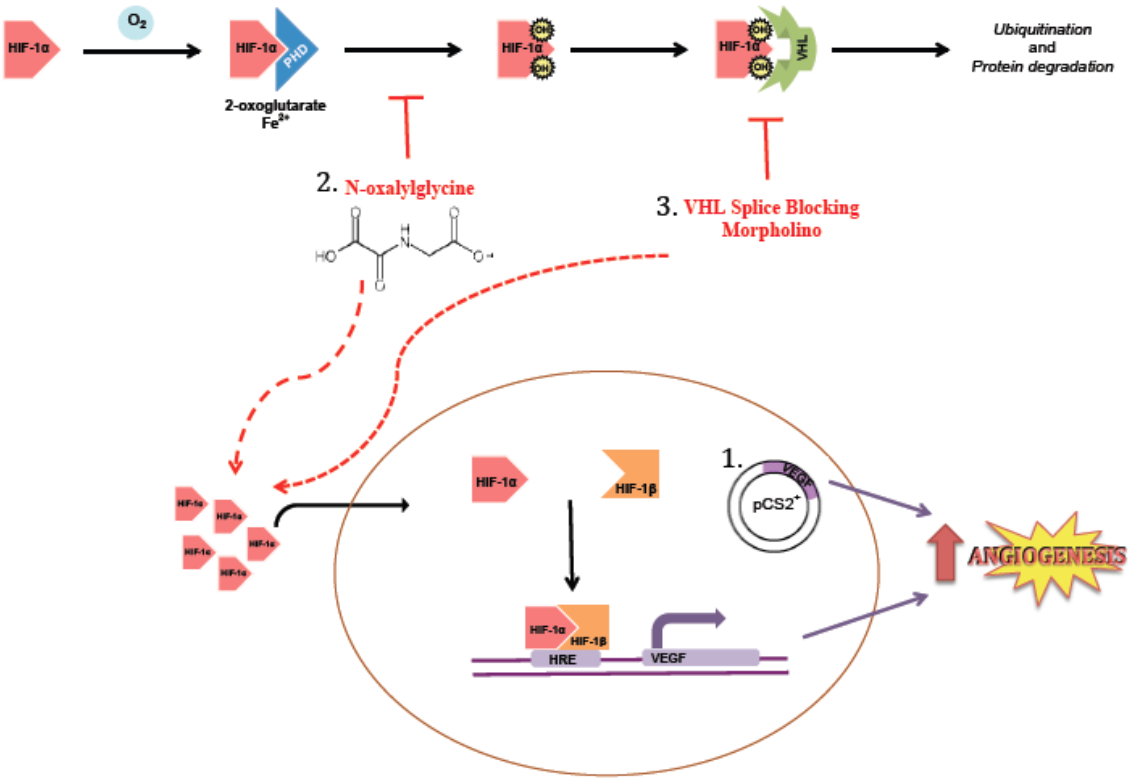

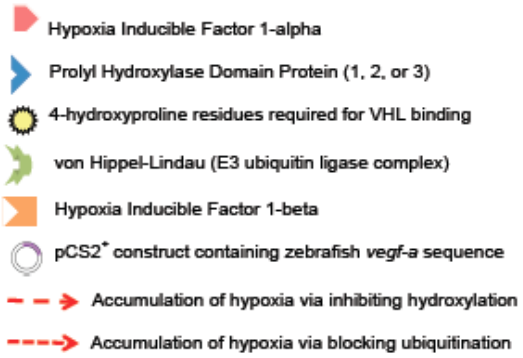

Figure 5.2. Rescue study design. Study 1.) A pCS2^{+} expression construct containing zebrafish *vegf-a* was injected into single cell embryos to over express the critical vascular protein. Study 2.) N-oxalylglycine (NOG) is a 2-oxoglutarate mimic and acts as a competitive inhibitor of PHD activity. Inhibiting PHD hydroxylation of Hif1-α, stabilizes Hif1-α and promote a localized hypoxic response. Study 3.) A morpholino was designed to knockdown functional protein levels of VHL (VHL-MO) and block HIF1α ubiquitination, which should indirectly lead to the stabilization of Hif1-α and translocation into the nucleus.

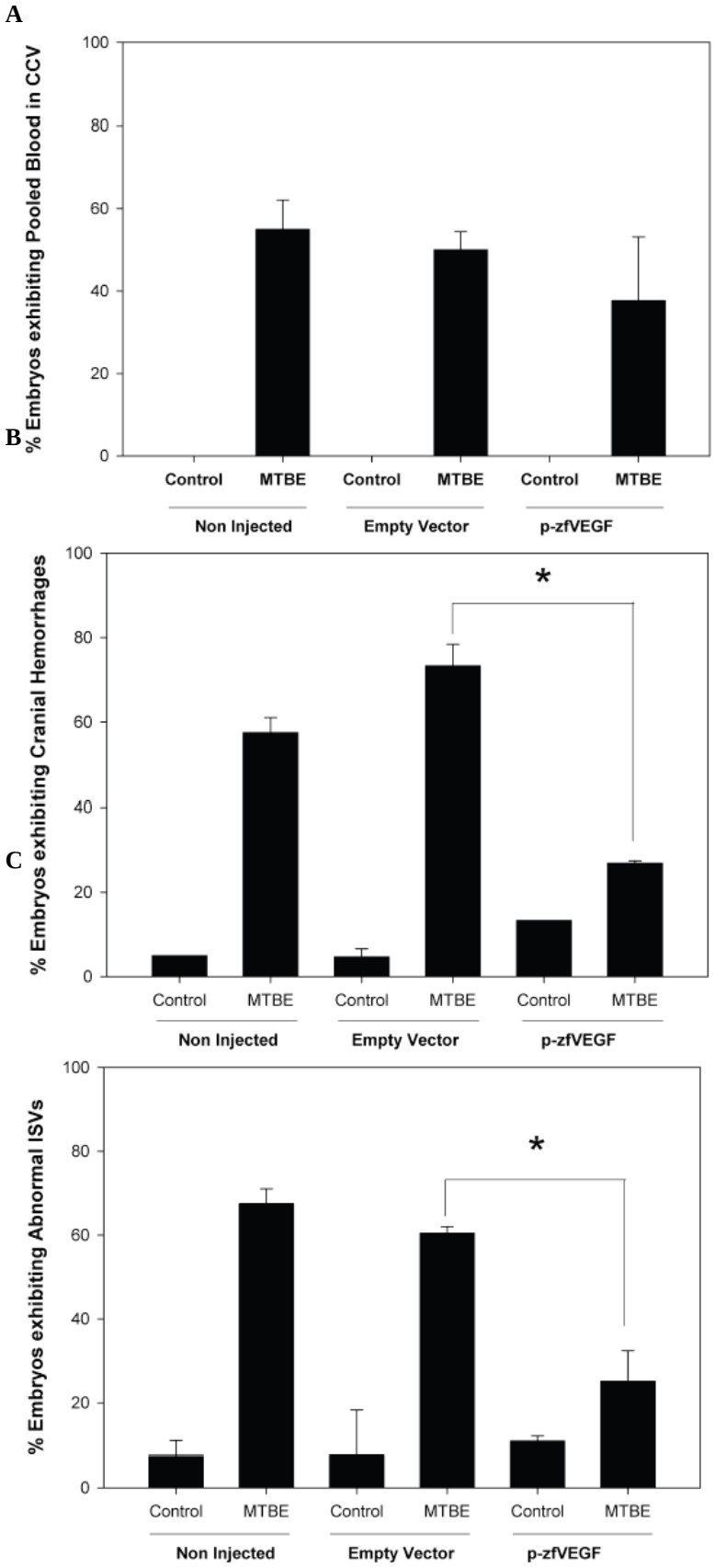

Figure 5.3. Over-expression of zebrafish *vegf-a* rescued some MTBE-induced vascular lesions. A) Exposure to 10 mM MTBE induced a significant increased in pooled blood in the common cardinal vein (CCV) in non-injected, empty vector, and p-zfVEGF embryos compared to the respective controls. Over-expression of *vegf-a* did not rescue the CCV lesion. B) Exposure to 10 mM MTBE induced cranial hemorrhages in non-injected and empty vector injected embryos, compared to controls, but not in embryos injected with p-zfVEGF. Overexpression of vegf-a rescued the occurrence of cranial hemorrhages following MTBE exposure (*). C) Exposure to 10 mM MTBE caused abnormal intersegmental vessel (ISV) development in non-injected and empty vector injected embryos, but not in embryos injected with p-zfVEGF. Overexpression of vegf-a rescued the occurrence of abnormal ISVs following MTBE exposure (*).

Table 5.1A. The effect of MTBE on mRNA transcript levels in Empty Vector injected embryos at 21-somites.

	Fold Δ between empty vector and empty vector + MTBE
vegf-a	- 1.60
vegf-c	- 2.00
vegfr2	- 1.88
hif1-α	- 1.70
mmp-9	- 1.58
egln3	- 3.55

Table 5.1B. Average fold change in mRNA transcript levels between Empty Vector and p-zfVEGF treated MTBE at 21-somites.

	Fold Δ between empty vector +MTBE and p-zfVEGF + MTBE
vegf-a	+ 1.87
vegf-c	+ 1.77
vegfr2	+ 1.65
hif1-α	+ 2.23
mmp-9	+ 2.26
egln3	+ 2.88

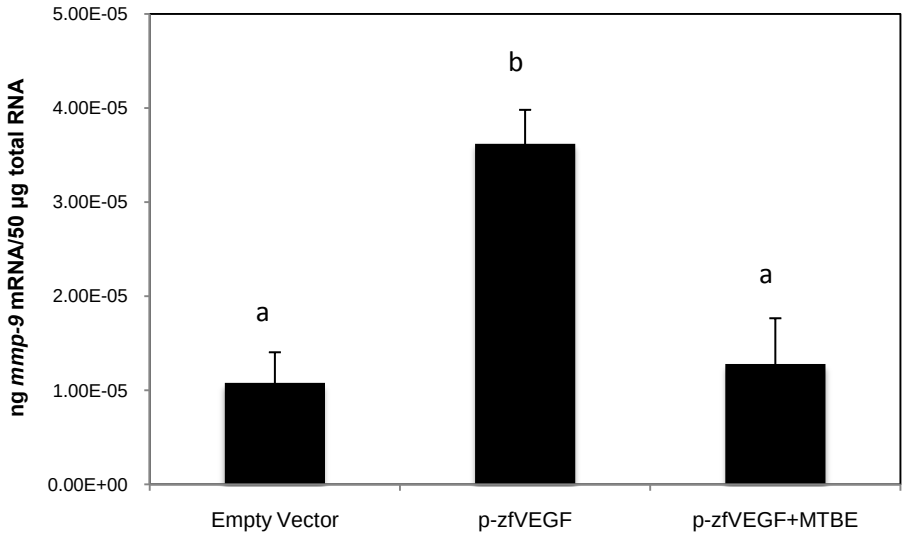

Figure 5.4: MTBE inhibits Vegf-A mRNA induction of *mmp-9*. Over-expression of *vegf-a* by injection of p-zfVEGF caused a significant increase in *mmp-9* transcript from empty vector control. However, p-zfVEGF injected embryos treated with 5 mM MTBE had a significantly lower expression than untreated p-zfVEGF embryos. Letters denote statistical significance.

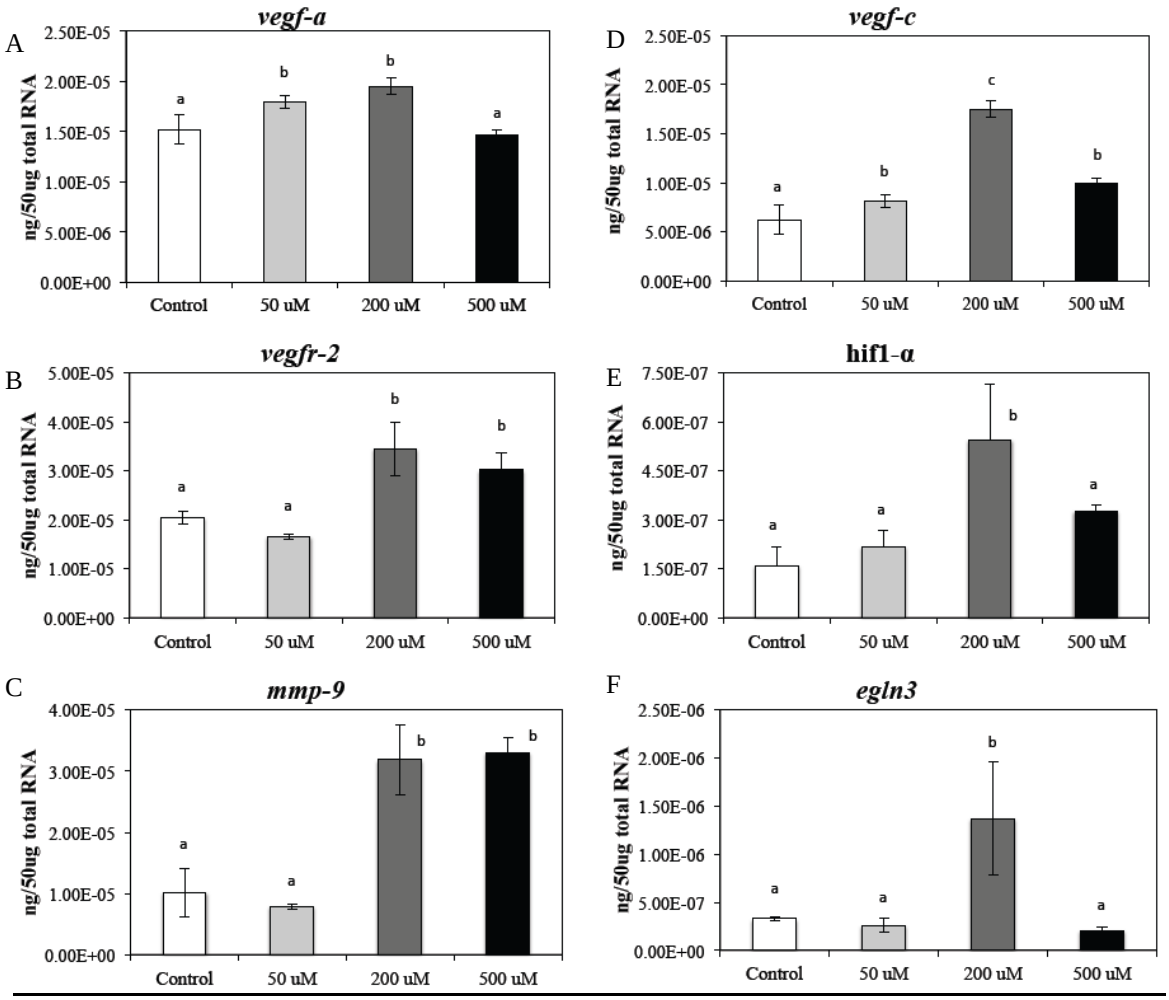

Figure 5.5. NOG upregulates the mRNA transcript levels of key genes involved in angiogenesis and hypoxia regulation. A 2 hr incubation with NOG at 21-somites demonstrated a similar trend in expression for all 6 genes: 50 µM NOG had virtually no effect on expression, while 200 µM NOG increased expression the most, and at 500 µM NOG, expression either decreases from 200 µM NOG or was about the same. The letters represent significantly different values determined by a One-Way ANOVA followed by a Student-Newman-Keuls post hoc. The difference in expression between 200 and 500 µM NOG was greatest for *egln3*. Based on the results of these studies, 200 µM NOG was chosen for the rescue studies.

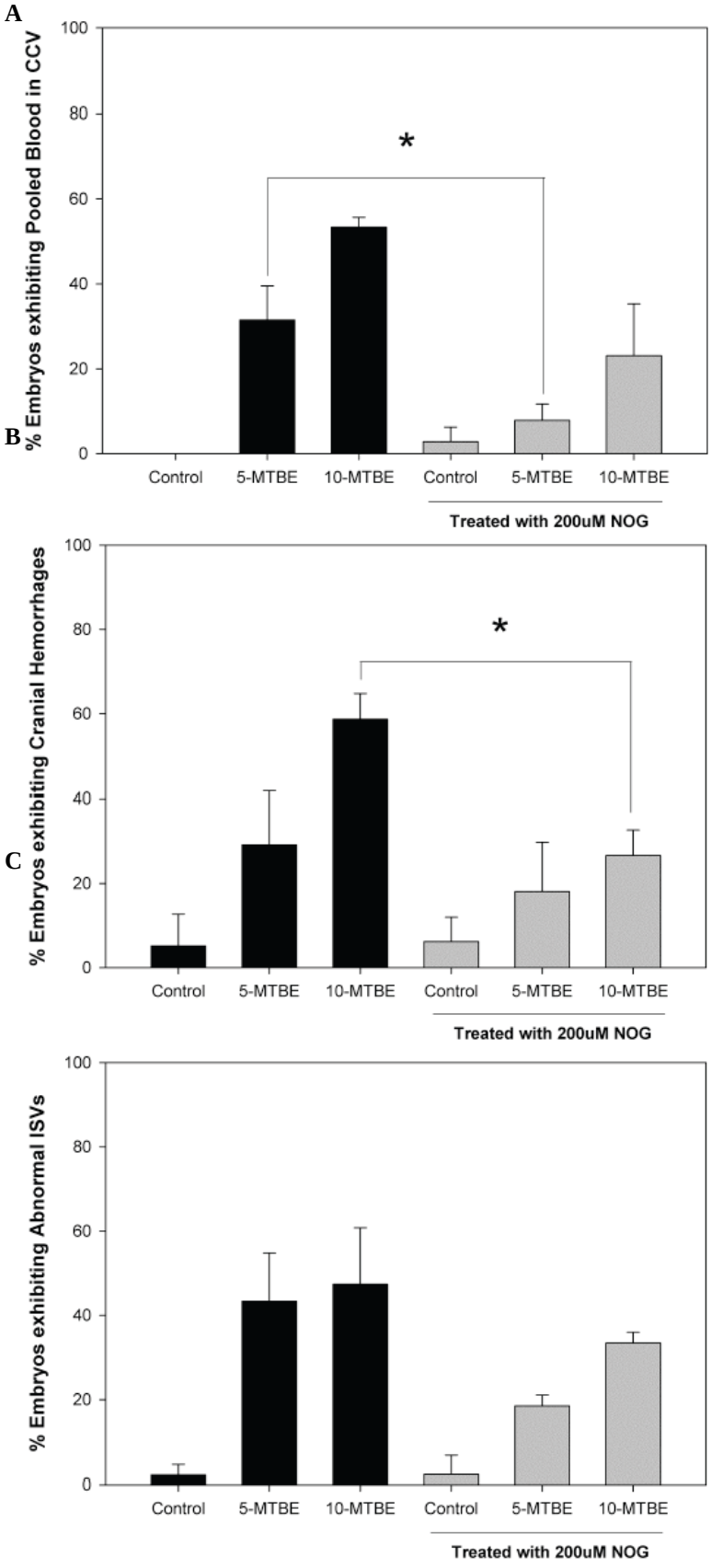

Figure 5.6. Co-exposure with N-oxalylglycine (NOG) rescued some MTBE-induced vascular lesions. A) Exposure to 5 or 10 mM MTBE induced a significant increased in pooled blood in the common cardinal vein (CCV). NOG significantly decreased the percent of embryos exhibiting this lesion in co-treatments with 5 mM MTBE (*), but not 10 mM MTBE. B) Exposure to 10 mM MTBE significantly increased cranial hemorrhages. NOG significantly decreased the percent of embryos exhibiting this lesion in co-treatments with 10 mM MTBE (*). C) Exposure to 5 or 10 mM MTBE caused abnormal intersegmental vessel (ISV). Co-treatment with NOG did not rescue the occurrence of this lesion at the concentration tested.

Table 5.2. Average fold change in mRNA transcripts levels between MTBE treatments and MTBE/NOG co-treatment at 21-somites

	Fold Δ
vegf-a	+ 2.35
vegf-c	+ 1.75
vegfr2	+ 2.40
hif1-α	+ 1.22
mmp-9	+ 2.65
egln3	-1.38

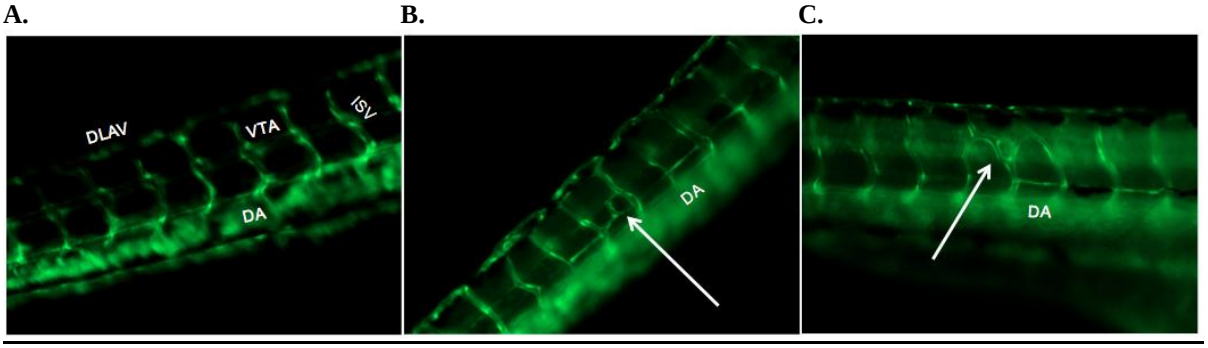

Figure 5.7. VHL-MO caused additional angiogenic sprouts in ISVs. At the Protruding Mouth stage, control embryos (A) exhibited normal dorsal vascular structures with intersegmental vessels [ISV] projecting perpendicular to the dorsal aorta [DA], connected dorsally by the dorsal longitudinal anastomotic vessel [DLAV] and in the middle by the vertebral artery [VA]. Aberrant angiogenic sprouts were observed in some embryos injected with 50 μM of VHL-MO at the same time point (B, C).

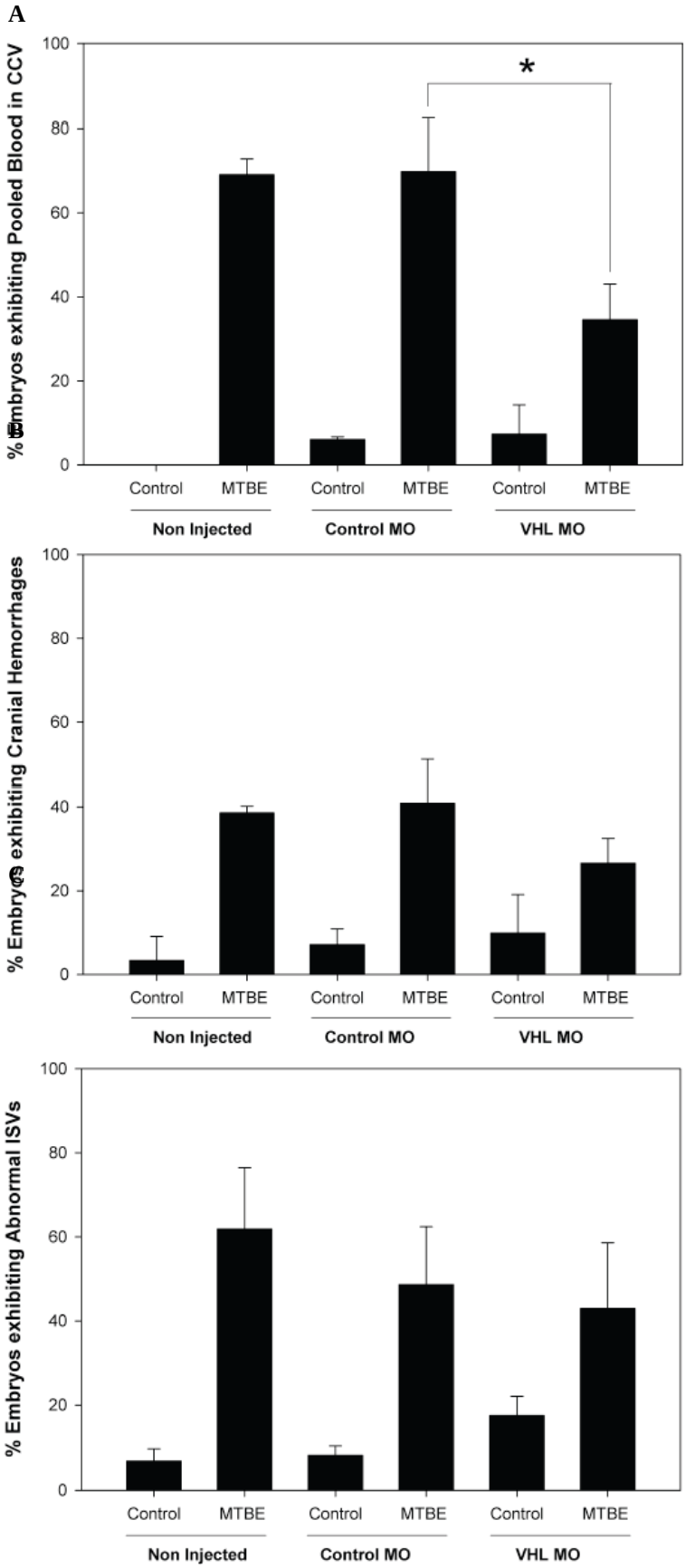

Figure 5.8. VHL knockdown rescues an MTBE-induced vascular lesion. A) Exposure to 10 mM MTBE induced a significant increased in pooled blood in the common cardinal vein (CCV) in non-injected and control morpholino (CoMO) injected embryos, but not in VHL morphants. VHL knockdown rescued the occurrence of pooled blood in the CCV following MTBE exposure (*). B) Exposure to 10 mM MTBE induced cranial hemorrhages in non-injected, CoMO, and VHL-MO injected embryos. VHL morphants were not protected against MTBE induced cranial hemorrhages. C) Exposure to 10 mM MTBE induced abnormal intersegmental vessel (ISV) development in non-injected, CoMO, and VHL-MO injected embryos. VHL morphants were not protected against MTBE induced abnormal ISV development.

Table 5.3A: The effect of MTBE on mRNA transcript levels in Co-MO injected embryos at 21-somites.

	Fold Δ between Co-MO and Co-MO + MTBE
vegf-a	- 1.53
vegf-c	- 1.69
vegfr2	- 1.04
hif1-α	- 1.20
mmp-9	- 1.31
egln3	- 3.19

Table 5.3B. Average fold change in mRNA transcripts levels between Co-MO treated with MTBE and VHL-MO treated with MTBE at 21-somites.

	Fold Δ between Co-MO + MTBE and VHL-MO + MTBE
vegf-a	+ 1.71
vegf-c	+ 2.02
vegfr2	+ 2.04
hif1-α	+ 1.61
mmp-9	+ 2.02
egln3	+ 2.17

Table 5.4. Summary of Morphology Rescue Studies (Average % rescue ± SD[#])

	N	Pooled Blood in the CCV	Cranial Hemorrhages	Abnormal ISVs
p-zfVEGF	2	12 ± 11.1	46 ± 5.5 *	35 ± 5.8 *
NOG (5 mM)	3	24 ± 6.0 *	11 ± 7.0	25 ± 12.8
NOG (10 mM)	3	30 ± 11.6	32 ± 3.9 *	14 ± 12.1
VHL-MO	3	35 ± 4.5 *	14 ± 13.9	6 ± 4.0

For zfVEGF Plasmid, ± range
* Statistically significant rescue

Chapter 6

General Discussion and Conclusions

The studies presented in this dissertation support the hypothesis that MTBE anti-angiogenesis is mediated by a disruption of the VEGF pathway. Specific MTBE-induced vascular lesions were associated with a decrease in mRNA transcripts of several genes important to angiogenesis within the critical period established for MTBE. Dose-response studies with structurally similar ETBE and TAME demonstrated that the addition of a single methyl group resulted in chemicals with greater toxicity to multiple organ systems, and emphasized the distinctive quality of MTBE to target developing vasculature. An analysis of the global gene expression changes in zebrafish exposed to MTBE during the critical period supported the hypothesis, and in addition, implicated alternative pathways that are affected by MTBE toxicity. Finally, manipulation of the HIF-VEGF pathway to rescue the specific MTBE induced vascular lesions, via an over-expression of *vegf-a* and inhibition of HIF degradation, demonstrated convincingly that MTBE toxicity is mediated by the down-regulation of VEGF at a critical time in the developing cardiovascular system. This research opens up new avenues for future studies to better understand the sensitivity of the vascular system to toxicants and identify new targets that can be useful in developing agents for up- or down-regulating angiogenesis in solid tumors, wound repair, and diabetes-induced vascular damage.

6.1 MTBE targets developing vasculature

The findings from chapters 2, 3, and data from Kozlosky et al. (2012) collectively demonstrated the specificity of MTBE's toxicity to developing vasculature. All of the

lesions present in MTBE exposed zebrafish were associated with the cardiovascular system, with no visible lesions observed in any other organ system (Table 2.3). The three predominant lesions were: pooled blood in the common cardinal vein (CCV), cranial hemorrhages, and abnormal intersegmental vessels (ISVs) (Fig. 2.3, 2.4, 2.5). Furthermore, these vascular lesions were not observed with the putative metabolites tert-butyl alcohol and formaldehyde, indicating the lesions was a result of exposure to the parent compound (Table 2.3). In contrast, embryonic exposure to the same molar concentrations of structurally similar ETBE or TAME resulted in greater toxicity than observed with MTBE, and in lesions in multiple organ systems (Tables 3.4, 3.5, 3.8). ETBE and TAME were also less effective in altering the mRNA expression of *vegf-a* and *vegf-c* when compared to MTBE, which significantly decreases the expression of both genes in addition to *vegfr2* (Table 3.7, Fig. 2.6). In Kozlosky et al. (2012), the capacity for MTBE to disrupt normal capillary formation in mammalian models of angiogenesis was demonstrated in rat brain embryonic endothelial cells, human umbilical vein endothelial cells (HUVECs), and a Matrigel plug assay in mice. An additional important observation made in the paper was the different levels of sensitivity between micro- and macrovasculature endothelial cells to MTBE. In the tube formation assay, MTBE inhibited the initiation of tube formation, and caused tubes to be shorter and thinner in HUVECS (Fig. 1.7, 1.8), but completely inhibited tube formation in the primary culture of rat brain endothelial cells. One difference between the two cell types is that the rat brain endothelial cells represent microvasculature while HUVECs are representative of large vessel endothelial cells, since they originate from the umbilical vein. When zebrafish embryos were exposed to MTBE, lesions were observed in the

microvasculature, while the major arteries and veins of the embryo appear unaffected. Differences in gene expression of the micro- and macrovascular endothelial cells have been shown between HUVECs and human microvascular endothelial cells, a primary cell line derived from neonatal dermis (Jackson and Ngyun, 1997). Several studies have demonstrated differences between endothelial cell types in response to VEGF stimulation (Dardik et al., 2009), secretion of angiogenic proteins (Jayasinghe et al., 2009), and activation of eNOS (Krause et al., 2012). All endothelial cells are, therefore, not the same, but they all appear to be targets of MTBE toxicity. Why endothelial cells are susceptible to MTBE toxicity, and why microvascular endothelial cells are more sensitive than macrovascular cells, could provide additional information toward understanding the mechanism of MTBE vascular toxicity. This information could be useful in designing different treatment approaches to inhibit or promote angiogenesis in vascular related diseases.

6.2 MTBE disrupts the HIF-VEGF regulation of angiogenesis.

MTBE's unique specificity to developing vasculature, even compared to two structurally related chemicals, drove the hypothesis that MTBE acted through a VEGF-dependent mechanism. MTBE significantly decreased mRNA transcripts of *vegf-a* and *vegf-c* at 21-somites, a stage critical to both angiogenesis and MTBE toxicity (Kimmel et al., 1995, Isogai et al., 2001; Bonventre et al. 2011). Hypoxia is the primary inducer of angiogenesis in developing embryos as it increases both transcription and stabilization of the VEGF mRNA (Ryan et al. 1998; Lee et al., 2001; Ramirez-Bergeron et al., 2004; Minchenko et al., 1994; Shima et al., 1995). The HIF-VEGF pathway (Fig. 1.2) was the

primary focus of this dissertation, rather than an alternative angiogenesis pathway, because during development the predominant growth factor initiating and regulating early angiogenesis is VEGF. While other important pro-angiogenesis factors, such as the Angiopoietin/Tie system, function in early development, their activity is understood to follow that of VEGF and its receptors (Dumont et al., 1994; Sato et al., 1995; Suri et al, 1996).

The rescue studies (Chapter 5: Fig. 5.2) demonstrated a clear role for the HIF-VEGF pathway in MTBE toxicity by reversing the three primary vascular lesions induced by MTBE (Table 5.4). Over expression of zebrafish *vegf-a* significantly reduced the occurrence of cranial hemorrhages and abnormal ISVs in MTBE exposed embryos, but did not rescue the pooled blood in the CCV lesion (Fig. 5.3). Co-exposure with the PHD chemical inhibitor significantly rescued the CCV lesion and cranial hemorrhages, while the knockdown of VHL rescued only the CCV lesion (Figures 5.6, 5.8). In addition, transcript levels of HIF-VEGF related genes were all increased from their respective MTBE treated controls (Tables 5.1, 5.2, and 5.3). The inhibition of Vegf-a driven *mmp-9* mRNA expression by MTBE clearly demonstrated a role for MTBE disruption of Vegf-a activity (Fig. 5.4). How MTBE disrupts VEGF activity is still unclear (Fig. 6.1). Studies investigating MTBE's effect on *vegf-a* promoter activity, mRNA stability and protein concentrations would provide further insight into the mechanism by which MTBE inhibits VEGF and disrupts angiogenesis.

MTBE may function by disrupting a mechanism upstream of VEGF; e.g., by interfering with HIF1-α regulation in the cytoplasm (Fig. 6.1: 1, 2, or 3). Under normoxic conditions, HIF1-α is hydroxylated by PHDs and funneled through the ubiquitination

pathway by VHL (Ivan et al., 2001; Jaakkola et al., 2001). Oxygen, 2-oxoglutarate, and Fe^{2+} are required for PHD activity, while PHD activity is required for VHL driven ubiquitination. If the decrease in *vegf-a* results from altered HIF activity, then MTBE could be acting through a PHD dependent mechanism. On a cellular level, MTBE may mimic an oxygenated environment by binding to PHD, and stimulating HIF1-α hydryoxylation (Fig. 6.1: 1, 2). Alternatively, MTBE may block HIF1-α translocation into the nucleus, binding to HIF1-β, or interfere with association with specific HREs (Fig. 6.1: 3, 4, or 5). Future studies will need to investigate how MTBE alters the stability of HIF1-α and activity of HIF. *In silico* studies could be utilized, in addition to wet chemistry, to examine protein interactions in the presence of MTBE.

6.3 MTBE alters other developmental pathways on a gene expression level.

The zebrafish gene-array analysis provided evidence for MTBE-disruption of HIF activation *in vivo*. Many of molecules altered by MTBE during the critical period were related to the cardiovascular system, while other molecules were associated with cellular energy homeostasis and signs of cell stress. In addition to VEGF, erythropoietin, and associated proteins activated HIF (HIF1-α + HIF1-β) is known to regulate metabolic functions in the cell (Goda and Kanai, 2012). Under normoxic conditions, aerobic respiration occurs in the cell. However, in the absence of oxygen, the electron transport chain and preceding TCA cycle are inhibited, and anaerobic respiration (glycolysis) takes over. Lack of oxygen stabilizes HIF-α subunits in the cytoplasm, as PHDs require oxygen and 2-oxoglutarate (TCA cycle) to function. If HIF activation were inhibited by MTBE exposure, this would result in the decreased *vegf-a* mRNA and may also result in a

decrease in HIF-driven metabolic pathways (Fig. 6.1: 8, 9). The conversion of 2-oxoglutarate to succinate in HIF1-α hydroxylation suggests that the system is sensitive to dysfunction of the citric acid (TCA) cycle. An accumulation of succinate or fumarate, as well as increased levels of pyruvate and lactate, stabilizes HIF1-α by inhibiting PHD activity (Pollard et al., 2005; Lu et al., 2002). Conversely, if 2-oxoglutarate levels are increased and/or pyruvate levels are decreased, PHD activity is stimulated, providing an alternative mechanism by which MTBE may dysregulate HIF function (Fig. 6.1: 7). Altered expression of molecules associated with metabolism and energy production was observed in the microarray analysis, which strongly supports the hypothesis that MTBE disrupts HIF activity.

6.4 General Conclusions

The studies discussed in this dissertation demonstrate a relationship between MTBE toxicity and the HIF-VEGF pathway. The decreased expression of VEGF mRNA in addition to altered HIF-driven pathways at a critical point in development suggests that MTBE plays a role in disrupting normal HIF activation. Does MTBE bind to PHDs and mimic an oxygenated environment at the cellular level? Alternatively, can MTBE drive Hif1-α degradation, even under hypoxic conditions? Whether general hypoxia could be used to ameliorate MTBE-induced lesions was not pursued. However, if the MTBE toxicity is specific to a certain cell type, as has been proposed, then rearing embryos in a hypoxic environment will not be able to answer the question of what occurs at the cellular level. Hypoxia is known to render the embryo in a state of suspended animation (Padilla et al., 2001); therefore in order to test if hypoxia rescued MTBE-induced

vascular lesions, a low level of oxygen that does not itself cause toxicity to the embryo would be necessary. The potential direct relationship between hypoxia and MTBE would be more appropriately pursued in cell culture, where the effect hypoxia on MTBE toxicity could be determined at the level of the endothelial cells.

One of the most remarkable observations made in this dissertation was the identification of a critical period for MTBE toxicity that occured 24 hours prior to the appearance of the first MTBE-induced lesion. This sensitive period correlated to the stage of early angiogenesis in the embryo, but preceeding to the formation of the vessels that are affected (Kimmel el al., 1995; Isogai et al., 2001). If the embryos were exposed to MTBE after the critical period, there was no significant increase in vascular lesions. Ultimately, an exposure of only 15 hours during the critical period was enough to induce MTBE vascular lesions 24, 48, and 72 hours later. This suggested that the cells most sensitive to MTBE exposure are the progenitor endothelial cells, from which other endothelial cells are derived. In a study with cardiomyocyte progenitor cells, short-term hypoxia was shown to increase both the migratory and invasive capacity of the cells, as induced proliferation and angiogenic secretions (van Oorschot et al., 2011). Endothelial cells and endothelial progenitor cells have been shown possess alternate mechanisms for adapting to hypoxia (Abaci et al., 2010). Specifically, under low oxygen tension human endothelial progenitor cells grow more slowly than at normal oxygen levels, where as HUVECs grow more rapidly under low oxygen (Abaci et al., 2010). These two studies suggest that a dysregulation of the oxygen sensing system by MTBE means that the MTBE-vascular lesions could be a result of decreased proliferation, migratory capacity, and invasiveness of the original progenitor endothelial cells in the embryo.

The hypothesis that MTBE induces vascular lesions in the developing zebrafish by dysregulating the Hif-Vegf pathway has been supported by the findings of this dissertation. Due to the conserved nature of angiogenesis and the evidence for MTBE toxicity to mammalian systems (Koslosky et al., 2012), the results of these studies contribute the scientific knowledge of angiogenesis, and in particular, developmental angiogenesis. The small window of toxicity identified for MTBE in the zebrafish corresponds to days 24-27 of gestation in human embryonic development (Moore and Persaud, 1993). While exposure of a human fetus to signicantly high enough concentrations of MTBE in utero would be unquestionably unlikely, the studies presented in this dissertation highlight the importance of understanding the sensitivity of early vascular development in the embryo. Because it is both critical to life and detrimental in disease, the questions concerning the initiation and termination of angiogenesis will continue to drive scientific research beyond the presense of any one specific chemical of interest.

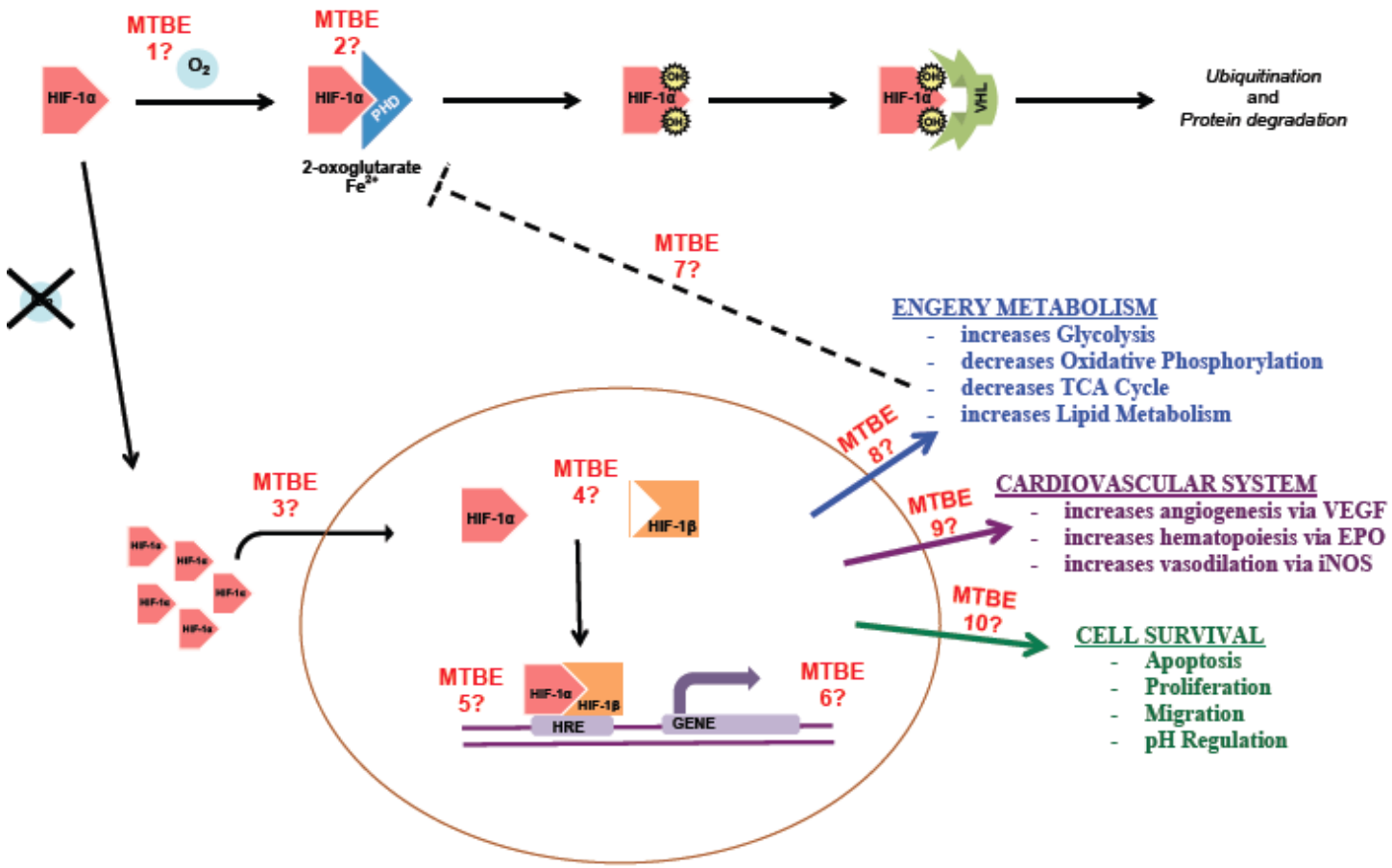

Figure 6.1. Possible locations for MTBE interference in the HIF-VEGF pathway. The rescue studies demonstrated a clear role for the HIF-VEGF pathway in MTBE toxicity by reversing the three primary vascular lesions induced by MTBE, but how MTBE disrupts VEGF activity is still unclear. MTBE could mimic oxygen in the microcellular environment or act as a substrate for PHD thereby activating the enzyme (1, 2). MTBE may inhibit HIF-α translocation into the nucleus, binding to HIF-β, or block the activated HIF complex from binding to HREs, or subsequent transcription of HIF dependent genes (3, 4, 5, 6). HIF mediates cell adaption to hypoxia by increases oxygen delivery (stimulated vascular growth) and a regulation of the cell's energy utilization. MTBE may act specifically on the cardiovascular endpoints of HIF activity (9), or as suggested by the gene array analysis, MTBE may alter energy metabolism (8) and cell survival (10), which could further impact HIF regulation in the cytoplasm (7).

170

Future Areas of Research

Angiogenesis is fundamental to development, but is contradictorily a common denominator in many diseases. As a result, anti-angiogenesis therapies play an important role in the treatment of such diseases, including cancer or retinopathies. Understanding basic mechanisms of angiogenesis are crucial to the development of new therapies. Chemicals with anti-angiogenic properties, such as MTBE, may be valuable tools to advance the science of angiogenesis, as well as provide insight into future anti-angiogenic pharmaceuticals.

The main questions that should be answered in future studies are how does MTBE disrupt HIF-VEGF regulation and why are endothelial cells more sensitive to MTBE? Possible avenues of research to pursue these questions have been discussed in sections 6.1, 6.2, and 6.3. Moreover, identifying if MTBE toxicity exerts a direct effect on VEGF specifically or on the entire HIF system is important to understanding the underlying mechanistic of action. The use of mRNA decay studies could be employed to determine if transcription or mRNA stability is affected by MTBE. Since HIF is involved both in VEGF transcription and mRNA stability, these studies would indicate an affect on HIF1 function. Due to the compensatory mechanisms involved in regulating angiogenesis, it would be interesting to knockdown the Angiopoietin/Tie system to see if and how it may be playing a role in compensating for the loss of VEGF incurred by MTBE exposure, or by other anti-VEGF compounds. This study would have implications in anti-VEGF therapies currently used in cancer treatments.

The rescue studies described in Chapter 5 suggest that the post-translational modification of HIF1-α is altered by MTBE exposure. *In vitro* studies could be

performed to determine if MTBE alters the number of hydroxylated HIF1-αs under normoxic or hypoxic conditions. If hydroxylated HIF1-αs increase in the presence of MTBE, it would suggest a mechanism by which MTBE is decreasing VEGF. Along the same lines, *in silica* studies with the crystalline structure of PHD could be used to determine if MTBE, either singular or polymerized can bind to the PHD and activate the enzyme under hypoxic conditions. Finally, *in vitro* kinetic studies could test the effect of MTBE on the rate of succinate production from 2-oxoglutarate by PHD. If more succinate is produced, then MTBE is indeed altering HIF1-α by interacting with PHD.

The ability of MTBE to inhibit invasion of endothelial cells into a Matrigel plug in the mouse model warrants further study (Kozlosky et al., 2012). Endothelial cells respond and migrate up a VEGF concentration gradient, but invasion into the matrix (or Matrigel) requires the hydrolysis of collagen and other extracellular matrix components. In Chapter 5, MTBE inhibited the increase in *mmp-9* transcript levels induced by an over expression of *vegf-a* (Figure 5.4). Transcription and secretion of MMP-9 is upregulated by the VEGF-A-VEGFR2 signaling cascade (Wang and Keiser, 1998; Pufe et al., 2002; Hollborn et al., 2007). Studies should be designed to determine if the lack of invasion is due to a reduced response to the VEGF contained in the Matrigel or an inability to break down the matrix components from inhibited MMP activity.

Another question that arose from this dissertation and the work in Kozlosky et al. (2012) is whether MTBE would be able to inhibit vascular growth in a solid tumor. Further studies with a standard mouse tumor model or a humanize mouse model injected with human tumor cells could be used to determine if MTBE exposure inhibits tumor growth *in vivo*. The primary difficulty with using MTBE to a solid tumor would be

maintaining concentrations of the chemical that would sustain the anti-angiogenic properties long enough to inhibit tumor growth. The concentrations of MTBE that have been shown to inhibit angiogenesis in fish, rodent, and cell studies are lower than the concentration administered to dissolve gallstones (Leuschner, 1986; Hellstern et al., 1998). However, since MTBE is rapidly broken down in a physiological system, a method of administering the chemical. Daily injections would be required, but they are painful and a useful tactic to treat a deep tissue tumor. Perhaps implanting a gel saturated with MTBE at the center of the tumor would allow for a delayed release. Co-administering MTBE and a known anti-angiogenic treatment, such as Avastin, may prove to be a more meaningful route of study.

While using MTBE as an anti-angiogenesis treatment alone is unlikely to inhibit tumor growth alone, it may be possible to develop an MTBE-based eye drop medication to inhibit the vascular remodeling that occurs in retinopathies. Again, administering the chemical would be the challenging, but in the form of a daily-use eye drop, it may be a plausible treatment, if the medication could penetrate the sclera and reach the retina. Studies would need to be carried out to determine if damage to the cornea would be sustained following MTBE exposure owing to the solvent properties of the chemical.

From the microarray studies discussed in Chapter 4, it was proposed that MTBE altered energy metabolism. While further studies would be needed to confirm this hypothesis, the idea raises important questions regarding the potential for MTBE in the treatment of solid tumors. Glycolysis is often more active in tumors than normal cells due to the increased hypoxia often associated with rapid growth (Hamanaka and Chandel, 2012). The effects of MTBE on metabolic function within a tumor are necessary

endpoints to study within the model. A mouse tumor study utilizing the microarray platform could be used to examine the effect of MTBE on a tumor compared to a tumor growing in the absence MTBE. If histology and morphometrics of the tumors were performed, then the gene expression changes would be anchored to a phenotype, providing a greater understanding of how MTBE toxicity affects tumor growth.

Studies examining the developmental toxicity of structurally related ETBE or TAME could also be pursed in the future. Developmental pathways upregulated during a critical time period of zebrafish development were identified and could be used to establish hypotheses for toxicants with unknown modes of action. ETBE and TAME were less effective in altering the mRNA expression of *vegf-a* and *vegf-c* compared to MTBE, but significantly decreased *wnts* and *mmps*. The IPA-derived networks created from the analysis of the stage-related changes in gene expression present a snapshot of the pathways activated early in development. The networks that include Wnt and MMPs could be used to generate hypotheses and design future experiments to determine how ETBE or TAME elicited their toxicity in the developing zebrafish. Examining the effect of ETBE or TAME on alternate molecules in the networks opens the door to pathways important to development.

An evaluation of MTBE's effect on a bone marrow may provide critical information on the sensitivity of early multipotent cardiovascular stem cells. The *in vivo* developmental vascular lesions observed with MTBE were shown only in piscine models, but *in vitro* studies with mammalian bone marrow could be used to explore the sensitivity of this system, critical for cardiovascular development, in the mammalian model system. These studies would explore the ability of MTBE to disrupt the differentiation of cell

types of the bone marrow. Altered cardiovascular stem cell differentiation could explain some of the MTBE-induced vascular lesions, including their latency (occurring 24 hrs after the critical period) and the fact that some vessels are more sensitive than other (differences in micro- and macrovasculature).

Kozlosky et al. (2012) reported that pregnant female rats exposed to at one time gavaged dose of 500 -1500 mg/kg of MTBE did not demonstrate treatment related effects in the pups. However, no histology was performed on the placenta, a highly vascularized organ wherein the maternal and fetal blood vessels meet to exchange nutrients and oxygen for waste and carbon dioxide. While it is unlikely that a mammalian female would be exposed to sufficient concentrations of MTBE to induce vascular lesions in her fetus, alterations in vascular structure of the placenta could be conceivable. This in turn would lead to nutrient deficiencies in the embryo, which have been shown to induce disease states later in life (Painter et al. 2005; Langley-Evans and McMullen et al., 2010). A reproductive study of chronic drinking water exposure should be conducted to determine if aberrations in the placenta vasculature occur.

Future studies with MTBE should be designed to better characterize the molecular targets for MTBE anti-angiogenesis. In order to be relevant to human applications, these studies must incorporate human tissues and correlate observed effects to relevant gene expression and biochemical pathways. As stated earlier, the use of MTBE to establish additional anti-angiogenic therapies could lead to new therapeutic approaches for either decreasing or increasing angiogenesis in a disease state.

ACKNOWLEDGEMENT OF PREVIOUS PUBLICATIONS

CHAPTER 1 (Figs. 1.7 & 1.8):

Kozlosky, J., **Bonventre, J.A.**, Cooper, K.R., (2012) Methyl tert butyl ether is anti-angiogenic in both in vitro and in vivo mammalian model systems. J Appl Toxicol, DOI 10.1002/jat.273 Epub Mar 8. *Reprinted with permission from the publisher, John Wiley and Sons (License #2902851441655).*

CHAPTER 2:

Bonventre, J.A., White, L.A., Cooper, K.R., (2011) Methyl tert butyl ether targets developing vasculature in zebrafish (*Danio rerio*) embryos. Aquatic Toxicol, 105: 29-40. *Reprinted with permission from the publisher, Elsevier B.V. (License #2823211137788)*

CHAPTER 3:

Bonventre, J.A., White, L.A., and Cooper, K.R. (2012) Craniofacial abnormalities and altered *wnt* and *mmp* mRNA expression in zebrafish embryos exposed to gasoline oxygenates ETBE and TAME. Aquat. Toxicol. Apr 25; 120-121C:45-53. *Reprinted with permission from the publisher, Elsevier B.V. (License #2923630292700)*

REFERENCES

Abaci, H.E., Truitt, R., Luong, E., Drazer, G., Gerecht, S., 2010. Adaptation to oxygen deprivation in cultures of human pluripotent stem cells, endothelial progenitor cells, and umbilical vein endothelial cells. Am. J. Physiol. Cell Physiol., 298(6): C1527-37.

Adelman, D.M., Maltepe, E., Simon, M.C., 1999. Multilineage embryonic hematopoiesis requires hypoxic ARNT activity. Genes Dev. 13, 2478–2483.

Ahmed, F.E., 2001. Toxicology and human health effects following exposure to oxygenated or reformulated gasoline. Toxicol. Lett. 123, 89–113.

Amberg, A., Rosner, E., Dekant, W., 2001. Toxicokinetics of methyl tert butyl ether and its metabolites in humans after oral exposure. Toxicol. Sci. 61, 62–67.

American Petroleum Institute (1995b) tert-Amyl Methyl Ether (TAME) - Acute Toxicity to Rainbow Trout (Oncorhynchus mykiss) under Flow-through Conditions, Project No. 93-3-4682, Springborn Laboratories, Inc, Wareham, MA, USA.

Ancillotti, F., and Fattore, V., 1998. Oxygenate fuels: market expansion and catalytic aspect of synthesis. Fuel Process Technol 57:163–194.

Antkiewicz, D.S., Burns, C.G., Carney, S.A., Peterson, R.E., Heideman, W., 2005. Heart malformation is an early response to TCDD in embryonic zebrafish. Toxicol. Sci. 84, 368–377.

Asano, Y., Ishikura, T., Kudoh, K., Haneda, R., Endoh, T., 2011. Prenatal developmental toxicity study of ethyl tertiary-butyl ether in rabbits. Drug Chem Toxicol, 34(3): 311–317.

Bahary, N., Goishi, K., Stuckenholz, C., Weber, G., Leblanc, J., Schafer, C.A., Berman, S.S., Klagsbrun, M., Zon, L.I., 2007. Duplicate VegfA genes and orthologues of the KDR receptor tyrosine kinase family mediate vascular development in the zebrafish. Blood 110 (10), 3627–3636.

Bedell, V.M., Westcot, S.E., Ekker, S.C., 2011. Lessons from morpholino-based screening in zebrafish. Brief Funct. Genomics, 10(4): 181-188.

Berra, E., Benizri, E., Ginouves, A., Volmat, V., Roux, D., Pouyssegur, J., 2003. HIF prolyl-hydroxylase 2 is the key oxygen sensor setting low steady-state levels of HIF-alpha in normoxia. EMBO J., 22:4082-4090.

Bevan, C., Tyl, R.W., Neeper-Bradley, T.L., Fisher, L.C., Panson, R.D., Douglas, J.F., and Andrews, L.S., 1997. Developmental toxicity evaluation of MTBE by inhalation in mice and rabbits. J Appl Toxicol Suppl 1:S21-29.

Brown, S., 1997. Atmospheric and potable water exposure to methyl tert–butyl ether. Regul. Toxicol. Pharm. 25, 256–276.

Brugmann, S.A., Goodnough, L.H., Gregorieff, A., Leucht, P., ten Berg, D., Fuerer, C., Clevers, H., Nusse, R., Helms, J.A., 2007. Wnt signaling mediates regional specifications in the vertebrate face. Develop. 134: 3283-3295.

Bonventre, J.A., White, L.A., Cooper, K.R., 2011. Methyl tert butyl ether targets developing vasculature in zebrafish (*Danio rerio*) embryos. Aquat. Toxicol., 105: 29-40.

Bonventre, J.A., White, L.A., Cooper, K.R., 2012. Craniofacial abnormalities and altered wnt and mmp mRNA expression in zebrafish embryos exposed to gasoline oxygenates ETBE and TAME. Aquat. Toxicol. Apr 25;120-121C:45-53. [Epub ahead of print] doi: 10.1016/j.aquatox.2012.04.008

Bugel, S.M., White, L.A., Cooper, K.R., 2010. Impaired reproductive health of killifish (*Fundulus heteroclitus*) inhabiting Newark Bay, NJ, a chronically contaminated estuary. Aquat. Toxicol. 96 (3), 182-193.

Carmeliet, P., Ferreira, V., Breier, G., Pollefeyt, S., Kieckens, L., Gertsenstein, M., Fahrig, M., Vandenhoek, A., Harpal, K., Eberhardt, C., Declercg, C., Pawling, J., Moons, L., Collen, D., Risau, W., Naggy, A., 1996. Abnormal blood vessel development and lethality in embryos lacking a single VEGF allele. Nature 380, 436–438.

Carney, M.W., Erwin, K., Hardman, R., Yuen, B., Volz, D.C., Hinton, D.E., Kullman, S.W., 2008. Differential developmental toxicity of naphthoic acid isomers in medaka (*Oryzias latipes*) embryos. Mar. Pollut. Bull. 57, 255–266.

Chevron Phillips, 2010. Material Safety Data Sheet: Ethyl-tert-Butyl Ether, version 1.2. MSDS Number:100000013976, p 7.

Chew, E.Y., 2005. Ocular manifestation of von Hippel-Lindau disease: clinical and genetic infestigations. Trans. Am. Ophthalmol. Soc., 103:495-511.

Childs, S., Chen, J.N., Garrity, D.M., Fishman, M.C., 2002. Patterning of angiogenesis in the zebrafish embryo. Develop. 129: 973-982.

Chiquet, B.T., Blanton, S.H., Burt, A., Ma, D., Stal, S., Mullikins, J.B., Hecht, J.T., 2008. Variation in WNT genes is associated with non-syndromic cleft lip with or without cleft palate. Human Mol. Gen. 17(14): 2212–2218.

Choi, K., Kennedy, M., Kazarov, A., Papadimitriou, J.C., Keller, G., 1998. A common precursor for hematopoietic and endothelial cells. Development 125, 725–732.

Cohen, T., Gitay-Goren, H., Sharon, R., Shibuya, M., Halaban, R., Levi, B.Z., Neufeld, G., 1995. VEGF121, a vascular endothelial growth factor (VEGF) isoform lacking heparin binding ability, requires cell-surface heparin sulfates for efficient binding to the VEGF receptors of human melanoma cells. J. Biol. Chem. 270(19):11322-6.

Conaway, C.C., Schroeder, R.E., and Snyder, N.K., 1985. Teratology evaluation of MTBE in rats and mice. J Toxicol Environ Health, 16(6):797-809.

Coons, R., 2008. Basic Chemicals & Plastics - Study suggests ETBE use to grow. Chemical Week, 170 (3), p30.

Covassin, L.D., Villefranc, J.A., Kacergis, M.C., Weinstein, B.M., Lawson, N.D., 2006. Distinct genetic interactions between multiple Vegf receptors are required for development of different blood vessel types in zebrafish. Proc. Natl. Acad. Sci. 103 (17), 6554–6559.

Dardik, R., Livnat, T., Seligsohn, U., 2009. Variable effects of alpha v suppression on VEGFR-2 expression in endothelial cells of different vascular beds. Thromb. Haemost. 102(5):975-82.

de Peyster, A., 2010. Ethyl t-butyl ether: review of reproductive and developmental toxicity. Birth Defects Res. B. Dev. Reprod. Toxicol. 89:239-263.

Dickmeis, T., Plessy, C., Rastegar, S., Aanstad, P., Herwig, R., Chalmel, F., Fischer, N, Strähle, U., 2004. Expression profiling and comparative genomics identify a conserved regulatory region controlling midline expression in the zebrafish embryo. Genome Res. 2004 Feb;14(2):228-38. Epub 2004 Jan 12.

Dong, W., Teraoka, H., Tsujimoto, Y., Stegeman, J.J., Hiraga, T., 2004. Role of aryl hydrocarbon receptor in mesencephalic circulation failure and apoptosis in zebrafish embryos exposed to 2,3,7,8–tetrachlorodibenzo–*p*–dioxin. Toxicol. Sci. 77, 109–116.

Du, H.F., Xu, L.H., Wang, H.F., Liu, Y.F., Tang, X.Y., Liu, K.X., Peng, S.X., 2005. Formation of MTBE–DNA adducts in mice measured with accelerator mass spectroscopy. Environ. Toxicol. 20, 397–401.

Dumont, D.J., Gradwohl, G., Fong, G.H., Puri, M.C., Gerstenstein, M., Auerbach, A., Breitman, M.L., 1994. Dominant-negative and targeted null mutations in the endothelial receptor tyrosine kinase, tek, reveal a critical role in vasculogenesis of the embryo. Genes Dev. 8: 1897-1909.

Elonen, G.E., Spehar, R.L., Holcombe, G.W., Johnson, R.D., Fernandez, J.D., Erickson, R.J., Tietge, J.E., Cook, P.M., (1998). Comparative toxicity of 2,3,7,8-

tetrachlorodibenzo-p-dioxin in seven freshwater fish species during early life-stage development. Environ Toxicol Chem. 17(3), 472-483.

Enholm, B., Karpanen, T., Jeltsch, M., Kubo, H., Stenback, F., Prevo, R., Jackson, D.G., Yla-Herttuala, S., Alitalo, K., 2001. Adenoviral expression of vascular endothelial growth factor-c induces lymphangiogenesis in the skin. Circul. Res. 88:623-629.

Eswaran, W., Lee, S.H., Inge, L., Guo, L., Goldbeck, C., Garrett, E., Wiesmann, M., Garcia, P.D., Fuller, J.H., Chan, V., Randazzo, F., Gundel, R., Warren, R.S., Escobedo, J., Aukerman, S.L., Taylor, R.N., Fantl, W.J., 2003. beta–Catenin regulates vascular endothelial growth factor expression in colon cancer. Cancer Res. 63 (12), 3145–3153.

Ferrara, N., Carver–Moore, K., Chen, H., Dowd, M., Lu, L., O'Shea, K.S., Powel–Braxton, L., Hillan, K.J., Moore, M.W., 1996. Heterozygous embryonic lethality induced by targeted inactivation of VEGF gene. Nature 308, 439–442.

Ferrara, N., Gerber, H.P., LeCouter, J., 2003. The biology of VEGF and its receptors. Nat. Med., 669–676.

Fraisl, P., Aragones, J., Carmeliet, P., 2009. Inhibition of oxygen sensors as therapeutic strategy for ischaemic and inflammatory disease. Nat Rev Drug Disc., 8: 139-152.

Forsythe, J.A., Jiang, B.H., Iyer, N.V., Agani, F., Leung, S.W., Koos, R.D., Semenza, G., 1996. Activation of vascular endothelial growth factor gene transcription by hypoxia–inducible factor 1. Mol. Cell Biol. 16 (9), 4604–4613.

Fujio, Y., Walsh, K., 1999. Akt mediates cytoprotection of endothelial cells by vascular endothelial growth factor in an anchorage-dependent manner. J. Biol. Chem. 274(23):16349-54.

Fukumura, D., Gohongi, T., Kadambi, A., Izumi, Y., Ang, J., Yun, C.O., Buerk, D.G., Huang, P.L., Jain, R.K., 2001. Predominant role of endothelial nitric oxide synthase in vascular endothelial growth factor-induced angiogenesis and vascular permeability. Proc Natl Acad Sci U S A. 98(5):2604-9.

Gavard, J., Gutkind, J.S., 2006. VEGF controls endothelial-cell permeability by promoting the beta-arrestin-dependent endocytosis of VE-cadherin. Nat. Cell Biol. 8(11):1223-34.

Gleadle, J.M., Ebert, B.L, Firth, J.D., Ratcliffe, P.J., 1995. Regulation of angiogenic growth factor expression by hypoxia, transition metals, and chelating agents. Am. J. Physiol., Jun;268(6 Pt 1):C1362-8.

Gnarra, J.R., Tory, K., Weng, Y., Schmidt, L., Wei, M.H., Li, H., Latif, F., Liu, S., Chen, F., Duh, F.M., Lubensky, I., Duan, D.R., Florence, C., Rozzatti, R., Walther,

M.M., Bander, N.H., Grossman, H.B., Brauch, H., Pomer, S., Brooks, J.D., Isaacs, W.B., Lerman, M.I., Zbar, B., Linehan, W.M., 1994. Mutations of VHL tumour suppressor gene in renal carcinoma. Nat. Genet. 7(1): 85-90.

Gnarra, J.R., Ward, J.M., Porter, F.D., Wagner, J.R., Devor, D.E., Grinberg, A., Emmert-Buck, M.R., Westphal., H., Klausner, R.D., Linehan, W.M., 1997. Defective placental vasculogenesis causes embryonic lethality in VHL-deficient mice. Proc. Natl. Acad. Sci., 94(17): 9102-7.

Goda, N., Kanai, M., 2012. Hypoxia-inducible factors and their roles in energy metabolism. Int. J. Hematol. 95(5):457-63.

Gonzalez Santander, R., Martinez Cuadrado, G., Gonzalez–Santander Marinez, M., Monteagudo, M., Martinez Alonso, F.J., Toledo Lobo, M.V., 1997. The use of different fixatives and hydrophilic embedding media (Historesiny and Unicryly) for the study of embryonic tissues. Microsc. Res. Tech. 36 (3), 151–158.

Habeck, H., Odenthal, J., Walderich, B., Maischein, H., Schulte–Merker, S., 2002. Analysis of zebrafish VEGF receptor mutant reveals specific disruption of angiogenesis. Curr. Biol. 12 (16), 1405–1412.

Hamada, S., Kim, T.D., Suzuki, T., Itoh, Y., Tsumoto, H, Nakagawa, H., Janknecht, R., Miyata, N., 2009. Synthesis and activity of N-oxalylglycine and its derivatives as Jumonji C-domain-containing histone lysine demethylase inhibitors. Bioorg. Med. Chem. Lett. 19(10):2852-5.

Hamanaka, R.B., Chandel, N.S., 2012. Targeting glucose metabolism for cancer therapy. J. Exp. Med. 209(2):211-5.

Heidman, W., Antkiewicz, D.S., Carney, S.A., Peterson, R.E., 2005. Zebrafish and cardiac toxicology. Cardiovasc. Toxicol. 5, 203–214.

Henry, T.R., Spitsbergen, J.M., Hornung, M.W., Abnet, C.C., Peterson, R.E., 1997. Early life stage toxicity of 2,3,7,8–tetrachlorodibenzo–*p*–dioxin in zebrafish (*Danio rerio*). Toxicol. Appl. Pharmacol. 142, 56–68.

Herbert, S.P., Huisken, J., Kim, T.N., Feldman, M.E., Houseman, B.T., Wang, R.A., Shokat, K.M., Stainier, D.Y.R., 2009. Arterial–venous segregation by selective cell sprouting: an alternative mode of blood vessel formation. Science 326, 294–298.

Hill, A.J., Teraoka, H., Heideman, W., Peterson, R.E., 2005. Zebrafish as a model vertebrate for investigating chemical toxicity. Toxicol. Sci. 86 (1), 6–19.

Hillegass, J.M., Villano, C.M., White, L.A., Cooper, K.R., 2007. Matrix metalloproteinase–13 is required for zebra fish (*Danio rerio*) development and is a target for glucocorticoids. Toxicol. Sci. 100 (1), 168–179.

Hillegass, J.M., Villano, C.M., White, L.A., Cooper, K.R., 2008. Glucocorticoids alter craniofacial development and increase expression and activity of matrix metalloproteinases in developing zebrafish (*Danio rerio*). Toxicol. Sci. 102, 413–424.

Hong, J.Y., Yang, C.S., Lee, M., Wang, Y.Y., Huang, W., Tan, Y., Patten, C.J., Bondoc, F.Y., 1997. Role of cytochromes P450 in the metabolism of methyl tert–butyl ether in human livers. Arch. Toxicol. 71, 266–269.

Hong, J.Y., Wang, Y.Y., Bondoc, F.Y., Lee, M., Yang, C.S., Hu, W.Y., Pan, J., 1999. Metabolism of Methyl tert–butyl ether and other gasoline ethers by human liver microsomes and heterologously expressed human cytochromes P450: identification of CYP2A6 as a major catalyst. Toxicol. Appl. Pharm. 160, 43–48.

Huttunen, H., Wyness, L.E., and Kalliokoski, P., 1997. Identification of environmental hazards of gasoline oxygenate *tert*-amyl methyl ether (TAME). Chemosphere, 35(6): 1199-1214.

IARC (2012) Agents Classified by the IARC Monographs, Volumes 1–104 http://monographs.iarc.fr/ENG/Classification/ClassificationsAlphaOrder.pdf updated March 27, 2012.

Incardona, J.P., Collier, T.K., Scholtz, N.L., 2004. Defects in cardiac function precede morphological abnormalities in fish embryos exposed to polycyclic aromatic hydrocarbon. Toxicol. Appl. Pharmacol. 196, 191–205.

Irwin, R.J. (Ed.), 1997. Environmental Contaminants Encyclopedia: MTBE entry. United Stages National Park Service, Water Resources Div., Water Operations Branch.

Isogai, S., Horiguchi, M., Weinstein, B.M., 2001. The vascular anatomy of the developing zebrafish: an atlas of embryonic and early larval development. Dev. Biol. 230 (2), 278–301.

Ivan, M., Kondo, K., Yang, H., Kim, W., Valiando, J., Ohh, M., Salic, A., Asara, J.M., Lane, W.S., Kaelin, W.G., 2001. HIFalpha targeted for VHL–mediated destruction by proline hydroxylation: implications for O2 sensing. Science 292 (5516), 464–468.

Iyer, V., Pumiglia, K., DiPersio, C.M., 2005. Alpha3 beta1 integrin regulates MMP-9 mRNA stability in immortalized keratinocytes: a novel mechanism of integrin-mediated MMP gene expression. J. Cell Sci. 118, 1185-1195.

Jaakola, P., Mole, D.R., Tian, Y.M., Wilson, M.I., Gielbert, J., Gaskell, S.J., Kriegsheim, A.V., Hebestreit, H.F., Mukherji, M., Shofield, C.J., Maxwell, P.H., Pugh, C.W., Ratcliffe, P.J., 2001. Targeting of HIF-alpha to the von Hippel-Lindaw

ubiquitylation complex of O2-regulated prolyl hydroxylation. Science, 292(5516): 468-72.

Jayasinghe, C., Simiantonaki, N., Michel-Schmidt, R., Kirkpatrick, C.J., 2009. Hypoxia-induced reduction of sVEGFR-2 levels in human colonic microvascular endothelial cells in vitro: Comparative study with HUVEC. Int. J. Mol. Med. 23(1):49-55.

Keith, B., Johnson, R.S., Simon, M.C., 2011. HIF1α and Hif2α: sibling rivalry in hypoxic tumour growth and progression. Nat. Rev. Cancer, 12(1):9-22. doi: 10.1038/nrc3183.

Kibel, A., Iliopoulos, O., DeCaprio, J. D., Kaelin, W. G., 1995. Binding of the von Hippel–Lindau tumor suppressor protein to elongin B and C. Science 269, 1444–1446.

Kim, W.Y., Safran, S., Buckley, M.R.M., Ebert, B.L., Glicman, G., Bosenberg, M., Regan, M., Kaelin, W.G. Jr., 2006. Failure to prolyl hydroxylate hyposia inducible factor alpha phenocopies VHL inactivation *in vivo*. EMBO J., 25, 4650-4662.

Kimmel, C.B., Ballard, W.W., Kimmel, S.R., Ullmann, B., Schilling, T.F., 1995. Stages of embryonic development of the zebrafish. Dev. Dynam. 203 (3), 253–310.

Kozlosky, J., Bonventre, J.A., Cooper, K.R., 2012. Methyl tert butyl ether is anti-angiogenic in both in vitro and *in vivo* mammalian model systems. J. Appl. Toxicol. DOI 10.1002/jat.273.

Krause, B.J., Prieto, C.P., Muños-Urrutia, E., San Martín, S., Sobrevia, L., Casanello, P., 2012. Role of arginase-2 and eNOS in the differential vascular reactivity and hypoxia-induced endothelial response in umbilical arteries and veins. Placenta 33(5):360-6.

Lamalice, L., Houle, F., Jourdan, G., Huot, J., (2004) Phosphorylation of tyrosine 1214 on VEGFR2 is required for VEGF-induced activation of Cdc42 upstream of SAPK2/p38. Oncogene **23**,434–445.

Lampugnani, M.G., Orsenigo, F., Gagliani, M.C., Tacchetti, C., Dejana, E., 2006. Vascular endothelial cadherin controls VEGFR2 internalization and signaling from intracellular compartments. J. Cell. Biol. 174 (4), 593–604.

Langley-Evans, S.C., and McMullen, S., 2010. Developmental origens of adult disease. Med. Princ. Pract. 19(2): 87-98.

Lawson, N.D., Weinstein, B.M., 2002. *In vivo* imaging of embryonic vascular development using transgenic zebrafish. Dev. Biol. 240, 307–318.

Le Gal, A., Dreano, Y., Gervasi, P.G., Berthou, F., 2001. Hyman cytochrome P450 2A6 is the major enzyme involved in the metabolism of three alkoxyethers used in oxyfuels. Toxicol. Lett. 124, 47–58.

Lee, Y.M., Jeong, C.H., Koo, S.Y., Son, M.J., Song, H.S., Bae, S.K., Raleigh, J.A., Chung, H.Y., Yoo, M.A., Kim, K.W., 2001. Determination of hypoxic region by hypoxia marker in developing mouse embryos *in vivo*: a possible signal for vessel development. Dev. Dyn. 220(2):175-86.

Levy, A.P., Levy, N.S., Wegner, S., Goldberg, M.A., 1995. Transcriptional regulation of the rat vascular endothelial growth factor gene by hypoxia. J. Biol. Chem. 270 (22), 13333–13340.

Liang, D., Xu, X., Chin, A.J., Balasubramaniyam, N.V., Teo, M.A., Lam, T.J., Weinberg, E.S., Ge, R., 1998. Cloning and characterization of vascular endothelial growth factor (VEGF) from zebrafish, *Danio rerio*. Biochim. Biophys. Acta 1397 (1), 14–20.

Litchfield, J.T., Wilcoxon, F., 1949. A simplified method of evaluating dose–effect experiments. J. Pharmacol. Exp. Ther. 96 (2), 99–113.

Lonergan, K. M. Iliopoulos. O., Ohh, M., Kamura, T., Conaway, RC., Conaway, J.W., Kaelin, W.G. Jr., 1998. Regulation of hypoxia-inducible mRNAs by the von Hippel–Lindau protein requires binding to complexes containing elongins B/C and Cul2. Mol. Cell. Biol., 18, 732–741.

Longo, S.E., 1995. Effects of methyl tert–butyl ether and napthaline on the embryo of the Japanese medaka. MS Thesis. Rutgers University, Graduate School, New Brunswick.

Lu, H., Forbes, R.A., Verma, A., 2002. Hypoxia-inducible factor 1 activation by aerobic glycolysis implicates the Warburg effect in carcinogenesis. J. Biol. Chem. 277(26):23111-5.

Madan, A., Varma, S., Cohen, H.J., 2002. Developmental stage-specific expression of the alpha and beta subunits of the HIF-1 protein in the mouse and human fetus. Mol. Genet. Metab. 75(3): 244-9.

Mackenzie, E.D., Selak, M.A., Tennant, D.A., Payne, L.J., Crosby, S., Frederiksen, C.M., Watson, D.G., Gottlieb, E., 2007. Cell-permeating alpha-ketoglutarate derivatives alleviate pseudohypoxia in succinate dehydrogenase-deficient cells. Mol. Cell. Biol., 27(9): 3282-9.

Mahabeleshwar, G.H., Feng, W., Phillips, D.R., Byzova, T.V., 2006. Integrin signaling is critical for pathological angiogenesis. J. Exp. Med. 203(11): 2495-507.

Malinin, N., Pluskota, E., Byzova, T.V., 2012. Integrin signaling in vascular function. Curr. Opp. 19(3): 206-211.

Marxsen, J.H., Stengel, P., Doege, K., Heikkinen, P., Jokilhto, T., Wagner, T., Jelkmann, W., Jaakkola, P., Metzen, E., 2004. Hypoxia-inducible factor-1 (HIF-1) promotes its degradation by induction of HIF-α-prolyl-4-hydroxylases. Biochem. J., 381(Pt 3): 761–767.

Matsumoto, T., Bohman, S., Dixelius, J., Berge, T., Dimberg, A., Magnusson, P., Wang, L., Wikner, C., Qi, J.H., Wernstedt, C., Wu, J., Bruheim, S., Mugishima, H., Mukhopadhyay, D., Spurkland, A., Claesson-Welsh, L., 2005. VEGF receptor-2 Y951 signaling and a role for the adapter molecule TSAd in tumor angiogenesis. EMBO J. 2005 Jul 6;24(13):2342-53.

Maxwell, P.H., Wiesener, M.S., Chang, G.W., Clifford, S.C., Vaux, E.C., Cockman, M.E., Wykoff, C.C., Pugh, C.W., Maher, E.R., Ratcliffe, P.J., 1999. The tumour suppressor protein VHL targets hypoxia-inducible factors for oxygen-dependent proteolysis. Nature, 399: 271–275.

Menezes, R., Letra, A., Kim, A.H., Küchler, E.C., Day, A., Tannure, P.N., Gomes da Motta, L., Paiva, K.B.S., Granjeiro, J.M., Vieira, A.R., Studies with Wnt genes and nonsyndromic cleft lip and palate. Birth Defects Res. A. Dev. Reprod. Toxicol. 88: 995-1000.

Mechtcheriakova, D., Wlachos, A., Holzmüller, H., Binder, B.R., Hofer, E., 1999. Vascular endothelial cell growth factor-induced tissue factor expression in endothelial cells is mediated by EGR-1. Blood, 93(11):3811-23.

Mole, D.R., Schlemminger, I., McNeill, L.A., Hewitson, K.S., Pugh, C.W., Ratcliffe, P.J., Shofield, C., 2003. 2-Oxoglutarate analogue inhibitors of HIF prolyl hydroxylase. Bioorgan. Medicin. Chem. Let., 13: 2677–2680.

Mone, S.M., Gillman, M.W., Miller, T.L., Herman, E.H., Lipshultz, S.E., 2004. Effects of environmental exposures on the cardiovascular system: prenatal period through adolescence. Pediatrics 113, 1058–1069.

Moore, K. L. and Persaud, T. V. N., 1993. The Developing Human: Clinically Oriented Embryology. 5th ed., (ed.), Philadelphia: WB Saunders.

Moreels, D., Van Cauwenberghe, K., Debaere, B., Rurangwa, E., Vromant, N., Bastiaens, L., Diels, L., Springael, D., Merckx, R., Ollevier, F., 2006a. Long–term exposure to environmentally relevant doses of methyl–tert–butyl ether causes significant reproductive dysfunction in the zebrafish (*Danio rerio*). Environ. Toxicol. Chem. 25 (9), 2388–2393.

Moreels, D., Lodewijks, P., Zegers, H., Rurangwa, E., Vromant, N., Bastiaens, L., Diels, L., Springael, D., Merckx, R., Ollevier, F., 2006b. Effect of short–term exposure to methyl–tert–butyl ether and tert–butyl alcohol on the hatch rate and development of the African catfish, *Clarias gariepinus*. Environ. Toxicol. Chem. 25 (2), 514–519.

Morris-Wiman, J., Burch, H., Basco, E., 2000. Temporospatial distribution of matrix metalloproteinase and tissue inhibitors of matrix metalloproteinases during murine secondary palate morphogenesis. Anat. Embryol. (Berl). 202:129–141.

Mostowska, A., Hozyasz, K.K., Biedziak, B., Wojcicka, P., Lianeri, M., Jagodzinski, P.P., 2012. Genotype and haplotype analysis of WNT genes in non-syndromic cleft lip with or without cleft palate. Eur. J. Oral Sci. 120: 1–8.

Naddafi, K., Nabizadeh, R., Baiggi, A., 2008. Bioassay of methyl tertiary–butyl ether (MTBE) toxicity on rainbow trout fish. J. Hazard. Mater. 154 (1–3), 403– 406.

Nasevicius, A., Larson, J., Ekker, S.C., 2000. Distinct requirements for zebrafish angiogenesis revealed by a VEGF–A morphant. Yeast 17, 294–301.

Nasevicius, A., Ekker, S.C., 2000. Effective targeted gene knockdown in zebrafish. Nat. Genet. 26 (2), 216–220.

Ohh, M., Yauch, R. L.,Lonergan, K. M., Whaley, J. M., Stemmer-Rachamimov, A. O., Louis, D. N., Gavin, B. J., Kley, N., Kaelin, W. G. Jr., Iliopoulos, O., 1998. The von Hippel-Lindau tumor suppressor protein is required for proper assembly of an extracellular fibronectin matrix. Mol. Cell.1: 959–968.

Ohh, M., Park, C.W., Ivan, M., Hoffman, M.A., Kim, T.Y., Huang, L.E., Pavletich, N., Chau, V., Kaelin, W.G., 2000. Ubiquitination of hypoxia-inducible factor requires direct binding to the beta-domain of the von Hippel-Lindau protein. Nat. Cell Biol., 2(7): 423-7.

Padilla, P.A., Roth, M.B., 2001. Oxygen deprivation causes suspended animation in the zebrafish embryo. Proc. Natl. Acad. Sci. U S A., 98:7331-7335.

Painter, R.C., Roseboom, T.J., Bleker, O.P. 2005. Prenatal exposure to the Dutch famine and disease in later life: an overview. Reprod. Toxicol. 20(3): 345-52.

Parker, S., Mai, C.T., Canfield, M.A., Rickard, R., Wang, Y., Meyer, R.E., Anderson, P., Mason, C.A., Collins, J.S., Kirby, R.S., Correa, A., National Birth Defects Prevention Network., 2010. Updated National Birth Prevalence estimates for selected birth defects in the United States, 2004-2006. Birth Defects Res A Clin Mol Teratol. 88(12):1008-16.

Phillips, S., Palmer, R.B., Brody, A., 2008. Epidemiology, toxicology, and healthy effects of methyl tert–butyl ether (MTBE). J. Med. Toxicol. 4 (2), 115–126.

Planutiene, M., Planutis, K., Holcombe, R.F., 2011. Lymphoid enhancer-binding factor 1, a representative of vertebrate-specific Lef1/Tcf1 sub-family, is a Wnt-beta-catenin pathway target gene in human endothelial cells which regulates matrix metalloproteinase-2 expression and promotes endothelial cell invasion. Vascular Cell. 3:28, doi:10.1186/2045-824X-3-28.

Pollard, P.J., Briere, J.J., Alam, N.A., Barwell, J., Barclay, E., Wortham, N.C., Hunt, T., Mitchell, M., Olphin, S., Moat, S.J., Hargreaves, I.P., Heales, S.J., Griffiths, J.R., Dangleish, A., McGrath, J.A., Gleeson, M.J., Hodgson, S.V., Poulsom, R., Rustin, P., Tomlinson, I.P., 2005. Accumulation of Krebs cycle intermeidates and over-expression of HIF1alpha in tumours wchi result from germline FH and SDH mutations. Hum. Mol. Genet. 14(15): 2231-9.

Post, G. (Ed.), 2001. MTBE in New Jersey's Environment. New Jersey Department of Environmental Protection.

Ramirez–Bergeron, D.L., Runge, A., Cowden Dahl, K.D., Fehling, H.J., Keller, G., Simon, C., 2004. Hypoxia affects mesoderm and enhances hemangioblast specification during early development. Development 131, 4623–4634.

Redondo-Muñoz, J., Ugarte-Berzal, E., García-Marco, J.A., del Cerro, M.H., Van den Steen, P.E., Opdenakker, G., Terol, M.J., García-Padro, A., 2008. Alpha4beta1 integring and 190-kDa CD44v constitute a cell surface docking complex for gelatinase B/MMP-9 in chronic leukemic but not in normal B cells. Blood. 112(1):169-78.

Rosell, M., Lacorte, S., Barcelo, D., 2006. Analysis, occurrence and fate of MTBE in the aquatic environment over the past decade. Trends Anal. Chem. 25, 1016– 1029.

Ryan, H.E., Lo, J., Johnson, R.S., 1998. Hif–1 alpha is required for solid tumor formation and embryonic vascularization. EMBO J. 17 (11), 3005–3015.

Sato, T.N, Tozawa, Y., Deutsch, U., Wolburg-Buchholz, K., Fujiwara, Y, Gendron-Maquire, Gridley, T., Wolburg, H., Risau, W., Qin, Y., 1995. Distinct roles of the receptor tyrosine kinases Tie-1 and Tie-2 in blood vessel formation. Nature, 376: 70–74.

Shalaby, F., Rossant, J., Yamaguchi, T.P., Gertsenstein, M., Wu, X.F., Breitman, M.L., Schuh, A.C., 1995. Failure of blood island formation and vasculogenesis in Flk–1–deficient mice. Nature 376 (6535), 62–66.

Shima, D.T., Deutsch, U., D'Amore, P.A., 1995. Hypoxic induction of vascular endothelial growth factor (VEGF) in human epithelial cells is mediated by increases in mRNA stability. FEBS Lett., 370(3): 203-8.

Sokol, S.Y., 2011. Maintaining embryonic stem cell pluripotency with Wnt signaling. Development. 138, 4341-4350.

Spitsbergen, J.M., Walker, M.K., Olson, J.R., Peterson, R.E., 1991. Pathologic alterations in early life stages of like trout, *Salvelinus namaycush*, exposed to 2,3,7,8–tetrachlorodibenzo–*p*–dioxin as fertilized eggs. Aquat. Toxicol. 19, 41–72.

Squillace, P.J., Moran, M.J., 2007. Factors associated with sources, transport, and fate of volatile organic compounds and their mixtures in aquifers of the United States. Environ. Sci. Technol. 41, 2123–2130.

Stein, I., Neeman, M., Shweiki, D., Itin, A., Keshet, E., 1995. Stabilization of vascular endothelial growth factor mRNA by hypoxia and hypoglycemia and coregulation with other ischemia-induced genes. Mol. Cell Biol., 15(10): 5363-8.

Suri, C., Jones, P.F., Patan, S., Bartunkova, S., Maisonpierre, P.C., Davis, S., Sato, T.N., Yancopoulos, G.D., 1996. Requisite role of Angiopoietin-1, a ligand for the Tie2 receptor, during embryonic angiogenesis. Cell, 87: 1171–1180.

Takahashi, T., Ueno, H., Shibuya, M., 1999. VEGF activates protein kinase C-dependent, but Ras-independent Raf-MEK-MAP kinase pathway for DNA synthesis in primary endothelial cells. Oncogene, 18(13):2221-30.

Takahashi, T., Yamaguchi, S., Chida, K., Shibuya, M., 2001. A single autophosphorylation site on KDR/Flk-1 is essential for VEGF-A-dependent activation of PLC-gamma and DNA synthesis in vascular endothelial cells. *EMBO J.*20, 2768–2778.

Taylor, J.S., Braasch, I., Frickey, T., Meyer, A., Van de Peer, Y., 2003. Gene duplication, a trait shared by 22,000 species of ray-finned fish. Genome Res., 13:382-390.

Ton, C., Stamatiou, D., Liew, C.C., 2003. Gene expression profile of zebrafish exposed to hypoxia during development. Physiol. Genomics, 16;13(2):97-106.

United States DOE–EAI, 2010. Monthly MTBE production, updated 12.30.10: http://tonto.eia.doe.gov/dnav/pet/pet_pnp_oxy_dc_nus_mbbl_m.htm (accessed December 2010).

United States EPA, 2007. State actions banning MTBE (Statewide). EPA420–B–07–013: http://www.epa.gov/MTBE/420b07013.pdf (accessed October 2009).

Van Wezel, A., Puijker, L., Vink, C., Versteegh, A., de Voogt, P., 2009. Odour and flavor thresholds of gasoline additives (MTBE, ETBE and TAME) and their occurrence in Dutch drinking water collection areas. Chemosphere 76 (5), 672–676.

Van Oorschot, A.A., Smits, A.M., Pardali, E., Doevendans, P.A., Goumans, M.J., 2011. Low oxygen tension positively influences cardiomyocytes progenitor cell function. J. Cell Mol. Med. 15(12): 2723-34.

Vogeli, K.M., Jin, S.W., Martin, G.R., Stainier, D.Y., 2006. A common progenitor for haematopoietic and endothelial lineages in the zebrafish gastrula. Nature 443, 337–339.

Wang, G.L., Semenza, G.L., 1993. Characterization of hypoxia inducible factor 1 and regulation of DNA binding activity by hypoxia. J. Biol. Chem. 268 (29), 21513–21518.

Wang, S., Li, X., Parra, M., Verdin, E., Bassel-Duby, R., Olson, E.N., 2008. Control of endothelial cell proliferation and migration by VEGF signaling to histone deacetylase 7. Proc Natl Acad Sci, 105(22): 7738-43.

Welsch, F., Elswick, B., James, R.A., Marr, M.C., Myers, C.B., Tyl, R.W., 2003. Developmental Toxicity evaluation of inhaled tertiary amyl methyl ether in mice and rats, J. Appl. Toxicol. 23, 387–395.

Werner, I., Koger, C.S., Deanovic, L.A., Hinton, D.E., 2001. Toxicity of methy–tert–butyl ether to freshwater organisms. Environ. Pollut. 111, 83–88.

Wilkinson, K.D., 2000. Ubiquitination and deubiquitination: Targeting of proteins for degradation by the proteasome Cell. Develop. Biol., 11: 141–148.

Wirthner, R., Balamurugan, K., Stiehl, D.P., Barth, S., Spielmann, P., Oehmen, F., Flamme, I, Katschinski, D.M., Wenger, R.H., Carmenisch, G., 2007. Determination and modulation of prolyl-4-hydroxylase domain oxygen sensor activity. Meth. Enzymol. 435: 43-60.

Wisk, J.D., Cooper, K.R., 1990a. The stage specific toxicity of 2,3,7,8–tetrachlorodibenzo–*p*–dioxin in embryos of the japanese medaka (*Oryzias latipes*). Environ. Toxicol. Chem. 9 (9), 1159–1169.

Wisk, J.D., Cooper, K.R., 1990b. Comparison of the toxicity of several polychlorinated dibenzo–*p*–dioxins and 2,3,7,8–tetrochlorobenzofuran in embryos of the Japanese medaka (*Oryzias latipes*). Chemosphere 20, 361–377.

Xu, Q., 1999. “Chapter 11: Microinjection into Zebrafish Embryos,” in Methods in Molecular Biology, vol. 127: Molecular methods in developmental biology:

Xenopus and Zebrafish. Edited by M. Gille, Humana Press, Inc., Totowa, NJ. Pg 125-132. DOI: 10.1385/1-59259-678-9:125.

Yang, L., Kemadjou, J.R., Zinsmeister, C., Bauer, M., Legradi, J., Müller, F., Pankratz, M., Jäkel, J., Strähle, U., 2007. Transcriptional profiling reveals barcode-like toxicogenomic responses in the zebrafish embryo. Genome Biol. 8(10):R227.

Yao, T., Yang, L., Li, P., Wu, H., Xie, H., Shen, X., Xie, X. 2011 Association of Wnt3A gene variants with non-syndromic cleft lip with or without cleft palate in Chinese population. Arch. Oral Biol. 56: 73-78.

Zhou, S., Dong, Q., Li, S., Guo, J., Wang, X., Zhu, G., 2009. Developmental toxicity of cartap on zebrafish embryos. Aquat. Toxicol. 95, 339–346.

Zitka, O., Kukacka, J., Krizkova, S., Huska, D., Adam, V., Masarik, M., Prusa, R., Kizek, R., 2010. Matrix Metalloproteinases, Curr. Med. Chem., 17: 3751-3768.